Utah State University

DigitalCommons@USU

12-2017

Behavior of Copper Oxide Nanoparticles in Soil Pore Waters as Influenced by Soil Characteristics, Bacteria, and Wheat Roots

Joshua Hortin
Utah State University

Follow this and additional works at: https://digitalcommons.usu.edu/etd

Part of the Civil and Environmental Engineering Commons

UtahStateUniversity
MERRILL-CAZIER LIBRARY

BEHAVIOR OF COPPER OXIDE NANOPARTICLES IN SOIL PORE WATERS

AS INFLUENCED BY SOIL CHARACTERISTICS, BACTERIA,

AND WHEAT ROOTS

by

Joshua Hortin

A thesis submitted in partial fulfillment
of the requirements for the degree

of

MASTER OF SCIENCE

in

Civil and Environmental Engineering

Approved:

_____   _____
Joan E. McLean, M.S.   Astrid R. Jacobson, Ph.D.
Major Professor   Committee Member

_____   _____
David W. Britt, Ph.D.   Anne J. Anderson, Ph.D.
Committee Member   Committee Member

_____   _____
Laurie S. McNeill, Ph.D.   Mark R. McLellan, Ph.D.
Committee Member   Vice President for Research and
                                                                    Dean of the School of Graduate Studies

UTAH STATE UNIVERSITY
Logan, Utah

2017

ABSTRACT

Behavior of Copper Oxide Nanoparticles in Soil Pore Waters

as Influenced by Soil Characteristics, Bacteria,

and Wheat Roots

by

Joshua M. Hortin, Master of Science

Utah State University, 2017

Major Professor: Joan E. McLean
Department: Civil and Environmental Engineering

Copper oxide nanoparticles, used in paints/coatings, electronics, and agriculture, will inevitably enter soils through land-application of wastewater effluent or biosolids, use as a foliar fungicide, or use as a crop fertilizer or drought treatment. Therefore, the solubility, surface transformations, and plant uptake of copper oxide nanoparticles were measured in pore water extractions from soils with varied organic matter additions, and in the rooting zone of wheat grown in sand for 10 days with selected soil pore waters.

Soil pore waters increased solubility of copper oxide nanoparticles above the solubility observed in 3.34 mM calcium nitrate at the comparable pH (> pH 8) driven by complexation with dissolved natural organic matter. Soluble organic matter (> 30 mg/L C) did not bind with dissolved copper at its predicted capacity, suppressing nanoparticle solubility. Coating of nanoparticles by organic matter was the theorized controller of solubility.

In sand with soil pore waters, copper oxide nanoparticles dissolved at levels in agreement with geochemical models. It is likely that the presence of sand surface area minimized the main controlling mechanism on solubility, coating, observed in the first study. Wheat increased nanoparticle solubility due to the production of copper complexing exudates. The presence of a root-colonizing bacterium, *Pseudomonas chlororaphis* O6, decreased copper oxide nanoparticle solubility primarily due to metabolism of root exudates. Nanoparticles in sand and 3.34 mM calcium nitrate shortened root lengths, but soil pore waters partially restored root length in the sand-nanoparticle matrix, despite having similar soluble copper levels. Although *Pseudomonas chlororaphis* O6 decreased nanoparticle solubility, the bacteria increased damage to wheat roots from nanoparticles likely via increased concentrations of the phytosiderophore 2'-deoxymugineic acid, which altered bioavailability of the dissolved copper to the wheat. Nanoparticles also increased the concentrations of 2'-deoxymugineic acid and citrate, which were associated with shortening roots, potentially in a feedback loop. Uptake of copper into the shoot was held at the level of the control or below.

Dissolved natural organic matter has potential to lessen copper oxide nanoparticle phytotoxicity in contaminated soils. Nanoparticles could be manipulated with organic compounds to deliver targeted fertilizer or pesticidal treatments.

(170 pages)

PUBLIC ABSTRACT

Behavior of Copper Oxide Nanoparticles in Soil Pore Waters

as Influenced by Soil Characteristics, Bacteria,

and Wheat Roots

Joshua M. Hortin

The goal of this project was to study the behavior of copper oxide nanoparticles in soil environments. Copper oxide nanoparticles have antimicrobial properties and may also be used in agricultural settings to provide a source of copper for plant health, but accidental or misapplication of these nanoparticles to soil may be damaging to the plant and its associated bacteria.

Dissolved soil organic matter that is present in soil pore waters dissolved nanoparticles, but did not dissolve the expected amounts from a geochemical model because the geochemical model did not take into account surface chemistry or coating of the nanoparticles by dissolved organic matter. Wheat grown in soil pore water increased the solubility of the nanoparticles. The nanoparticles and dissolved copper were harmful to wheat, but dissolved soil organic matter remediated a portion of the damage. These studies were conducted with Utah soils and wheat, a highly valuable Utah crop.

These results suggest that contamination of soils by copper oxide nanoparticles will be partially mitigated by the organic matter content of the soil. Producers of fertilizers and fungicides may use various forms of organic matter to deliver products that are targeted to specific plants or pathogens and avoid damage to non-target organisms.

ACKNOWLEDGMENTS

Thesis writing has been one of the largest, if not most intense, challenges of my life. With that in mind, I would like to thank those who supported me and who made this possible.

I'd like to thank Joan McLean at the Utah Water Research Laboratory for hiring me as an undergraduate with no idea about research or laboratories, for encouraging me to pursue undergraduate and graduate research, and for tireless feedback and direction. I thank my committee for their input, insight, encouragement, and review of my work.

I am grateful for funding over four years from the Utah Water Research Laboratory, the Utah Mineral Lease Fund, and the Engineering Undergraduate Research Program. These funds allowed me to pursue four years of focused research.

I thank my family and friends for celebrating the decision to pursue graduate education, for listening to complaints, and for supporting me through the process.

I thank my husband, Shaun Anderson, for discussions, meals, rides, encouragement, sympathy, and whatever else I needed at the time over two years. Shaun helped me navigate not only school but concurrent crises during thesis writing – the challenges of belonging to the LGBT+ population and managing a faith crisis.

Lastly, to peers, professors, the broader USU community – thank you for being here with me, being friendly and open and helpful, and making up the school I love.

Joshua Hortin

CONTENTS

LIST OF TABLES

LIST OF FIGURES

LIST OF NOTATIONS

Word, name, or phrase	Notation
"Agricultural Millville"	AgrM
Analysis of variance	ANOVA
Bioaccumulation factor	BAF
Bioconcentration factor	BCF
Biotic ligand model	BLM
Colony forming units	CFU
Copper	Cu
Copper, aqueous phase	$Cu_{(aq)}$
Copper, solid phase	$Cu_{(s)}$
Copper ions, uncomplexed	Cu^{2+}
Copper oxide	CuO
2'-deoxymugineic acid	DMA
Dissolved natural organic mater	DNOM
Dynamic light scattering	DLS
Energy dispersive X-ray spectroscopy	EDS
Extracellular polymeric substances	EPS
Fulvic acid(s)	FA
Fourier transform infrared spectroscopy	FTIR
"Garden (community) Millville"	GM
Honestly significant difference	HSD
Humic acid(s)	HA(s)
Inductively coupled plasma mass spectrometry	ICP-MS
"Iron-deficient (grassland) Millville"	IDM
Low molecular weight organic acid(s)	LMWOA(s)
Luria-Bertani	LB
Molecular weight cutoff	MWCO
Nanoparticle(s)	NP(s)
"Organic farm Millville"	OrgM
Point of zero charge	PZC
Principal component analysis	PCA
Pseudomonas chlororaphis O6	*Pc*O6
Pyoverdine	PVD
Root mean square error	RMSE
Scanning electron microscopy	SEM

LIST OF NOTATIONS (CONT.)

Word, name, or phrase	Notation
(Soil) pore water(s)	(S)PW(s)
Warm Springs	WS
X-ray diffraction	XRD

CHAPTER 1

INTRODUCTION

Nanoparticles (NPs), particles less than 100 nm in at least one dimension, have a

much higher surface area than larger "bulk" particles per unit weight. NPs' increased

surface area gives NPs differing properties over bulk particles. Specialized NP properties

may include faster kinetics of dissolution, potential toxicity, or other material-dependent

properties that suit particular NPs for specific industrial applications.

Research into NP fate and toxicity has lagged behind their use. Studies on

nanoparticle toxicity and nanoecotoxicology (with the origination of the term) began in

2003 and 2006, respectively, despite research on nanoparticles extending back before

1990 (Kahru and Dubourguier 2010). Consequently, many household, industrial, and

agricultural products use NPs without an adequate understanding of their environmental

implications and end-of-life fate.

Copper oxide (also termed cupric oxide, tenorite, or CuO) NPs are highly likely

to contact soil through several routes. CuO NPs are primarily used in catalysts,

electronics, and as an antimicrobial in paints/coatings (Keller et al. 2013). In 2010, 18%

of the global flow of Cu-based NPs were disposed of in soils (Keller et al. 2013), mostly

through deposition of CuO NPs into biosolids from wastewater treatment plants

(Cornelis et al. 2014; Otero-Gonzalez et al. 2014). CuO NPs applied to soil or

agricultural foliage intentionally, with the objectives of remediation, fertilization, or

antimicrobial action (Cornelis et al. 2014; Servin et al. 2015; Elmer and White 2016),

may also contaminate soil. The fate and behavior of NPs in the soil environment is, however, not understood well (Fang et al. 2013; Pan and Xing 2012).

CuO NPs are thus a concern in the agricultural soil environment due to toxic responses observed under well-defined media or hydroponic systems in plants (Dimkpa et al. 2012; Ko and Kong 2014), bacteria (Gajjar et al. 2009; Dimkpa et al. 2011; Frenk et al. 2013; Martineau et al. 2014), and fungi (Zabrieski et al. 2015). The mode of toxicity of CuO NPs is debated and is theorized to be 1) toxicity due to soluble Cu ions (Dimkpa et al. 2011), 2) NP-specific effects (such as generation of reactive oxygen species, Trojan-horse cellular effects (Cronholm et al. 2013) as NPs approach the size of pores in root cell walls of ~5 nm (Carpita et al. 1979), or aerobic vs. anaerobic effects), or 3) a combination of both (Jiang et al. 2017).

Despite the limits of research on the toxicity and behavior of CuO NPs in soils, principles of chemistry and limited research of CuO NPs in natural waters indicate how CuO NPs may act in soils. Solubility of the NPs is controlled by pH, organic and inorganic ligands, ionic strength, and contributions of organisms through plant and bacterial exudates. The solubility of CuO decreases with increasing pH (log K_{sp} = -7.9; Lindsay et al. 1979). The presence of organic (soil organic matter or organic acids) and inorganic (carbonate, chloride, phosphate) ligands, which complex Cu ions, increases CuO solubility. Ligands may increase CuO NP solubility even at high pH.

pH, ionic strength (Sousa et al. 2013), and solution cations/anions such as phosphate/alkalinity (Conway et al. 2015) affect the negative surface charge of the CuO NPs below the point of zero charge at ~pH 10, which affects aggregation. Aggregation

of NPs indirectly affects the rate of solubility. Organic molecules (particularly humic and fulvic acids) coat CuO NPs (Peng et al. 2015; Zhao et al. 2013) and reduce their contact and toxicity with organisms. Coatings also decrease the solubility of CuO NPs in laboratory or natural media (Conway et al. 2015). Living cells (such as bacteria or roots) alter these aforementioned processes via secretion of organic components (McManus 2016; Martineau et al. 2014) and bacterial exudates/extracellular polymeric substances (Dimkpa et al. 2011; Miao et al. 2015). The bioavailability and toxicity of Cu ions to soil organisms such as wheat or bacteria are dependent on competing cations for surface sorption sites and complexing ligands, which make the Cu less bioavailable according to the Biotic Ligand Model (Luo et al. 2008), but this model has not been applied to CuO NPs. A full literature review of how these variables impact CuO NP dissolution, aggregation, and toxicity in soils or other media is found in Chapter 2.

Altogether, previous research suggests that dissolved organic matter in soils and other soil properties will be very important in CuO NP chemistry, yet the mechanisms and effects of dissolved organic matter on CuO NPs are not well-defined. Furthermore, toxicity and uptake of CuO NPs to wheat may correlate with soil properties. For example, pH correlates with NP solubility (Anderson et al. 2017), cation competition correlates with root adsorption/uptake of Cu ions or NPs (Stewart et al. 2015), and root exudate production correlates with enhanced uptake of Cu (McManus 2016).

The goals of this study were to determine how variables present in semi-arid agricultural soils (fulvic acids, orthophosphate, alkalinity) and time affected the solubility and surface chemistry of CuO NPs in soil pore waters (SPWs) (Chapter 4), and

how SPWs and microbes alter the solubility, forms of Cu present, and uptake of CuO

NPs to wheat (Chapter 5). These data will build knowledge about the fate of CuO NPs in

soil (particularly high pH, calcareous soils characteristic of arid regions), potential

remediation techniques for CuO NP-contaminated soil, and may shed further light on

uses for CuO NPs in agriculture.

References

Anderson, A., McLean, J., McManus, P., and Britt, D. (2017). "Soil chemistry influences the phytotoxicity of metal oxide nanoparticles." *Int. J. Nanotechnol.*, 14(1-6), 15-21.

Carpita, N., Sabularse, D., Montezinos, D., and Delmer, D. P. (1979). "Determination of the pore size of cell walls of living plant cells." *Science*, 205(4411), 1144-1147.

Conway, J. R., Adeleye, A. S., Gardea-Torresdey, J., and Keller, A. A. (2015). "Aggregation, dissolution, and transformation of copper nanoparticles in natural waters." *Environ. Sci. Technol.*, 49(5), 2749-2756.

Cornelis, G., Hund-Rinke, K., Kuhlbusch, T., Van den Brink, N., and Nickel, C. (2014). "Fate and bioavailability of engineered nanoparticles in soils: A review." *Crit. Rev. Environ. Sci. Technol.*, 44(24), 2720-2764.

Cronholm, P., Karlsson, H. L., Hedgerg, J., Lowe, T. A., Winnberg, L., Elihn, K., Wallinder, I. O., and Möller, L. (2013). "Intracellular uptake and toxicity of Ag and CuO nanoparticles: A comparison between nanoparticles and their corresponding metal ions." *Small*, 9(7), 970-982.

Dimkpa, C. O., Calder, A., Britt, D. W., McLean, J. E., and Anderson, A. J. (2011). "Responses of a soil bacterium, *Pseudomonas chlororaphis* O6 to commercial metal oxide nanoparticles compared with responses to metal ions." *Environ. Pollut.*, 159(7), 1749-1756.

Dimkpa, C. O., McLean, J. E., Latta, D. E., Manangon, E., Britt, D. W., Johnson, W. P., Boyanov, M. I., and Anderson, A. J. (2012). "CuO and ZnO nanoparticles: Phytotoxicity, metal speciation, and induction of oxidative stress in sand-grown wheat." *J. Nanopart. Res.*, 14(9).

Elmer, W. H., and White, J. C. (2016). "The use of metallic oxide nanoparticles to enhance growth of tomatoes and eggplants in disease infested soil or soilless medium." *Environ. Sci.: Nano*, 3(5), 1072-1079.

Fang, T., Watson, J. L., Goodman, J., Dimkpa, C. O., Martineau, N., Das, S., McLean, J. E., Britt, D. W., and Anderson, A. J. (2013). "Does doping with aluminum alter the effects of ZnO nanoparticles on the metabolism of soil pseudomonads?" *Microbiol. Res.*, 168(2), 91-98.

Frenk, S., Ben-Moshe, T., Dror, I., Berkowitz, B., and Minz, D. (2013). "Effect of metal oxide nanoparticles on microbial community structure and function in two different soil types." *PLoS One*, 8(12).

Gajjar, P., Pettee, B., Britt, D. W., Huang, W., Johnson, W. P., and Anderson, A. J. (2009). "Antimicrobial activities of commercial nanoparticles against an environmental soil microbe, *Pseudomonas putida* KT2440." *J. Biol. Eng.*, 3(9).

Gustaffson, J. P. (2013). "Visual MINTEQ."

Jiang, C., Castellon, B. T., Matson, C. W., Aiken, G. R., and Hsu-Kim, H. (2017). "Relative contributions of copper oxide nanoparticles and dissolved copper to Cu uptake kinetics of Gulf Killifish (*Fundulus grandis*) embryos." *Environ. Sci. Technol.*, 51(3), 1395-1404.

Kahru, A., and Dubourguier, H. (2010) "From ecotoxicology to nanoecotoxicology." *Toxicol.*, 269, 105-119.

Keller, A. A., McFerran, S., Lazareva, A., and Suh, S. (2013). "Global life cycle releases of engineered nanomaterials." *J. Nanopart. Res.*, 15(6).

Ko, K. S., and Kong, I. C. (2014). "Toxic effects of nanoparticles on bioluminescence activity, seed germination, and gene mutation." *Appl. Microbiol. Biotechnol.*, 98(7), 3295-3303.

Lindsay, W. L. (1979). Chemical Equilibria in Soils, John Wiley & Sons, New York.

Luo, X. S., Li, L. Z., and Zhou, D. M. (2008). "Effect of cations on copper toxicity to wheat root: Implications for the biotic ligand model." *Chemosphere*, 73(3), 401-406.

Martineau, N., McLean, J. E., Dimkpa, C. O., Britt, D. W., and Anderson, A. J. (2014). "Components from wheat roots modify the bioactivity of ZnO and CuO nanoparticles in a soil bacterium." *Environ. Pollut.*, 187, 65-72.

McManus, P. (2016). "Rhizosphere interactions between copper oxide nanoparticles and wheat root exudates in a sand matrix: influences on bioavailability and uptake," thesis, Utah State University, Logan.

Miao, L. Z., Wang, C., Hou, J., Wang, P. F., Ao, Y. H., Li, Y., Lv, B. W., Yang, Y. Y., You, G. X., and Xu, Y. (2015). "Enhanced stability and dissolution of CuO nanoparticles by extracellular polymeric substances in aqueous environment." *J. Nanopart. Res.*, 17(10).

Otero-Gonzalez, L., Field, J. A., and Sierra-Alvarez, R. (2014). "Inhibition of anaerobic wastewater treatment after long-term exposure to low levels of CuO nanoparticles." *Water Res.*, 58, 160-168.

Pan, B, and Xing, B. (2012). "Applications and implications of manufactured nanoparticles in soils: A review." *Eur. J. Soil Sci.*, 63(4), 437-456.

Peng, C., Zhang, H., Fang, H. X., Xu, C., Huang, H. M., Wang, Y., Sun, L. J., Yuan, X. F., Chen, Y. X., and Shi, J. Y. (2015). "Natural organic matter-induced alleviation of the phytotoxicity to rice (Oryza Sativa L.) caused by copper oxide nanoparticles." *Environ. Toxicol. Chem.*, 34(9), 1996-2003.

Servin, A., Elmer, W., Mukherjee, A., De La Torre-Roche, R., Hamdi, H., White, J. C., Bindraban, P., and Dimkpa, C. (2015). "A review of the use of engineered

nanomaterials to suppress plant disease and enhance crop yield." *J. Nanopart. Res.*, 17(2).

Stewart, J., Hansen, T., McLean, J. E., McManus, P., Day, S., Britt, D. W., Anderson, A. J., and Dimkpa, C. O. (2015). "Salts affect the interaction of ZnO or CuO nanoparticles with wheat." *Environ. Toxicol. Chem.*, 34(9), 2116-2125.

Sousa, V. S., and Teixeira, M. R. (2013). "Aggregation kinetics and surface charge of CuO nanoparticles: The influence of pH, ionic strength and humic acids." *Environ. Chem.*, 10(4), 313-322.

Zabrieski, Z., Morrell, E., Hortin, J., Dimkpa, C., McLean, J., Britt, D., and Anderson, A. (2015). "Pesticidal activity of metal oxide nanoparticles on plant pathogenic isolates of Pythium." *Ecotoxicology*, 24(6), 1305-1314.

Zhao, J., Wang, Z. Y., Dai, Y. H., and Xing, B. S. (2013). "Mitigation of CuO nanoparticle-induced bacterial membrane damage by dissolved organic matter." *Water Res.*, 47(12), 4169-4178.

CHAPTER 2

LITERATURE REVIEW

CuO NP occurrence, use, and exposure to soil

NP use in commercial products is growing at an exponential rate. Keller et al. (2013) estimated that approximately 200 metric tons of Cu/Cu-oxides NPs were used and disposed of worldwide in 2010 with 36 metric tons residing in soil, and these statistics will be higher in 2017.

Suppan (2013) states that environmental contamination of NPs in general is likely to occur through land application of biosolids, wastewater effluent, and agriculture. Outside studies validate each of Suppan's exposure routes. Keller et al. (2013) modeled the exposure of commercial NPs to the environment, estimating that 18% of global Cu and Cu-oxides NPs were disposed of in soils primarily after passing through a water treatment plant (Figure 2-1). Westerhoff et al. (2015) used microscopy and spectroscopy to verify the presence of NPs in wastewaters, including copper-containing colloids. As most of the NPs which pass through a wastewater treatment plant originate from paints and coatings, according to Keller et al. (2013), Adeleye et al. (2016) confirmed release of Cu_2O NPs from a commercial paint in seawater and freshwater which transformed to CuO under oxic conditions. CuO NPs also show promise as a foliar fungicide (Servin et al. 2015) and they may contact agricultural soils through overspray or leaf litter from treated crops.

Principles of CuO NP behavior in aqueous systems

When NPs are in suspension, they may remain as nanoparticles (Figure 2-1A), aggregate (B), or dissolve forming Cu ions (C). The CuO NPs may transition between these forms through dissolution, precipitation, aggregation, and/or fragmentation. Any form of the CuO NP (A, B, C) may be coated or complexed with organic or inorganic ligands (D), sorb to minerals, organic surfaces in soils, or roots (E), or be uptaken by plants and/or microbes (F). These processes are confirmed by outside publications (Figure 1 of Thwala et al. 2016, Figure 2 of Delay & Frimmel 2012).
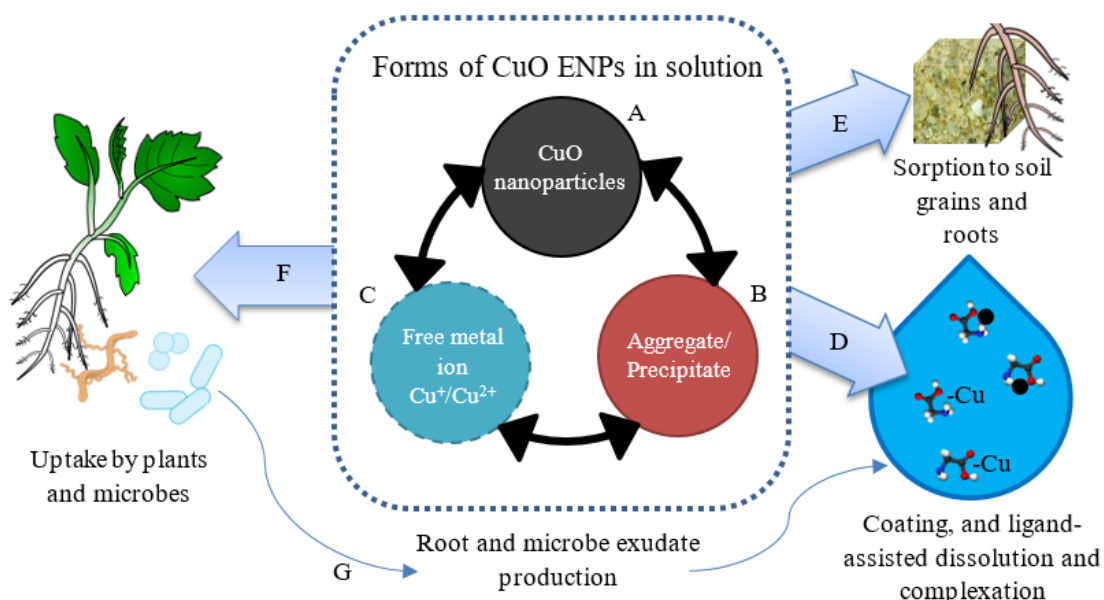
Figure 2-1: Behavior of CuO NPs in aqueous environments.

All of these processes have been previously observed: dissolution, aggregation, and fragmentation of CuO NPs (Conway et al. 2015), coating and ligand-assisted dissolution of CuO NPs (D; Wang et al. 2013; Wang et al. 2015; Conway et al. 2015), sorption of CuO NPs (E) to soil (Julich and Gath 2014) and wheat roots (Zhou et al.

2011), and sub-lethal toxicity of CuO NPs (F) to wheat (Dimkpa et al. 2013a; Dimkpa et al. 2012c) and microbes (Dimkpa et al. 2011; Dimkpa et al. 2012a, b, d). Many of these studies, however, are limited to well-defined solution matrices not relevant to the soil environment.

Although these processes have been observed, they are not yet well understood. For example, plants and microorganisms (F) are selective as to the form of metal uptaken (i.e., solid vs. dissolved, redox state, complexed with certain ligands) limiting the bioavailability. Plants increase the dissolution of CuO NPs (Dimkpa et al. 2013a), probably through acidification of the rooting zone (the volume of soil filled by roots) or release of organic exudates (G), yet the plant responses are not well known and increased dissolution may not always cause increased toxicity, especially when complexing or competing ligands are present (Luo et al. 2008). Many studies are seemingly contradictory (i.e., ligands increase or suppress dissolution of CuO NPs under different circumstances; Table 2-1), and some studies are the first of their types (such as the sorption studies of Julich and Gath (2014) and Zhou et al. (2011)). More knowledge is needed to understand the complex interplay between NPs in soil with microbes and plants.

The hypotheses and objectives in this study will consider all processes shown in Figure 2-1, but the processes primarily measured will be dissolution, complexation, and sub-lethal toxicity of NPs to gain a greater understanding of the processes that are not yet well-detailed by the literature. The following sections will investigate the factors that affect the processes outlined in Figure 2-1. General factors affecting the aggregation,

Table 2-1: Increase of or suppression of CuO NP solubility as affected by dissolved natural organic matter under varying conditions.

Author	Ligand	Result on CuO NP dissolution
Adeleye et al. (2014)	Suwannee River organic matter (pH 4)	Suppressed
	Extracellular polymeric substances (pH 4)	Suppressed
	Suwannee River organic matter (pH 7, 11)	Increased
	Extracellular polymeric substances (pH 7, 11)	Increased
Conway et al. (2015)	Freshwater organic matter (pH 6.3)	Suppressed
	Stormwater runoff organic matter (pH 6.6)	Suppressed
	Wastewater organic matter (pH 7.6)	Increased
Peng et al. (2015)	Humic acid (pH 7)	Increased
Jiang et al. (2017)	Humic acid (pH 7)	Increased
	Fulvic acid (pH 7)	Increased
	Williams Lake Hydrophobic acid (pH 7)	Suppressed or no change

dissolution, sorption, coating, and uptake of CuO NPs are solution pH, soil ligands and their concentrations, and ionic strength.

Solution pH

Solution pH affects several parts of the CuO NP picture: NP dissolution, NP surface charge, and anion protonation. These three effects are discussed in the following paragraphs.

In general, NPs are expected to have the same solubility product as their bulk counterpart materials, but more rapid equilibrium because of increased surface area (Misra et al. 2012); although David et al. (2012) demonstrated that for 6 nm ZnO NPs, the solubility product was higher than that of the mineral form, zincite. Misra et al. (2012) stated that enough evidence had been gathered to show that CuO NPs' equilibrium solubility concentration increases with decreasing NP size, although this statement is not well supported in the literature.

The log K_{sp} for CuO (tenorite) is 7.66 (Lindsay 1979), and the equilibrium solubility of CuO to Cu^{2+} increases tenfold for every 0.5 unit of pH decrease (Figure 2-2). Regardless of pH, if the system is undersaturated with respect to copper, dissolution of CuO NPs will proceed (Kent & Vikesland 2016). Vencalek et al. (2016), following up the work of Kent & Vikesland (2016), determined that pH ultimately affected the rate of dissolution more than organic matter content.
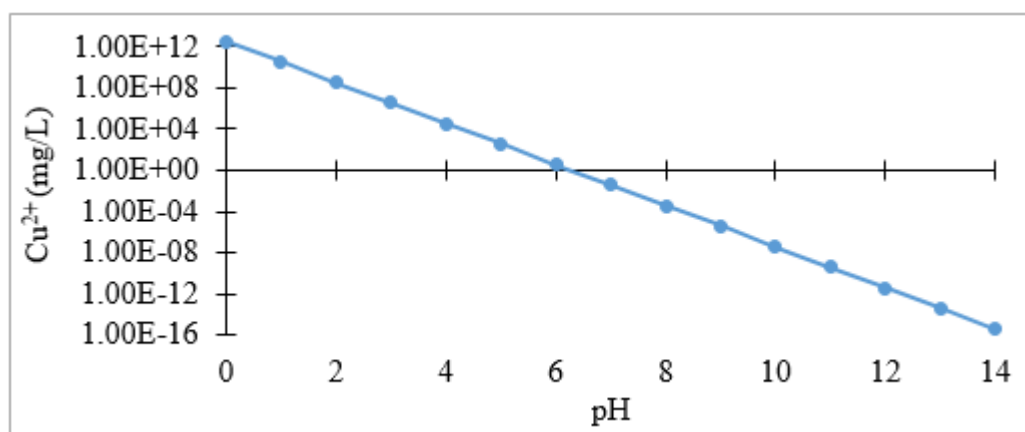
Figure 2-2: Theoretical solubility of Cu^{2+} ions from $CuO_{(s)}$ with pH.

CuO NP surface charge is affected by pH. CuO NPs, like all materials, have a point of zero charge (PZC), which is the pH at which the net surface charge on the particle is zero. The PZC of CuO NPs has been reported as pH 6 (Conway et al. 2015) and pH 10 (Sousa and Teixeira 2013) depending on crystalline structure and surface area. The NPs are expected to have their PZC near pH 10. Below the PZC CuO NPs are positively charged, and above the PZC negatively charged. The charge on the NPs is often measured as the zeta potential, and has great implications for homoaggregation (aggregation of CuO NPs with themselves, Figure 2-3), heteroaggregation (aggregation of CuO NPs with other materials, such as clays, Figure 2-3), and adsorption of materials

to the NP surface (such as ions or dissolved organic matter). A zeta potential on colloids

greater than 20 to 30 mV or less than -20 to -30 mV typically indicates a stable

suspension, while a charge between -20 and 20 mV indicates aggregation is more likely

to occur. When the pH of the solution is near the PZC of the CuO NPs, the zeta potential

is small and aggregation of the CuO NPs increases (Sousa and Teixeira 2013; Heinlaan

et al. 2016) when no other factors are present. Conversely, when the zeta potential is

large (positive or negative), the particles repel each other and aggregation is reduced

(Cornelis et al. 2014). The same principle applies to heteroaggregates and adsorption of

ions to the NP surface: phosphate adsorbs best to positively charged NPs (Conway et al.

2015), while calcium adsorbs to negatively charged NPs.
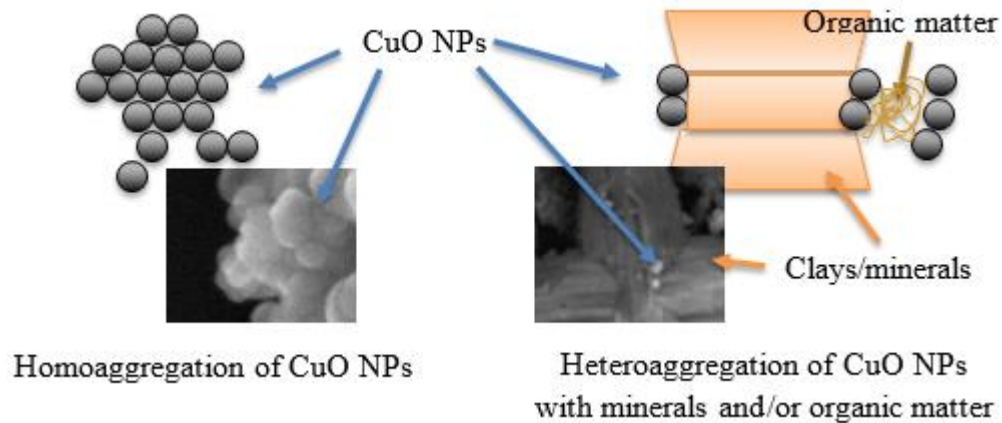
Figure 2-3: Homo- and heteroaggregation of CuO NPs.

pH also affects protonation of organic and inorganic compounds. Most dissolved

natural organic matter (DNOM) becomes partially deprotonated (negatively charged)

around pH 3-4. Negatively charged DNOM adsorbs best to CuO NPs when the NPs are

positively charged. The adsorption of negatively charged humic acids, fulvic acids, or

inorganic anions (such as phosphate) causes the surface charge of NPs to switch from positive to negative (Sousa and Teixeira 2013; Wang et al. 2011); whereas, adsorption of uncharged DNOM (carbohydrates, amino acids) may not be as important (Figure 2-4; Tian et al. 2015). Cornelis et al. (2014) compiled data from several studies and noted that the PZC decreased for a wide variety of NPs after adsorption of organic matter (equivalent to causing the surface charge to become more negative), and was dependent on the concentration of DNOM in solution.
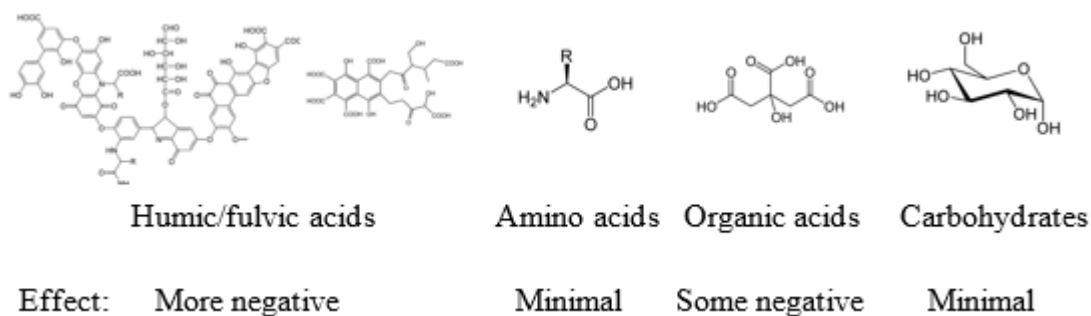
Figure 2-4: Potential effects of coatings on CuO NPs on subsequent charge of the CuO NPs. Adapted from Tian et al. (2015).

Soil ligand type

Soil ligand background

Ligands present in soil may be organic (organic matter) or inorganic (chloride, sulfate, nitrate, carbonate, bicarbonate, phosphate, hydroxide). Inorganic ions typically originate from the dissolution of minerals (such as $CaCO_3$) or the dissolution of gases into solution (CO_2). According to the equilibrium constants of inorganic complexes with Cu^{2+} stored in MINTEQ v3.1, only a $CuHPO_4$ complex is more stable than a Cu-fulvic

acid complex (Gustaffson 2013), so inorganic Cu-complexes are not considered in this review.

Organic ligands originate from soil organic matter or living organisms. Soil organic matter is defined as the fraction of soil which is organic yet non-living, in various states of decomposition, and originating from plants, animals, and microbes. Soil organic matter varies among soils but can be divided into classes loosely based on origin and extent of decomposition. The most basic classes of soil organic matter are non-humic materials (recognizable plant and animal debris which are not highly degraded and are removed from analysis), biochemicals (peptides, proteins, carbohydrates, lipids, low molecular weight organic acids), and humic materials (unidentifiable, highly transformed, darkly colored organic matter) (Swift 1996). Solubilized organic material, DNOM, is generally the more important form of soil organic matter as it relates to CuO NPs (Cornelis et al. 2014). DNOM in this study includes soluble components of soil pore water (root exudates, humic/fulvic acids, proteins, etc.)

Root exudates are defined for the purposes of this study as the biochemicals that a root emits to fulfill specific purposes in the rooting zone. These purposes include chelating metals for graminaceous monocot (Strategy II plants) uptake (phytosiderophores, Figure 2-5), defense against toxic metal levels (low molecular weight organic acids), symbiotic colonization of the root (carbohydrates, amino acids), microbial signaling, or acidification of the root zone. Other chemicals are exuded by roots, such as inorganic K (to balance ion flow into the root), but these chemicals are (generally) not exuded to achieve a purpose outside of the root. Wheat has been

observed to produce significant levels of low molecular weight organic acids (such as acetate, succinate, malate, and isocitrate) (Martineau et al. 2014), carbohydrates, and a phytosiderophore, 2'-deoxymugineic acid (DMA, Figure 2-5), among other components. The composition of the root exudates varies according to the plant; Shukla et al. (2011) compiled a review of approximately 115 organic compounds which have been detected in a variety of root exudates. Synthetic root exudates are frequently used in the literature in lieu of actual root exudates because of the difficulty of generating root exudates and/or defining their composition. Two examples of compositions of synthetic root exudates for generic roots and maize, are given by LeFevre et al. (2013) and Tian et al. (2015) respectively.
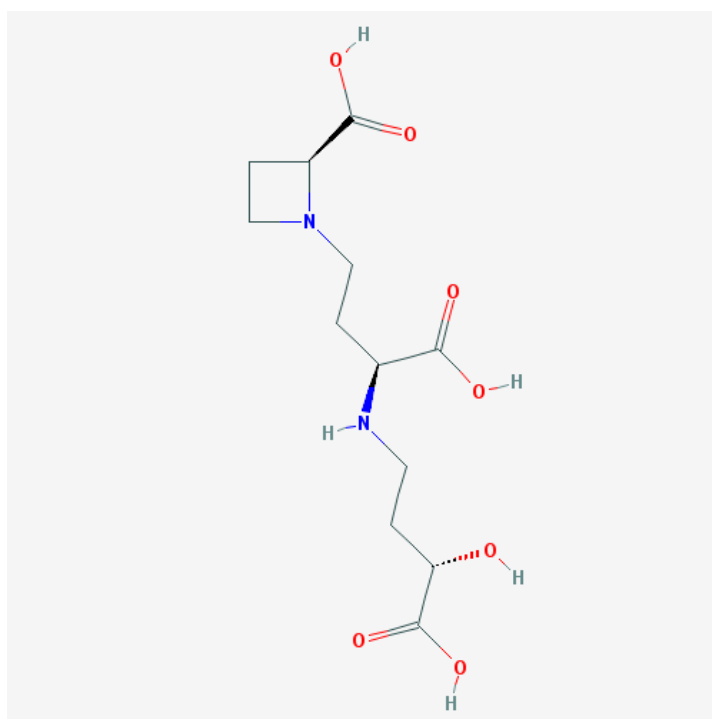
Figure 2-5: Structure of 2'-deoxymugineic acid, a phytosiderophore of wheat and other Strategy-II graminaceous plants.

Bacteria also produce siderophores and other exudates, including LMWOAs. Over 500 siderophores have been identified in bacteria (Ali and Vidhale 2013). Pseudomonads, such as *PcO6*, produce pyoverdines (PVDs) with differences in the amino acid chains (Figure 2-6).
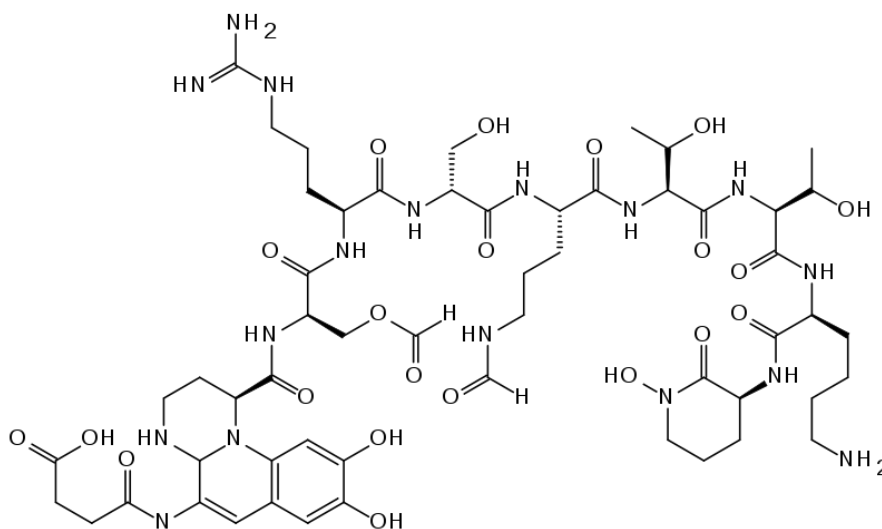
Figure 2-6: Chemical structure of pyoverdine. Differing isolates of Pseudomonads produce differences in the amino acid chain.

Humic materials are organic molecules composed of aromatic groups with carboxyl, carbonyl, hydroxyl, aliphatic, and substituted aromatic groups attached (Figure 2-7). Unlike biochemicals, there is no consistent structure among humic materials. Humic materials are often associated with mineral surfaces or divalent/trivalent cations. They are not very soluble, but at high pH the carboxyl and hydroxyl groups may dissociate and become charged, causing humic materials to become more soluble. Extractions of soil organic matter are typically done in 0.1 M NaOH for this reason. Because of the changes in charge and solubility of humic materials across all pH, humic

substances can be further fractionated into humin (colloidal material insoluble at all pH),

humic acids (soluble only at high pH) and fulvic acids (soluble at all pH) (Swift 1996).

Humic materials can weigh from as little as one kiloDalton (kDa) to more than

1,000 kDa. Fulvic acids range from approximately 1-30 kDa peaking at about 1-5 kDa;

humic acids range from approximately 2-100 kDa peaking at about 2-10 kDa (Beckett et

al. 1987; Perminova et al. 2003). Soil proteins range from 10-200 kDa peaking at about

40 kDa (Schulze 2005). Phytosiderophores range from 0.5 to 1 kDa (Ahmed and

Holmstrom 2014). Relative to fulvic acids, humic acids are larger, have proportionately

more C/N but less O, and are more "lignin-like" (Figure 2-7) (Swift 1996).
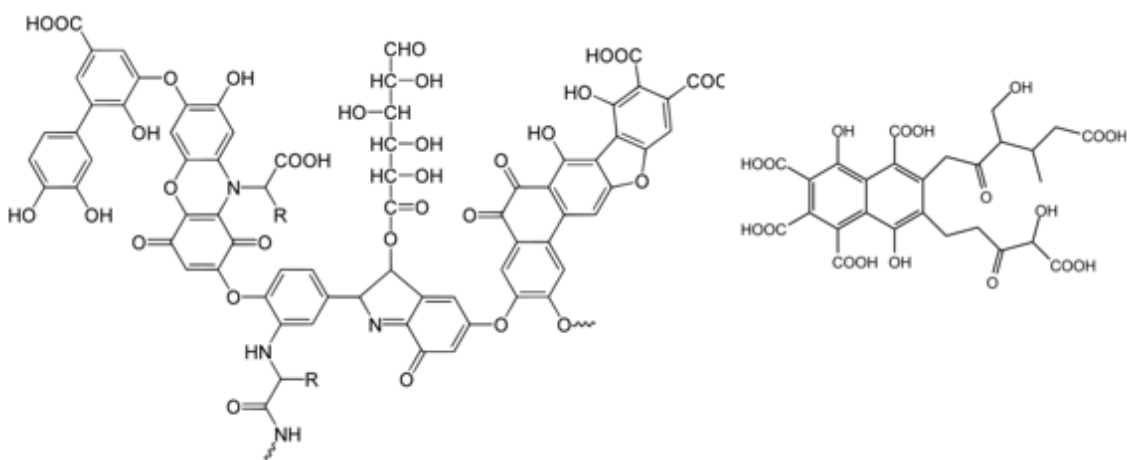
Figure 2-7: Models of a representative humic acid molecule (left) and fulvic acid molecule (right).

Soil ligand effects on CuO NPs

DNOM and inorganic anions may competitively adsorb to NPs. These sorption

processes may enhance or decrease aggregation of CuO NPs affecting dissolution of

CuO NPs, and thus the toxicity of CuO NPs.

Of the several mechanisms that enable DNOM and ions to adsorb to CuO NPs (Figure 2-8; Philippe and Schaumann 2014), electrostatic and ligand exchange reactions dominate over other adsorption reactions on nano-oxides (Yang et al. 2009). Proteins (Miao et al. 2015), fulvic acids (Zhao et al. 2013), humic acids (Yang et al. 2009), and phosphate (Conway et al. 2015) have all been previously detected on the surface of CuO NPs.
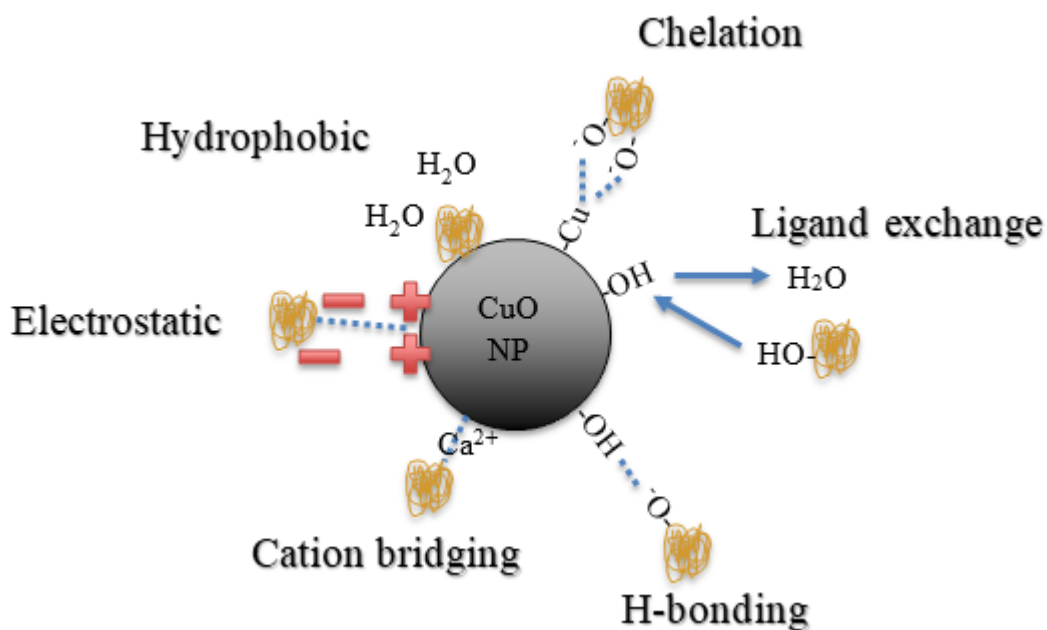
Figure 2-8: Possible interactions between NPs and dissolved organic matter. Adapted from Philippe and Schaumann (2014).

Phosphate competes with DNOM for adsorption and is affected by the same conditions as DNOM (Conway et al. 2015; Hiemstra et al. 2010). Calcium or other positively charged ions may adsorb to negatively-charged NPs, neutralizing their charge (Schwyzer et al. 2012).

DNOM and/or ions may also help solubilize the CuO NPs. Early studies of CuO NP solubility were typically conducted in carefully-defined laboratory-prepared waters or poorly-defined biological growth media. Luria-Bertani (LB) broth, a mixture of yeast extract (undefined organic molecules), tryptone, and salt, dissolved 100% of CuO NPs (150-900 mg/L) after 6 hours (Gunawan et al. 2011). Citric/oxalic acid (1-10 mM) and benzoic acid (1-10 mg/L) increased dissolution of CuO NPs compared with the control with no LMWOA addition from at pH 7.8 and pH 3-11, respectively (Mudunkotuwa et al. 2012; Wang et al. 2016). A series of individual amino acids (11 tested), as well as Roswell Park Memorial Institute medium and Dulbecco's Modified Eagle's medium (two media containing amino acids, salts, glucose, and vitamins) increased dissolution of CuO NPs (Wang et al. 2013). However some of the tested organic components, such as glucose and some buffering agents, have no effect on CuO NP solubility (Wang et al. 2013), likely because they do not form complexes with copper. Extracellular polymeric substances (molecules such as polysaccharides and proteins, detached from the surfaces of cells; EPS) enhanced dissolution of CuO NPs at pH 7-11 but decreased dissolution of CuO NPs at pH 4 (Adeleye et al. 2014) due to coating of the NPs, adsorption of protons by EPS, and adsorption of Cu^{2+} by EPS. Another study utilizing EPS at pH 7 agreed with the results of Adeleye et al. (2014), finding that EPS increased CuO NP solubility (Miao et al. 2015). Components from a root wash of wheat (containing LMWOAs and undefined organic molecules) increased dissolution of CuO NPs over 1 hour (Martineau et al. 2014).

Studies with natural waters showed mixed effects upon the dissolution of CuO NPs, though these studies are not common. Natural organic matter in storm runoff (unidentified molecules) and simulated freshwater (Suwanee River fulvic acid) decreased dissolution of CuO NPs even at pH < 7, while organic matter in wastewater increased dissolution above the two previously mentioned waters even at pH > 7 (Conway et al. 2015). Conway et al. (2015) attributed the reduction of dissolution to coating of the NP surface by DNOM. Another study of CuO NPs in lake waters found that dissolution of CuO NPs was more dependent on pH over ionic strength or DNOM concentration (Odzak et al. 2015). CuO NPs dissolved rapidly in a stream (Kent & Vikesland 2016). A study in a freshwater mesocosm found significant dissolution of CuO NPs at pH 7-9, although ultimately less dissolution than deionized water at pH 5.8 (Vencalek et al. 2016). Thus studies of CuO NPs in natural waters are of paramount importance.

In summary, a broad range of organic components seem to increase the dissolution of CuO NPs when accounting for pH (Adeleye et al. 2014; Gunawan et al. 2011; Martineau et al. 2014; Miao et al. 2015; Mudunkotuwa et al. 2012; Wang et al. 2013), but the organic components and the NP both affect this interaction and some organic molecules may actually decrease solubility, possibly via coating (Adeleye et al. 2014; Conway et al. 2015), or have little effect at all (Odzak et al. 2015).

The biggest disagreements regarding the effect of DNOM on NP dissolution seem to revolve around humic and fulvic acids. Some authors find that these substances increase dissolution of CuO NPs (Adeleye et al. 2014; Peng et al. 2015; Wang et al.

2011), while others find that they or other unidentified organics decrease solubility in CuO NPs (Conway et al. 2015). A similar effect on CuO NP dissolution reported by Conway et al. (2015) was seen in coating by organic matter from soil decreasing dissolution of Ag NPs in a soil solution (Klitzke et al. 2015). Furthermore, in preliminary experiments soil DNOM at high concentrations seemed to inhibit dissolution of CuO NPs, yet increased dissolution of CuO NPs at lower DNOM concentrations (Chapter 4).

As far as aggregation, DNOM coating the surface of NPs usually results in more charged and dispersed NPs (Dimkpa et al. 2011; Cornelis et al. 2014; Philippe and Schaumann 2014; Miao et al. 2016). As an example, humic acid stabilized and prevented aggregation in a suspension of CuO NPs in 0.01 mM NaCl for several hours (Ben-Moshe et al. 2010), presumably because of a large zeta potential.

However, occasionally DNOM promotes more aggregated NPs (Dimkpa et al. 2013a, b; Wang et al. 2016). In one example, 80 mg/L humic acid caused ZnO NPs to aggregate to larger sizes than water alone (Watson et al. 2015). In another, 5 mg/L fulvic acid increased the diameter of aggregates of CuO NPs (Zhao et al. 2013). These examples seem counterintuitive because DNOM could increase the negative charge on the NPs, and charged particles should be more repulsive. The answer may lie in whether the main adsorption mechanism is electrostatic: if there is only enough DNOM present to neutralize the positive charge, then the decreased repulsion can lead to more aggregation (Philippe and Schaumann 2014). Another explanation is the type of DNOM that coats the surface; humic and fulvic acids tend to stabilize NPs, whereas long-chain

DNOM may have bridging-flocculation effect in the presence of multivalent cations, increasing aggregation (Miao et al. 2016, Figure 2-9).
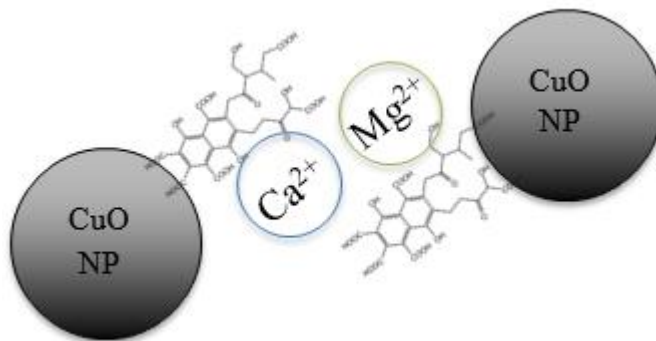
Figure 2-9: Cation-assisted bridging-flocculation behavior between NPs and long-chain DNOM. Adapted from Philippe and Schaumann (2014).

Like DNOM coatings, inorganic coatings also affect aggregation by altering zeta potential (Conway et al. 2015), such as in the case where Dimkpa et al. (2012b) speculated that inorganic oxyanions Si and P may have affected NP aggregation during experiments in sand medium with CuO NPs and planted wheat. If Ca^{2+} ions or other multivalent cations neutralize the negative charge on CuO NPs, aggregation of NPs may increase. In one example, Ca^{2+} promoted aggregation in Ag NPs by reducing the negative surface charge (Calder et al. 2012). Multivalent cations may also increase aggregation through bridging-flocculation (Miao et al. 2016; Figure 2-11), which can bind long-chained DNOM together by connecting two ends of negatively charged DNOM adsorbed to differing NPs. One must be cautious not to interpret coagulated humic or fulvic acids as NPs during analysis, however (Wang et al. 2015). Cation bridging as a means of both bridging-flocculation (Figure 2-9) and DNOM adsorption (Figure 2-8) may be very relevant at pHs seen in calcareous soils.

As far as toxicity, organic components usually alter CuO NPs, protecting organisms from damage – with a few important exceptions. EPS protected *Pseudomonas chlororaphis* O6 from both Cu ions and CuO NPs (Dimkpa et al. 2011). Wheat root exudates protected a root colonizer, *Pseudomonas putida* KT2440 against CuO NPs, but not Cu^{2+} ions; the protective effect originated from coating of the NP surfaces (Martineau et al. 2014). Humic acid protected bacterial and fungal decomposers from CuO NPs (Pradhan et al. 2016) and rice seedlings from CuO NPs by coating NPs and increasing repulsion between the root wall and the NPs (Peng et al. 2015). Natural river waters varying in dissolved organic carbon contents protected two crustaceans against CuO NPs (Blinova et al. 2010). However, certain low molecular weight organic acids may actually increase CuO NP toxicity. For example, citrate increased Cu^{2+} bioavailability to the root colonizer *Pseudomonas putida* (McLean et al. 2013) and benzoic acid increased toxicity of CuO NPs to an alga *Scenedesmus obliquus* (Wang et al. 2016).

Organisms may have different sensitivities to the same organic matter: Zhao et al. (2013) found that a natural pond water and Suwannee River fulvic acid partially protected *Escherichia coli* from CuO NPs. Bulk CuO had no toxic effect, showing that the NP effect was size-specific. However, two years earlier the same group reported that the same fulvic acid and pond water increased damage against an alga, *Microcystis aeruginosa* (Wang et al. 2011).

Soil ligand concentration

The concentration of DNOM or ions matters for adsorption. DNOM concentration affects DNOM adsorption because adsorption is limited if there is not sufficient opportunity for DNOM and CuO NPs to contact. Observations from Chen et al. (2012) with humic acid and TiO_2 NPs agree that increasing DNOM concentration aids DNOM adsorption.

The CuO NPs are saturated with fulvic acid at approximately 40 mg/g DOC/CuO NPs (Sousa and Teixeira 2013). Above the equivalent concentration in aqueous solution, there may little more adsorption of additional DNOM onto CuO NPs.

Ionic strength

Ionic strength affects DNOM/ion adsorption and homo-/hetero-aggregation by compressing the electrostatic double layer around CuO NPs, allowing particles to move closer in suspension. At very low ionic strengths (< about 4 mM), disaggregation of homoaggregated CuO NPs may occur (Conway et al. 2015). The compression of the electrostatic double layer of CuO NPs begins at about 11 mM (Ben-Moshe et al. 2010; Conway et al. 2015) and increases with ionic strength until 150 mM, at which point the apparent compression remains constant (Sousa and Teixeira 2013). The suppression of the electrostatic double layer of CuO NPs allows DNOM/ions more potential to adsorb to the NPs and more aggregation potential (Heinlaan et al. 2016).

In practice, other factors such as pH influence aggregation of NPs, which may partially explain the results of Miao et al. (2016), who saw the same trends (increasing aggregation of CuO NPs with increasing ionic strength) but differing concentrations for

the lower and upper bounds. Aggregation of CuO NPs was not apparent at 5 mM (for Na^+) or 1.5 mM (for Ca^{2+}), increased over the range of 10-50 mM (for Na^+) or 3-15 mM (for Ca^{2+}), and had no further effect above 50 mM (for Na^+) or 3-15 mM (for Ca^{2+}).

Increasing ionic strength also may aid CuO NP dissolution, if the added ligands such as chloride or carbonate can complex copper ions (Adeleye et al. 2014). Complexation with ions may prevent the toxicity and generation of reactive oxygen species often caused by copper ions.

<u>Research Needs</u>

Studies thus far typically used model DNOMs to interact with CuO NPs, such as Suwannee River fulvic acid or commercial humic acids. There is little information available about fulvic and humic acids from soil and their interactions with CuO NPs, including measurements of aggregation, dissolution, and toxicity. Other components of soil, such as divalent cations, may also have appreciable impacts on CuO NP aggregation (cation-bridging or charge neutralization) or dissolution.

Furthermore, the exact roles of various types of DNOM in their interactions with CuO NPs are unknown or seemingly contradictory. Many studies find that DNOM increases or decreases dissolution of CuO NPs, for example. Toxicity and aggregation are other variables which will increase or decrease in the presence of DNOM.

Sources of uncertainty in CuO NP dissolution

Unfortunately, there is doubt surrounding the dissolution of NPs, particularly because separating NPs from the truly dissolved components remains a challenge. Dissolved metal species have been operationally defined as metal species that pass

through a 0.45-micron filter, or later a 0.2-micron filter; however, NPs (diameter < 100 nm) can pass both of these filters, creating a problem of defining what metals are truly dissolved in NP suspensions.

Many different methods of NP separation have been applied to NP dissolution studies. Filtration removes particles from solution (particles > 200 nm in diameter with a 0.2-micron filter (Mudunkotuwa et al. 2012), and particles approximately > 3 nm in diameter with an ultrafilter (Conway et al. 2015)), but may leave smaller, undissolved particles in solution. Centrifugation removes particles as a function of particle diameter, particle density, g-force, time centrifuged, and centrifuge radius, but may only achieve partial removal of very small particles and risks resuspension of the sedimented particles during analysis. An ion-selective electrode will read free Cu^{2+} ions' activity, but will not read free or complexed Cu^+ or complexed Cu^{2+} ions (Son et al. 2015). Other techniques, such as membrane dialysis (Odzak et al. 2014) and diffusive gradients in thin films (Odzak et al. 2015) rely on diffusion driven by concentration gradients into aqueous media or resin, respectively; these techniques are passive and require time and thus can only return time-averaged measurements. Thus using a 0.2-micron filter vs. centrifugation vs. an ultrafilter vs. an ion selective electrode vs. concentration gradient techniques, has the potential to produce significantly different "dissolved" metal results with each method.

Copper redox chemistry

Aqueous copper exists as Cu^+ or Cu^{2+}. Cu^{2+} is the oxidized form and is expected to be the dominant form in oxic waters. In the presence of oxygen, free Cu^+ ions are

generally rapidly oxidized to Cu^{2+} ions. When Cu^+ is oxidized by oxygen, superoxide (O_2^-) followed by hydrogen peroxide (H_2O_2) is formed. Hydrogen peroxide may also oxidize Cu^+. However, Cu^{2+} can be back-reduced to Cu^+ by superoxide. Sunlight may also reduce Cu^{2+}, leading to the detection of Cu^+ in oceans (Moffett and Zika 1983).

pH, chloride, and bicarbonate concentrations affect oxidation rates. Chloride slows oxidation because the copper chloride complexes do not oxidize as quickly. Bicarbonate enhances copper oxidation, possibly because copper carbonates oxidize faster, especially under high pH. pH is the least sensitive variable of the three (Yuan et al. 2012). Amino acids, such as glutathione and cysteine, form very stable complexes with Cu^+, particularly in seawater because of the thiol groups, preventing copper ion oxidation. The thiol groups bind with Cu^+ in a 2:1 ratio (Leal and Van den Berg 1998).

Fulvic acid can reduce Cu^{2+}, even under oxic conditions. Under anoxic conditions (pH 8, 0.7 M NaCl, 2 mM $NaHCO_3$, 0.25-8 mg/L fulvic acid, 0.2-0.4 μM Cu^{2+}), there is an initial phase of rapid reduction followed by a slower, long-term second phase of reduction. In the presence of oxygen, the initial phase of rapid reduction is not altered, but the second phase is altered, especially at a high concentration of fulvic acid (2-8 mg/L fulvic acid) because some Cu^+ is oxidized back to Cu^{2+}. Hydrogen peroxide was detected in oxic samples. Fulvic acid did not affect the oxidation of Cu^+ (Pham et al. 2012).

A significant amount of the dissolved copper from CuO NPs is expected to be present in a reduced form in soil pore waters because of complexation with fulvic acids. This is significant because Strategy I plants (all plants except grasses) uptake copper as

Cu^+, which may have implications for Cu toxicity to plants, while Strategy II plants (grasses, including wheat) employ phytosiderophores to chelate and uptake Cu^{2+} (Marschner and Romheld 1994). Strategy II plants may even take up copper as Cu^+, too. Furthermore, even in aerobic soils, micropores may harbor anaerobic zones where Cu^+ will be the dominant species.

CuO NP phytotoxicity to wheat

CuO NPs have direct, well-measured effects on wheat. Shoot and root lengths are reduced in a dose-dependent manner (0-500 mg/kg CuO NP/sand, Figure 2-10). In one study, shoot length was reduced by 13% by 500 mg/kg CuO NPs and root length was reduced 59% by 500 mg/kg CuO NPs/sand compared to the controls (Dimkpa et al. 2012c). Additionally, lateral roots increased by 42%. In another study under the same conditions, root length was decreased by 64% (Dimkpa et al. 2013a). Similar effects are seen with the addition of Cu ions (Dimkpa et al. 2012c). By the use of x-ray absorption near-edge spectroscopy, CuS was detected in shoots (CuO was also detected, but this was possibly due to external CuO NP contamination) (Dimkpa et al. 2013a; Dimkpa et al. 2012c).

For 14-day-old wheat grown in sand over 10 days with a 1 mM $Ca(NO_3)_2$ background, Cu in shoots increases from ~23 mg/kg Cu/dry shoot (in control samples with 0 mg CuO NPs/kg sand) to ~38 mg/kg Cu/dry shoot with 300 mg/kg CuO NPs/sand (McManus 2016). With increasing Cu dose, K, Ca, Mg, Fe, Ni, and Mn decrease in shoots. In roots, Cu increases from <100 mg/kg Cu/dry root (in 0 mg/kg CuO NPs/sand) to >3500 mg/kg root (in 300 mg/kg CuO NPs/sand), although much of this may be NPs

Figure 2-40: Reduction of root length in wheat by exposure to CuO NPs in sand.

associated with the root surface. K, Ca, Mg, Ni, and Mn also decrease in roots with

increasing CuO NP dose (McManus 2016).

CuO NP fate in soil

Important factors in NP fate in soil include NP surface charge, NP stability, and

soil physical and chemical parameters, which control NP dissolution, transport,

bioavailability, and fate in soil (Dimkpa et al. 2013b; Misra et al. 2012; Servin et al.

2015). Overall, the fate of NPs in soil is not well-studied (Reddy et al. 2016).

Size (bulk or nano) seems to make little difference on the ultimate fate of the

particles (Dimkpa et al. 2013a). This may be because NPs aggregate in soils and planted

environments to a larger extent than in water alone (Dimkpa 2014), which modifies

bioreactivity and transport properties. Agreeing with Dimpka et al. (2013a), Cornelis et

al. (2014) state that the fate of NPs in soil is similar to that of natural colloids as many of

the same processes govern colloids and NPs; these processes include

homoaggregation/heteroaggregation, fragmentation/dissolution, sedimentation, and

transport (Figure 2-11). Transport is not considered here because it is not involved in the

hypotheses of the study, and is expected to be minimal as CuO NPs tend to sorb to soils

(Julich and Gath 2014).
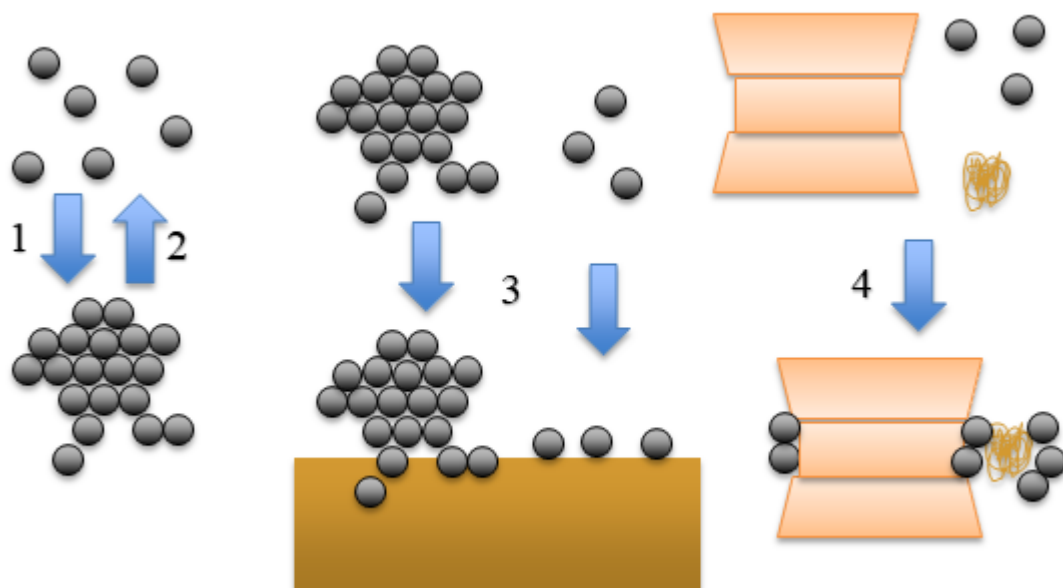
Figure 2-51: Main processes of NPs and colloids in soil. 1) Homoaggregation 2) Fragmentation 3) Sedimentation 4) Heteroaggregation. Transport processes not included in this figure. Adapted from Cornelis et al. (2014).

Components in the soil, such as organic matter, may coat and stabilize NPs

(Dimkpa et al. 2013b), which could be viewed as a form of heteroaggregation. Frenk et

al. (2013) suggested that higher clay and organic matter contents reduce toxicity of CuO

NPs to soil microbial communities, but did not identify if the specific effect was due to

NP coating or heteroaggregation. NPs may also alter levels of soluble metals, although CuO NPs did not do so in a planted bean study (Dimkpa et al. 2015). If NPs increase the pH of the system, then precipitation may remove aqueous copper originating from CuO NPs from the system (Servin et al. 2015). In planted systems, a portion of NPs associate with roots and may be uptaken by plants (Dimkpa et al. 2012c; Zhou et al. 2011).

References

Adeleye, A. S., Conway, J. R., Perez, T., Rutten, P., and Keller, A. A. (2014). "Influence of extracellular polymeric substances on the long-term fate, dissolution, and speciation of copper-based nanoparticles." *Environ. Sci. Technol.*., 48(21), 12561-12568.

Adeleye, A. S., Oranu, E. A., Tao, M., Keller, A. A. (2016). "Release and detection of nanosized copper from a commercial antifouling paint." *Water Res*., 102, 374-382.

Ahmed, E., and Holmstrom, S. J. M. (2014). "Siderophores in environmental research: Roles and applications." *Microb. Biotechnol.*, 7(3), 196-208.

Ali, S. S., and Vidhale, N. N. (2013). "Bacterial siderophore and their application: A review." *Int. J. Curr. Microbiol. Appl. Sci.*, 2(12), 303-312.

Beckett, R., Jue, Z., and Giddings, J. C. (1987). "Determination of molecular-weight distributions of fulvic and humic acids using flow field-flow fractionation." *Environ. Sci. Technol.*, 21(3), 289-295.

Ben-Moshe, T., Dror, I., and Berkowitz, B. (2010). "Transport of metal oxide nanoparticles in saturated porous media." *Chemosphere*, 81(3), 387-393.

Blinova, I., Ivask, A., Heinlaan, M., Mortimer, M., and Kahru, A. (2010). "Ecotoxicity of nanoparticles of CuO and ZnO in natural water." *Environ. Pollut.*, 158(1), 41-47.

Calder, A. J., Dimkpa, C. O., McLean, J. E., Britt, D. W., Johnson, W., and Anderson, A. J. (2012). "Soil components mitigate the antimicrobial effects of silver nanoparticles towards a beneficial soil bacterium, *Pseudomonas chlororaphis* O6." *Sci. Total Environ.*, 429, 215-222.

Chen, G. X., Liu, X. Y., and Su, C. M. (2012). "Distinct effects of humic acid on transport and retention of TiO_2 rutile nanoparticles in saturated sand columns." *Environ. Sci. Technol.*, 46(13), 7142-7150.

Conway, J. R., Adeleye, A. S., Gardea-Torresdey, J., and Keller, A. A. (2015). "Aggregation, dissolution, and transformation of copper nanoparticles in natural waters." *Environ. Sci. Technol.*, 49(5), 2749-2756.

Cornelis, G., Hund-Rinke, K., Kuhlbusch, T., Van den Brink, N., and Nickel, C. (2014). "Fate and bioavailability of engineered nanoparticles in soils: A review." *Crit. Rev. Environ. Sci. Technol.*, 44(24), 2720-2764.

David, C. A., Galceran, J., Rey-Castro, C., Puy, J., Companys, E., Salvador, J., Monne, J., Wallace, R., and Vakourov, A. (2012). "Dissolution kinetics and solubility of ZnO nanoparticles followed by AGNES." *J. Phys. Chem. C*, 116(21), 11758-11767.

Delay, M., and Frimmel, F. H. (2012). "Nanoparticles in aquatic systems." *Anal. Bioanal. Chem.*, 402(2), 583-592.

Dimkpa, C. O. (2014). "Can nanotechnology deliver the promised benefits without negatively impacting soil microbial life?" *J. Basic Microbiol.*, 54(9), 889-904.

Dimkpa, C. O., Calder, A., Britt, D. W., McLean, J. E., and Anderson, A. J. (2011). "Responses of a soil bacterium, *Pseudomonas chlororaphis* O6 to commercial metal oxide nanoparticles compared with responses to metal ions." *Environ. Pollut.*, 159(7), 1749-1756.

Dimkpa, C. O., Latta, D. E., McLean, J. E., Britt, D. W., Boyanov, M. I., and Anderson, A. J. (2013a). "Fate of CuO and ZnO nano- and microparticles in the plant environment." *Environ. Sci. Technol.*, 47(9), 4734-4742.

Dimkpa, C. O., Mclean, J. E., Britt, D. W., and Anderson, A. J. (2012a). "CuO and ZnO nanoparticles differently affect the secretion of fluorescent siderophores in the beneficial root colonizer, *Pseudomonas chlororaphis* O6." *Nanotoxicology*, 6(6), 635-642.

Dimkpa, C. O., McLean, J. E., Britt, D. W., and Anderson, A. J. (2013b). "Antifungal activity of ZnO nanoparticles and their interactive effect with a biocontrol bacterium on growth antagonism of the plant pathogen *Fusarium graminearum*." *BioMetals*, 26(6), 913-924.

Dimkpa, C. O., McLean, J. E., Britt, D. W., and Anderson, A. J. (2015). "Nano-CuO and interaction with nano-ZnO or soil bacterium provide evidence for the interference of nanoparticles in metal nutrition of plants." *Ecotoxicology*, 24(1), 119-129.

Dimkpa, C. O., McLean, J. E., Britt, D. W., Johnson, W. P., Arey, B., Lea, A. S., and Anderson, A. J. (2012b). "Nanospecific inhibition of pyoverdine siderophore production in *Pseudomonas chlororaphis* O6 by CuO nanoparticles." *Chem. Res. Toxicol.*, 25(5), 1066-1074.

Dimkpa, C. O., McLean, J. E., Latta, D. E., Manangon, E., Britt, D. W., Johnson, W. P., Boyanov, M. I., and Anderson, A. J. (2012c). "CuO and ZnO nanoparticles: Phytotoxicity, metal speciation, and induction of oxidative stress in sand-grown wheat." *J. Nanopart. Res.*, 14(9).

Dimkpa, C. O., Zeng, J., McLean, J. E., Britt, D. W., Zhan, J. X., and Anderson, A. J. (2012d). "Production of indole-3-acetic acid via the indole-3-acetamide pathway in the plant-beneficial bacterium *Pseudomonas chlororaphis* O6 is inhibited by ZnO nanoparticles but enhanced by CuO nanoparticles." *Appl. Environ. Microbiol.*, 78(5), 1404-1410.

Frenk, S., Ben-Moshe, T., Dror, I., Berkowitz, B., and Minz, D. (2013). "Effect of metal oxide nanoparticles on microbial community structure and function in two different soil types." *PLoS One*, 8(12).

Gunawan, C., Teoh, W. Y., Marquis, C. P., and Amal, R. (2011). "Cytotoxic origin of copper(II) oxide nanoparticles: Comparative studies with micron-sized particles, leachate, and metal salts." *ACS Nano*, 5(9), 7214-7225.

Gustaffson, J. P. (2013). "Visual MINTEQ."

Heinlaan, M., Muna, M., Knöbel, M., Kistler, D., Odzak, N., Kühnel, D., Müller, J., Gupta, G. S., Kumar, A., Shanker, R., and Sigg, L. (2016). "Natural water as the test medium for Ag and CuO nanoparticle hazard evaluation: An interlaboratory case study." *Environ. Pollut.*, 216, 689-699.

Hiemstra, T., Antelo, J., van Rotterdam, A. M. D., and van Riemsdijk, W. H. (2010). "Nanoparticles in natural systems II: The natural oxide fraction at interaction with natural organic matter and phosphate." *Geochim. Cosmochim. Acta*, 74(1), 59-69.

Julich, D., and Gath, S. (2014). "Sorption behavior of copper nanoparticles in soils compared to copper ions." *Geoderma*, 235, 127-132.

Keller, A. A., McFerran, S., Lazareva, A., and Suh, S. (2013). "Global life cycle releases of engineered nanomaterials." *J. Nanopart. Res.*, 15(6).

Kent, R. D. and Vikesland, P. J. (2016). "Dissolution and persistence of copper-based nanomaterials in undersaturated solutions with respect to cupric solid phases." *Environ. Sci. Technol.*, 50, 6772-6781.

Klitzke, S., Metreveli, G., Peters, A., Schaumann, G. E., and Lang, F. (2015). "The fate of silver nanoparticles in soil solution - sorption of solutes and aggregation." *Sci. Total Environ.*, 535, 54-60.

Leal, M. F. C., and Van den Berg, C. M. G. (1998). "Evidence for strong copper(I) complexation by organic ligands in seawater." *Aquat. Geochem.*, 4(1), 49-75.

LeFevre, G. H., Hozalski, R. M., and Novak, P. J. (2013). "Root exudate enhanced contaminant desorption: An abiotic contribution to the rhizosphere effect." *Environ. Sci. Technol.*, 47(20), 11545-11553.

Lindsay, W. L. (1979). *Chemical Equilibria in Soils*. John Wiley & Sons, New York.

Luo, X. S., Li, L. Z., and Zhou, D. M. (2008). "Effect of cations on copper toxicity to wheat root: Implications for the biotic ligand model." *Chemosphere*, 73(3), 401-406.

Marschner, H., and Romheld, V. (1994). "Strategies of plants for acquisition of iron." *Plant Soil*, 165(2), 261-274.

Martineau, N., McLean, J. E., Dimkpa, C. O., Britt, D. W., and Anderson, A. J. (2014). "Components from wheat roots modify the bioactivity of ZnO and CuO nanoparticles in a soil bacterium." *Environ. Pollut.*, 187, 65-72.

McLean, J. E., Pabst, M. W., Miller, C. D., Dimkpa, C. O., and Anderson, A. J. (2013). "Effect of complexing ligands on the surface adsorption, internalization, and bioresponse of copper and cadmium in a soil bacterium, *Pseudomonas putida*." *Chemosphere*, 91(3), 374-382.

McManus, P. (2016). "Rhizosphere interactions between copper oxide nanoparticles and wheat root exudates in a sand matrix: Influences on bioavailability and uptake," thesis, Utah State University, Logan.

Miao, L. Z., Wang, C., Hou, J., Wang, P. F., Ao, Y. H., Li, Y., Lv, B. W., Yang, Y. Y., You, G. X., and Xu, Y. (2016). "Effect of alginate on the aggregation kinetics of copper oxide nanoparticles (CuO NPs): Bridging interaction and hetero-aggregation induced by Ca^{2+}." *Environ. Sci. Pollut. Res.*, 23(12), 11611-11619.

Miao, L. Z., Wang, C., Hou, J., Wang, P. F., Ao, Y. H., Li, Y., Lv, B. W., Yang, Y. Y., You, G. X., and Xu, Y. (2015). "Enhanced stability and dissolution of CuO nanoparticles by extracellular polymeric substances in aqueous environment." *J. Nanopart. Res.*, 17(10).

Misra, S. K., Dybowska, A., Berhanu, D., Luoma, S. N., and Valsami-Jones, E. (2012). "The complexity of nanoparticle dissolution and its importance in nanotoxicological studies." *Sci. Total Environ.*, 438, 225-232.

Moffett, J. W., and Zika, R. G. (1983). "Oxidation-kinetics of Cu(I) in seawater - implications for its existence in the marine-environment." *Mar. Chem.*, 13(3), 239-251.

Mudunkotuwa, I. A., Pettibone, J. M., and Grassian, V. H. (2012). "Environmental implications of nanoparticle aging in the processing and fate of copper-based nanomaterials." *Environ. Sci. Technol.*, 46(13), 7001-7010.

Odzak, N., Kistler, D., Behra, R., and Sigg, L. (2014). "Dissolution of metal and metal oxide nanoparticles in aqueous media." *Environ. Pollut.*, 191, 132-138.

Odzak, N., Kistler, D., Behra, R., and Sigg, L. (2015). "Dissolution of metal and metal oxide nanoparticles under natural freshwater conditions." *Environ. Chem.*, 12(2), 138-148.

Peng, C., Zhang, H., Fang, H. X., Xu, C., Huang, H. M., Wang, Y., Sun, L. J., Yuan, X. F., Chen, Y. X., and Shi, J. Y. (2015). "Natural organic matter-induced alleviation of the phytotoxicity to rice (*Oryza Sativa* L.) caused by copper oxide nanoparticles." *Environ. Toxicol. Chem.*, 34(9), 1996-2003.

Perminova, I. V., Frimmel, F. H., Kudryavtsev, A. V., Kulikova, N. A., Abbt-Braun, G., Hesse, S., and Petrosyan, V. S. (2003). "Molecular weight characteristics of humic substances from different environments as determined by size exclusion chromatography and their statistical evaluation." *Environ. Sci. Technol.*, 37(11), 2477-2485.

Pham, A. N., Rose, A. L., and Waite, T. D. (2012). "Kinetics of Cu(II) reduction by natural organic matter." *J. Phys. Chem. A*, 116(25), 6590-6599.

Philippe, A., and Schaumann, G. E. (2014). "Interactions of dissolved organic matter with natural and engineered inorganic colloids: A review." *Enviro. Sci. Technol.*, 48(16), 8946-8962.

Pradhan, A., Geraldes, P., Seena, S., Pascoal, C., and Cássio, F. (2016). "Humic acid can mitigate the toxicity of small copper oxide nanoparticles to microbial decomposers and leaf decomposition in streams." *Freshwater Biol.*, 61, 2197-2210.

Reddy, P. V. L., Hernandez-Viezcas, J. A., Peralta-Videa, J. R., Gardea-Torresdey, J. L. (2016). "Lessons learned: Are engineered nanomaterials toxic to terrestrial plants?" *Sci. Total Environ.*, 568, 470-479.

Schulze, W. X. (2005). "Protein analysis in dissolved organic matter: What proteins from organic debris, soil leachate and surface water can tell us - a perspective." *Biogeosciences*, 2(1), 75-86.

Schwyzer, I., Kaegi, R., Sigg, L., Smajda, R., Magrez, A., and Nowack, B. (2012). "Long-term colloidal stability of 10 carbon nanotube types in the absence/presence of humic acid and calcium." *Environ. Pollut.*, 169, 64-73.

Servin, A., Elmer, W., Mukherjee, A., De La Torre-Roche, R., Hamdi, H., White, J. C., Bindraban, P., and Dimkpa, C. (2015). "A review of the use of engineered nanomaterials to suppress plant disease and enhance crop yield." *J. Nanopart. Res.*, 17(2).

Shukla, K. P., Sharma, S., Singh, N. K., Singh, V., Tiwari, K., and Singh, S. (2011). "Nature and role of root exudates: Efficacy in bioremediation." *Afri. J. Biotechnol.*, 10(48), 9717-9724.

Son, J., Vavra, J., and Forbes, V. E. (2015). "Effects of water quality parameters on agglomeration and dissolution of copper oxide nanoparticles (CuO-NPs) using a central composite circumscribed design." *Sci. Total Environ.*, 521, 183-190.

Sousa, V. S., and Teixeira, M. R. (2013). "Aggregation kinetics and surface charge of CuO nanoparticles: The influence of pH, ionic strength and humic acids." *Environ. Chem.*, 10(4), 313-322.

Suppan, S. (2013). "Nanomaterials in soil." Institute for Agriculture and Trade Policy, Minneapolis, MN.

Swift, R. S. (1996). "Organic matter characterization." *Methods of Soil Analysis: Part 3-Chemical Methods*, edited by D. L. Sparks, Soil Science Society of America, Inc. & American Society of Agronomy, Inc., Madison, WI, 1011-1069.

Thwala, M., Klaine, S. J., and Musee, N. (2016). "Interactions of metal-based engineered nanoparticles with aquatic higher plants: A review of the state of current knowledge." *Environ. Toxicol. Chem.*, 35(7), 1677-1694.

Tian, Y., Liu, C. H., Smucker, A. J. M., Li, H., and Zhang, W. (2015). "Plant root exudates decrease mobility of smectite colloids in porous media in contrast to humic acid." *Soil Sci. Soc. Am. J.*, 79(2), 467-475.

Vencalek, B. E., Laughton, S. N., Spielman-Sun, E., Rodrigues, S. M., Unrine, J. M., Lowry, G. V., and Gregory, K. B. (2016) "*In situ* measurement of CuO and $Cu(OH)_2$ nanoparticle dissolution rates in quiescent freshwater mesocosms." *Environ. Sci. Technol. Lett.*, 3, 375-380.

Wang, L. F., Habibul, N., He, D. Q., Li, W. W., Zhang, X., Jiang, H., and Yu, H. Q. (2015). "Copper release from copper nanoparticles in the presence of natural organic matter." *Water Res.*, 68, 12-23.

Wang, Z., Fang, H., and Wang, S. (2016). "Benzoic acid interactions affect aquatic properties and toxicity of copper oxide nanoparticles." *Bull. Environ. Contam. Toxicol.*, 97, 159-165.

Wang, Z. Y., Li, J., Zhao, J., and Xing, B. S. (2011). "Toxicity and internalization of CuO nanoparticles to prokaryotic alga *Microcystis aeruginosa* as affected by dissolved organic matter." *Environ. Sci. Technol.*, 45(14), 6032-6040.

Wang, Z. Y., Von Dem Bussche, A., Kabadi, P. K., Kane, A. B., and Hurt, R. H. (2013). "Biological and environmental transformations of copper-based nanomaterials." *ACS Nano*, 7(10), 8715-8727.

Watson, J. L., Fang, T., Dimkpa, C. O., Britt, D. W., Mclean, J. E., Jacobson, A., and Anderson, A. J. (2015). "The phytotoxicity of ZnO nanoparticles on wheat varies with soil properties." *BioMetals*, 28(1), 101-112.

Westerhoff, P., Lee, S., Yang, Y., Gordon, G. W., Hristovski, K., Halden, R. U., and Herckes, P. (2015). "Characterization, recovery opportunities, and valuation of metals in municipal sludges from US wastewater treatment plants nationwide." *Environ. Sci. Technol.*, 49(16), 9479-9488.

Yang, K., Lin, D. H., and Xing, B. S. (2009). "Interactions of humic acid with nanosized inorganic oxides." *Langmuir*, 25(6), 3571-3576.

Yuan, X., Pham, A. N., Xing, G. W., Rose, A. L., and Waite, T. D. (2012). "Effects of pH, chloride, and bicarbonate on Cu(I) oxidation kinetics at circumneutral pH." *Environ. Sci. Technol.*, 46(3), 1527-1535.

Zhao, J., Wang, Z. Y., Dai, Y. H., and Xing, B. S. (2013). "Mitigation of CuO nanoparticle-induced bacterial membrane damage by dissolved organic matter." *Water Res.*, 47(12), 4169-4178.

Zhou, D. M., Jin, S. Y., Li, L. Z., Wang, Y., and Weng, N. Y. (2011). "Quantifying the adsorption and uptake of CuO nanoparticles by wheat root based on chemical extractions." *J. Environ. Sci.*, 23(11), 1852-1857.

CHAPTER 3

HYPOTHESES AND OBJECTIVES

Null hypothesis 1: Soil pore waters (SPWs) from agricultural soils differing in concentration of dissolved natural organic matter, or SPW components alkalinity/fulvic acid/phosphate, do not affect CuO NP solubility or surface chemistry.

Objective 1.1: Measure dissolution and surface chemistry of CuO NPs with time for 10 days in characterized SPWs.

Approach: Cations, low molecular weight organic acids (LMWOAs), orthophosphate, chloride, sulfate, nitrate, alkalinity, dissolved organic carbon, humic acids, and fulvic acids were characterized in five soil pore waters to geochemically model theoretical CuO NP dissolution in the soil pore waters. All SPWs were dosed with 12.5 mg/L CuO NPs (10 mg/L Cu) at a starting pH of 7.5. The samples were shaken over 10 days and sub-sampled over time for pH, dissolved Cu after centrifugation (removing particles > 10 nm) or ultrafiltration (removing particles > 1 nm), dissolved Cu speciation (free Cu^{2+} ions), and CuO NP surface alterations (organic coatings).

Objective 1.2: Measure dissolution and surface chemistry of CuO NPs with time for 10 days in 3.34 mM $Ca(NO_3)_2$ with varying fulvic acid, phosphate, and alkalinity concentrations.

Approach: 3.34 mM $Ca(NO_3)_2$ solutions containing, separately: fulvic acid, phosphate, or alkalinity were generated. All solutions were dosed with 12.5 mg/L CuO NPs (10 mg/L Cu) and processed and analyzed as described for Objective 1.1.

Null hypothesis 2: SPWs do not mitigate CuO NP uptake and toxicity to wheat grown in a sand matrix.

Objective 2: Determine the influence of SPWs on CuO NPs' uptake, solubility, and form in sterile, planted wheat systems dosed with 100 mg/kg Cu/sand from CuO NPs.

Approach: Wheat seedlings were grown in sterile sand watered with one of three previously characterized, filter-sterilized SPWs or a filter-sterilized 3.34 mM $Ca(NO_3)_2$ solution as control. After 10 days' growth, the sand pore water was analyzed for pH, cations, anions and LMWOAs, dissolved Cu after centrifugation (removing particles >10 nm) or ultrafiltration (removing particles >1 nm), and dissolved Cu speciation (Cu complexes and free Cu^{2+} ions). Root and shoot length and metal content were also measured after 10 days' growth.

Null hypothesis 3: A root-colonizing bacterium, *Pseudomonas chlororaphis* O6, does not mitigate CuO NP uptake and toxicity to wheat grown in a sand matrix.

Objective 3: Determine the influence of root-colonizing bacterium, *Pseudomonas chlororaphis* O6, on CuO NPs' solubility, form, and uptake in planted wheat systems dosed with 100 mg/kg Cu/sand from CuO NPs.

Approach: Wheat seedlings were grown as described under objective 2.1 in the presence of a root-colonizing soil bacterium, *Pseudomonas chlororaphis* O6. Plants were grown, harvested, and analyzed as described in Objective 2.1.

CHAPTER 4

SOLUBILITY OF COPPER OXIDE NANOPARTICLES IN CALCAREOUS SOIL

PORE WATERS VARIES WITH ALKALINITY AND DISSOLVED NATURAL

ORGANIC MATTER

Abstract

CuO nanoparticles (NPs) have the potential to contact agricultural soils through byproduct of biosolids or wastewater reuse, or applications of fungicides or fertilizers to or over soil. As soluble soil components may modify CuO NP behavior, the solubility and surface transformations of CuO NPs were examined in batch dissolution studies with soil pore waters (SPWs) extracted from semi-arid agricultural calcareous soils differing in crop management and 3.34 mM $Ca(NO_3)_2$ with defined concentrations of fulvic acid, alkalinity, and phosphate. SPW and $Ca(NO_3)_2$ batches amended with 10 mg/L Cu from CuO NPs were shaken and monitored over 10 days for pH and dissolved copper after separation of the aqueous phase from the NPs. Ultrafiltration and centrifugation were compared for NP removal efficiency. Fulvic acid, alkalinity, and all SPWs increased Cu solubility compared to the control (3.34 mM $Ca(NO_3)_2$). However, geochemical models of the SPWs predicted up to an order of magnitude more dissolved copper at equilibrium than was observed. Dissolved natural organic matter (DNOM) complexed dissolved copper when SPWs were diluted to <30 mg/L C, but suppressed CuO NP solubility at concentrations >30 mg/L C. The mechanism of suppression was hypothesized to be NP coatings. Ultrafiltration was

determined to be an appropriate NP separation method only in solutions lacking DNOM > 3 kiloDaltons (kDa), as ultrafilters removed DNOM > 3 kDa and a portion of the dissolved copper complexes. Centrifugation therefore was the most appropriate NP separation method for solutions with DNOM > 3 kDa.

1. Introduction

Agricultural soils may be contaminated by nanoparticles (NPs) by intentional or unintentional means. NPs are particles less than 100 nm in at least one dimension and are being increasingly incorporated into consumer products for their unique properties attributable to their nano-size. Copper oxide (CuO) NPs have strong potential for use near soils when formulated into agricultural products such as fungicides, fertilizers, or drought treatments.[1-3] Cu may be needed as a micronutrient fertilizer to strengthen crops against disease, and is an ingredient in some patented nano-fertilizers.[1] Accidental exposure of CuO NPs to agricultural or non-agricultural soils may occur through land application of wastewater effluent and biosolids bearing CuO NPs; as an example, CuO NPs concentrated into biosolids in an anaerobic wastewater treatment reactor, but an appreciable portion (20-32%) remained in the effluent.[4] An estimated 36 metric tons (18% of global flow) of industrial Cu-containing NPs were released in soils in 2010 as an end of life fate, primarily from paints and coatings after passing through a wastewater treatment plant.[5]

CuO NPs in soils may be toxic to soil organisms at least partially through ion release. CuO NPs show toxicity to soil microbes and microbial communities,[6-11] inhibit seed germination,[12] and are toxic to common crops.[6,13-14] The toxicity of CuO NPs is not always

replicated through equivalent doses of soluble Cu ions. Measurement of CuO NP solubility is thus essential when considering soil contamination and toxicity to soil organisms.

The small size of NPs presents challenges when measuring solubility of the NPs. The operational definition of dissolved metals is those that pass through a 0.45-micron filter.[15] Individual NPs would pass a 0.45-micron filter, or even the commonly used 0.2-micron filter, yet are not dissolved. Thus, techniques for measuring CuO NP solubility must be utilized that remove the solid phase nano- and micro-particle fractions (referred to as $Cu_{(s)}$) from the dissolved fraction (referred to as $Cu_{(aq)}$). Two NP removal techniques (centrifugation, and ultrafiltration with molecular weight cutoff of 3 kDa) were selected and compared for use to achieve this resolution.

NP dissolution depends on physical properties of the NPs (such as size, aggregation), characteristics of the solution (such as pH, ligand availability) and surface chemistry (such as capping agents or coatings).[16] Prior studies on CuO NP solubility typically use laboratory-prepared solutions or biological media with specified composition. These studies confirm increasing dissolution of CuO NPs with decreasing solution pH[17] and through Cu ion complexation with organic ligands such as many amino acids,[17-18] low molecular weight organic acids (LMWOAs),[19] and humic[20] and fulvic[21] acids (HA and FA), common components of the dissolved natural organic matter (DNOM) in soils (supporting information Table A-1). DNOM may coat CuO NPs, as has been seen for HA[20] and FA.[22] DNOM coatings on CuO NPs reduced solubility in some studies,[23] yet did not inhibit solubility in other studies.[20] Inorganic anions, such as chloride[24] and carbonate,[25] could also increase CuO NP solubility as they also complex Cu. Phosphate alters CuO NP

surface chemistry,[23] which could influence solubility. Consequently, studies on CuO NPs in soils need careful consideration of pH, DNOM, alkalinity, and phosphate. These challenges are addressed by 1) measurement of dissolved Cu as influenced by pH, HA/FA, LMWOAs, phosphate, and alkalinity in soil pore waters (SPWs), and 2) by sensitivity analyses in geochemical equilibrium models.

The objectives of this study were to investigate how soil pore waters (SPWs, waters extracted from saturated soils),[26] DNOM, alkalinity, and phosphate concentrations affected dissolution of CuO NPs. Soils with similar properties (soil series, pH, texture) but varied cultivation practices (i.e., organic matter or fertilizer additions) were collected for extraction of SPWs. Batch CuO NP solubility experiments in SPWs and laboratory waters were shaken for ten days. At various time points, the solution chemistry of the suspensions (pH, electrical conductivity, cations and trace metals, anions) was characterized to investigate CuO NP dissolution. Particulates from suspension were also collected to image with scanning electron microscopy (SEM), energy dispersive X-ray spectroscopy (EDS), and Fourier transform infrared spectroscopy (FTIR) to investigate NP transformations. The results showed that while DNOM in SPWs complexed Cu ions and increased CuO NP dissolution, DNOM aggregated NPs and was associated with the NP surfaces. Only concentrations of DNOM less than about 30 mg/L C complexed Cu ions to the full potential of modeled FA and HA.

2. Materials and Methods

2.1 Chemical sources and treatment of supplies

The CuO nanopowder (<50 nm; Sigma-Aldrich) used in this study was characterized by X-ray diffraction (XRD, Panalytical X'Pert Pro), FTIR (Nicolet 6700), inductively coupled plasma mass spectrometry (ICP-MS, Agilent 7700x, USEPA Method 6020), and SEM/EDS (FEI Quanta FEG 650/Oxford, X-Max detector).

Amicon-ultra centrifugal ultrafilters (3 kDa, Millipore) with estimated pore size 1.3 nm[27] were employed to separate CuO NPs from suspension. The filters were rinsed three times with DI water immediately prior to use to eliminate organic carbon contamination in the filtrates. The ultrafilters permitted a 93±2.3% and 92±1.6% recovery of Cu ions when tested with 0.5 and 5 mg/L Cu^{2+}, respectively.

2.2 Soils and pore water

Five soils were collected from agricultural and unaltered sites in Cache County, UT, USA (Millville series, coarse-silty, carbonatic, mesic *Typic Haploxerolls*) and Weber County, UT, USA (Warm Springs series, fine-loamy, mixed, active, mesic *Oxyaquic Calcixeroll*). The Millville soils were silty loams with pH 7.7-7.8, from an organic farm, a commercial wheat farm, a grassland field, and a community garden, and were named OrgM, AgrM, IDM, and GM (name origins shown in Table A-2). The differing cultivations changed the organic matter (5.6, 3.0, 3.1, and 4.1% organic matter), phosphorus (62.1, 10.1, 12.6, and 19.3 mg/kg P/soil), and alkalinity contents (14.6, 14.1, 4.3, and 16.1% $CaCO_3$) for the OrgM, AgrM, IDM, and GM soils, respectively (Table A-2). The Warm Springs soil was a sandy loam with pH 7.3 from a home garden and had a very high organic

matter (8.7% organic matter) and phosphorus (324 mg/kg P/soil) content with a lower alkalinity content (6.2% $CaCO_3$) (Table A-2). Soils were collected from the upper 10 cm, air-dried, sieved through a 2-mm screen, and stored covered at room temperature (~20° C) until use (less than one month).

SPW was generated by creating a saturation paste with the soil and deionized (18.2 MΩ) water,[26] equilibrating for 18 hours, and centrifuging at 3,000 x g for 25 minutes with a swinging bucket rotor (Beckman J2-21, rotor JS 7.5). The supernatant was removed and vacuum-filtered twice through a 0.2-micron nylon membrane filter to filter-sterilize the solutions. Each SPW was analyzed by standard methods[15] for pH (Accumet Excel XL25, Fisher Scientific), electrical conductivity (Accumet model 30 conductivity meter), and DNOM via dissolved organic carbon (DOC) by combustion with infrared detection (Apollo 9000, Teledyne Tekmar). SPW was also analyzed for major anions and low molecular weight organic acids by ion chromatography (Dionex ICS-3000, Dionex method 123), major cations and trace metals by ICP-MS (Agilent 7700x, USEPA Method 6020), free Cu^{2+} ion activity by ion selective electrode (Orion, Rachou method)[28], and HA and FA by acidification, sorption on XAD-8 resin, desorption with 0.1 M NaOH (Supelco method),[29] and analysis for HA and FA as DOC by standard methods.[15]

Visual MINTEQ 3.1[30] was used to predict the saturation level of dissolved Cu from CuO NPs, as well as to perform sensitivity analyses of CuO NP dissolution by altering various SPW characteristics in the geochemical model.

2.3 Batch CuO NP dissolution studies

Batch CuO NP dissolution studies were performed in 100 mL of solution at a dose of 12.5 mg/L CuO NPs (10 mg/L Cu) in 250 mL glass Erlenmeyer flasks. The concentration of CuO NPs was chosen to saturate the SPWs with Cu (geochemical models predicted the highest concentration of Cu in any SPW was ~5 mg/L Cu). All glassware contacting solutions was acid-rinsed by 50% nitric acid and then deionized water to eliminate metal contamination and autoclaved prior to use. $Ca(NO_3)_2$ solutions were autoclaved and SPWs were filter-sterilized with a 0.2-micron filter. Suspension pH was adjusted to 7.5 using CO_2 gas or minimal $NaHCO_3$ prior to addition of NPs.

The treatments were the five SPWs, one control, and three control solutions with added components. The control was sterile 3.34 mM $Ca(NO_3)_2$ (henceforth named "control"), because high concentrations of both calcium and nitrate were typically found in the SPWs. The ionic strength of the control (10 mM) was the approximate median of the SPWs. The added components were alkalinity (750 mg/L CaCO3 as $NaHCO_3$), FA (20 mg/L C as Suwannee River FA), or phosphate (5 mg /L PO_4-P). The FA was tested using a Pierce BCA protein assay kit (ThermoFisher Scientific) to assay for reduction of Cu^{2+} ions.

The treatments were shaken, in triplicate, on a rotary shaker at 200 RPM and in a constant-temperature room at 25 ± 1 °C in the dark for up to 240 h. Samples (7 mL) were taken with sterile pipettes without replacement at 0, 2, 4, 8, 24, 48, 96, 144, and 240 hours. The pH and electrical conductivity were measured followed by NP removal. To measure $Cu_{(aq)}$, two NP separation methods were used: centrifugation of 3 mL at 20,800 x g for 15

minutes (Eppendorf 8504, Eppendorf rotor F45-30-11) and centrifugal ultrafiltration of 4 mL with a 3 kDa molecular weight cutoff (MWCO) (Millipore). The centrifugation speed and time was calculated by the Stokes-Einstein equation to remove NPs with a diameter > 10 nm, a method previously used,[8,12,14] and the 3 kDa ultrafilter was estimated to remove CuO NPs > 1.3 nm in diameter.[27] Dynamic light scattering (DLS) was employed to check for remaining particles after centrifugation/ultrafiltration. After separation of the NPs, samples of the solution were analyzed for anions and cations/trace elements (after acidification for cation samples).

At the final sampling point (240 hours), DOC, free Cu^{2+} ion activities, and alkalinity were additionally measured in the treatments. Samples of particulates from the suspensions were isolated by centrifugation (as described previously); the supernatant was carefully removed with a pipette (to avoid disturbing the pellet), and the pellet was air-dried and stored under desiccated air until analysis by SEM/EDS and FTIR to determine coatings and morphology of the NPs. The pellets were analyzed by resuspending the pellet in 5 μL deionized water and drying on an aluminum stage (SEM/EDS) or glass slide (FTIR). After complete drying, SEM/EDS samples were imaged under high vacuum mode without coating under a 10 keV beam (FEI Quanta FEG 650, Oxford EDS with X-Max detector). FTIR data were collected in attenuated total reflectance (ATR) mode, 250 scans from 525-4000 cm^{-1}.

2.4 Effects of DNOM on CuO NP solubility

After the SPW solubility studies, two follow-up studies were conducted to confirm observations regarding DNOM and the NPs. The follow-up studies were performed to

determine: 1) if DNOM in the SPWs was suppressing or increasing $Cu_{(aq)}$ release at various concentrations, and 2) if sorption of Cu^{2+} to precipitated DNOM was suppressing Cu release. These batch solubility studies were performed as previously described with the following changes: 1) In both follow-up studies, the volume of SPW was decreased to 50 mL and only one sampling time (48 hours) was used, based on stable pH conditions from the first set of batch solubility studies; and 2) in both studies, only $Cu_{(aq)}$, pH, and EC were measured at the 48-hour sampling.

In the first follow-up study ("Does DNOM in the SPWs suppress or increase $Cu_{(aq)}$ release at various concentrations?", Section 3.5), the SPWs were diluted serially (SPW/diluent: 80/20%, 60/40%, 40/60%, 20/80%) with an equal ionic strength $Ca(NO_3)_2$ salt solution to maintain constant ionic strength but vary the organic ligand concentration, and then the solubility study was performed as described in Section 2.3, but with the modifications listed above over 48 hours. A $Ca(NO_3)_2$ control solution (SPW/diluent: (0/100%) and full strength SPW (SPW/diluent: 100/0%) was also tested for each SPW treatment.

In the second follow-up study ("Does sorption of Cu^{2+} to colloidal natural organic matter occur in SPWs?", Section 3.5), the SPWs were spiked with Cu^{2+} from a $CuNO_3$ salt instead of CuO NPs to match the 48-hour reaction time $Cu_{(aq)}$ concentration measured previously for each SPW. The solubility study was performed as described in Section 2.3 but with the modifications listed above over 48 hours. A $Ca(NO_3)_2$ control solution was also tested.

2.5 Statistical methods

All measurements were made in independent triplicates unless otherwise noted, and represented as the mean ± Student's t-test or Tukey's honestly significant difference (HSD) statistical significance bar. Within treatments, pH and $Cu_{(aq)}$ data points were compared by one-way analysis of variance (ANOVA; factors were NP separation technique or time point) and Tukey's HSD test or Student's t-test with $\alpha = 0.05$ in JMP 8. A logarithmic transformation on $Cu_{(aq)}$ was employed to maintain independent distributions of the residuals. Across treatments, all treatments were compared to the control at each time point by Dunnett's test with $\alpha = 0.05$.

First order models were fitted by R to dissolved Cu data with the equation:

$$C_{Cu} = C_{Cu,0} * e^{-k*t} + C_{Cu,eq} * (1 - e^{-k*t})$$

where C_{Cu} represents the concentration of dissolved Cu at any time t (hours), $C_{Cu,eq}$ represents the estimated dissolved Cu equilibrium concentration (μg/L), $C_{Cu,0}$ represents the initial measured dissolved Cu (μg/L), and k represents the rate (in hour^{-1}).

3. Results and Discussion

3.1 Characterization of NPs and SPWs prior to experiments

XRD identified the CuO NPs as tenorite (CuO) with possible ferrite (Fe_3O_4) contamination (supporting information Table A-3, Figure A-1). Acid digestions of the NPs confirmed trace contaminants, including Fe. All metals except K, Be, V, Se, and Sb assayed under USEPA method 6020 by ICP-MS were detectable, as observed in a previous batch from the same manufacturer[12] (Table A-4). Organic contaminants were detected by FTIR through a peak at 1436 cm^{-1}, but were undetectable by loss-on-

ignition (changes in weight associated with removal of organic carbon by calcination). The purity of the CuO NPs was estimated to be $\geq 99.2\%$. FTIR peaks at 533 cm^{-1} and 590 cm^{-1} were matched with characteristic peaks of CuO[31] (Figure A-2). SEM images of the NPs showed strong aggregation resulting from both dry and wet states (Figure A-3). The distribution of NP diameters (N = 30 from 3 images) was log-normal with an average of 46 nm and a median of 38 nm, generally agreeable to the manufacturer's specifications (D < 50 nm) (Figure A-4). The point of zero charge was not measured, but was expected to be about pH 10.[32]

The SPWs varied in DNOM (measured as DOC), FA, nitrate, phosphorus, and alkalinity by up to about an order of magnitude (Table 4-1) and varied less in HA, calcium, and initial Cu$_{(aq)}$. A full characterization may be found in the supporting information (Table A-5). The quantified DNOM (HA, FA, LMWOAs) accounted for 48% (WS) to 69% (OrgM, IDM) of the DOC. FA accounted for > 50% of the total DNOM apart from IDM where a major fraction was associated with LMWOAs, and WS where a major fraction was unidentified. IDM was from an unmanaged grassland whereas all other soils were associated with crop production. WS was the most modified soil, resulting in a broader array of DNOM than could be quantified here. The balance of DNOM is likely accounted for in protein, sugars, and carbohydrates which are unlikely to be complexing ligands for Cu. Amino acids and phenolics may also be present.

Table 4-1: Initial characteristics of 3.34 mM Ca(NO$_3$)$_2$ control and SPWs before addition of CuO NPs. "<" = below detection with detection limit following.

Soil name	Control	OrgM	AgrM	IDM	GM	WS
Initial pH	5.62	8.18	8.34	8.38	8.15	8.49
EC (μS/cm)	695	735	391	1100	3380	2030
Ca (mg/L)	119	168	97.4	187	373	200
Initial Cu$_{(aq)}$ (μg/L)	<2.5	13.4	22.8	22.7	81.2	123
Alkalinity (mg/L CaCO$_3$)	<10	340	450	1010	490	1270
NO$_3^-$ (mg/L N)	130	149	12.6	<0.5	574	71.5
PO$_4^{2-}$ (mg/L P)	<0.5	<0.5	<0.5	0.91	1.99	8.52
DOC (mg/L C)	<0.8	42.7	73.4	270	305	388
HA (mg/L C)	0	<0.8	<0.8	14.2	4.3	16.5
FA (mg/L C)	0	28.3	38.0	67.5	165	169
LMWOAs (mg/L C)	0	0.98	1.43	104	5.02	<0.5

3.2 Effects of changing variables on CuO NP solubility: Geochemical models

Before solubility experiments began, the geochemical model Visual MINTEQ 3.1 was used to help predict the most important factors in SPWs for CuO NP dissolution. Visual MINTEQ 3.1 was chosen because it is the most widely used speciation model and contained detailed databases modeling metal-DNOM complexes. The dissolution of CuO NPs was simulated in each solution/SPW while changing the composition of the solution to test which components had the most effect on the NP dissolution. Conditions used within the model are given in the supplementary information (Table A-6). The range of cation/anion balances in the SPWs was 2.7-19%, 2.2-30%, 34-37%, 22%, and 2.1-23% for the OrgM, AgrM, IDM, GM, and WS SPWs, respectively.

Predicted Cu$_{(aq)}$ concentrations increased with increasing FA and alkalinity concentrations, but not phosphate concentrations (Figure 4-1A). Cu$_{(aq)}$ was more sensitive to FA than alkalinity. Likewise, all SPWs (which contained FA, HA, other forms of DNOM, and alkalinity) enhanced theoretical Cu$_{(aq)}$ compared to the control

(Figure 4-1B). The modeled Cu in the SPWs was associated primarily with FA and HA. Overall, the order of increasing predicted dissolution was control < OrgM < AgrM < IDM < GM < WS.

The modeled total dissolved Cu ($Cu_{(aq)}$, red line) in control solutions or SPWs was generally decreased by increasing pH in the model (Figure 4-1C, D). The pH range used was that observed in this study (section 3.4). In 3.34 mM $Ca(NO_3)_2$, with and without alkalinity/FA/phosphate, modeled total dissolved copper decreased above pH 7.5 and was strongly dependent on pH, as illustrated by the control + alkalinity treatment (Figure 4-1C; remaining treatments shown in Figure A-5). In the SPWs (except GM) above pH 7.5, modeled total dissolved copper decreased by 0.5-27%, though the decrease was not consistent over the whole range, as illustrated by the OrgM SPW (Figure 4-1D; remaining SPWs shown in Figure A-6). The GM SPW increased in modeled total dissolved copper above pH 7.5 by about 6% (Figure A-6).

3.3 Effect of NP separation technique in measuring CuO NP dissolution

Centrifugation and ultrafiltration rely on differing processes to remove NPs from suspension, and neither method is immune from error. Both methods' advantages, disadvantages and experimental results are detailed here.

Centrifugation separates particles using sedimentation velocities based on particle density, particle geometry, particle diameter, liquid viscosity, container length, g-force, and time. The Stokes-Einstein equation was used to calculate a speed and time to separate spherical CuO NPs ≥ 10 nm in diameter from suspension in 15 minutes. Greater times or speeds were not feasible and provided little theoretical improvement over the
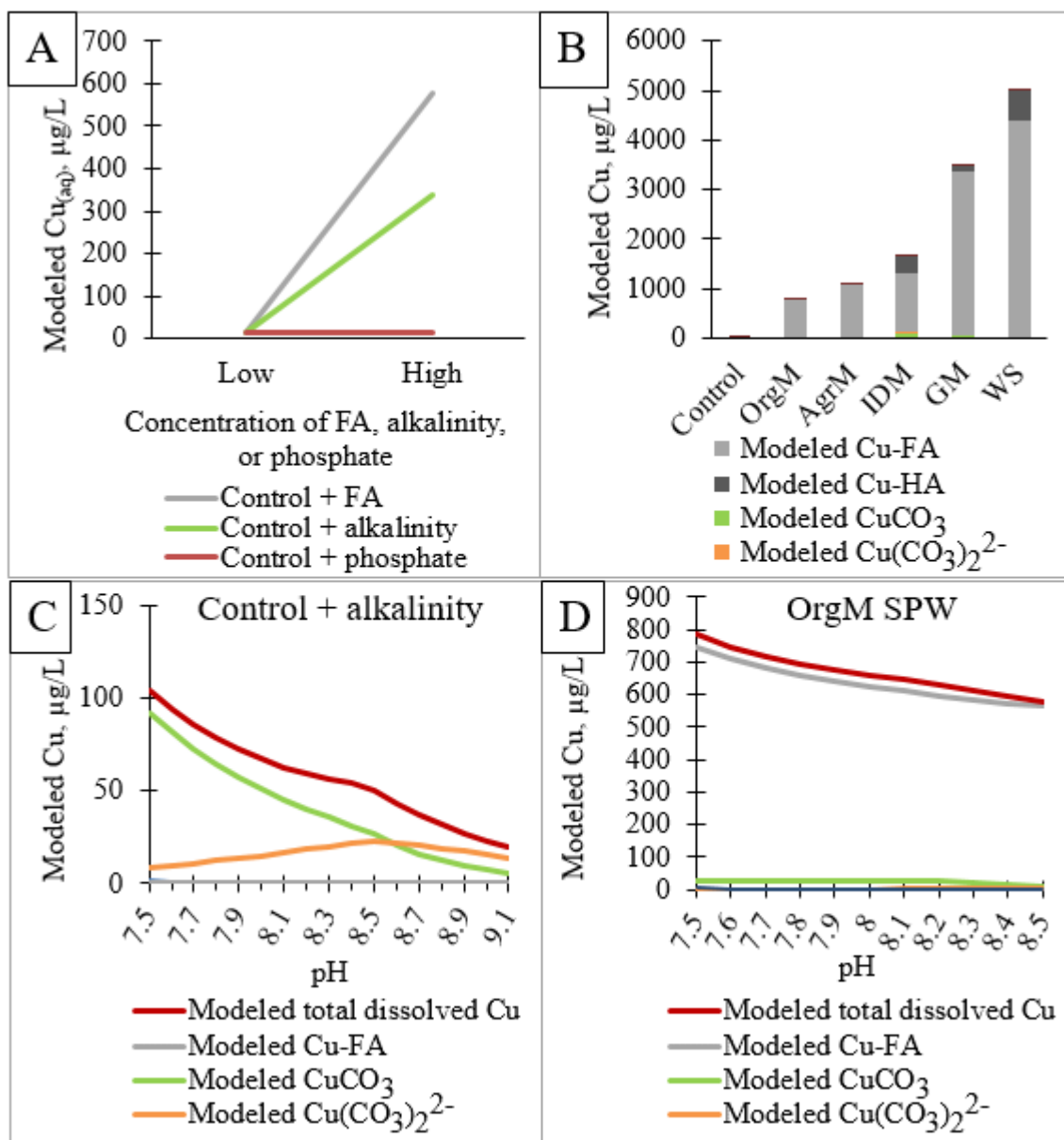
Figure 4-1: Modeled $Cu_{(aq)}$ in 3.34 mM $Ca(NO_3)_2$ with 0 and 5 mg/L PO_4-P (control + phosphate), 0 and 20 mg/L FA as C (control + FA), or 0 and 750 mg/L $CaCO_3$ as $NaHCO_3$ (control + alkalinity) (A), modeled forms of Cu in 3.34 mM $Ca(NO_3)_2$ (control) and all SPWs, (B), modeled forms of Cu in 3.34 mM $Ca(NO_3)_2$ with 750 mg/L $CaCO_3$ (C), and modeled forms of Cu in OrgM SPW (D). Note scale changes among graphs. "$Cu_{(aq)}$" (red line) in C, D is the sum of all other Cu forms. Geochemically modeled graphs for all other control solutions and SPWs are located in Appendix B (Figures A-5, A-6).

10-nm diameter cutoff. Processes that aggregate NPs, however, cause faster sedimentation because of increasing particle diameters. "Pelleted" NPs (those adhered to the wall or bottom of the container after centrifugation) are susceptible to resuspension, and nanoparticles smaller than 10 nm in diameter would not be removed.

Ultrafiltration uses a membrane based on a MWCO (3 kDa in this case) and is typically used for protein concentration. The MWCO is the point at which 90% of proteins of a given molecular weight are rejected by the filter. Pore size is not commonly reported for ultrafiltration membranes, but is estimated to be approximately 1.3 nm.[27] As the MWCO is not exact, some fraction of NPs may pass through the ultrafilter.

To test for NPs after separation (by centrifugation or ultrafiltration), DLS was employed. SPWs were equilibrated with CuO NPs (10 mg/L Cu) for 10 days followed by centrifugation and ultrafiltration. DLS detected particles in centrifuged supernatants (Figure 4-2A, OrgM SPW with CuO NPs after centrifugation, shown as an illustration), but not ultrafiltrates. DLS scans of ultrafiltrates never met quality control criteria, like scans of pure distilled water. The particulates were primarily nano-sized in all SPWs. DLS does not indicate whether these particles were NPs, colloidal (e.g. 5 nm peak in Figure 4-2A) minerals, or DNOM.

As nano-sized particulates were found in centrifuged supernatants but not in ultrafiltrates, differences in $Cu_{(aq)}$ were determined in all solutions by one-way ANOVA (separation method) by combining all data points with time. The difference between separation methods was always significant, except for the control + alkalinity (Figure 4-2B), but the magnitude of the difference varied by solution. The smallest differences
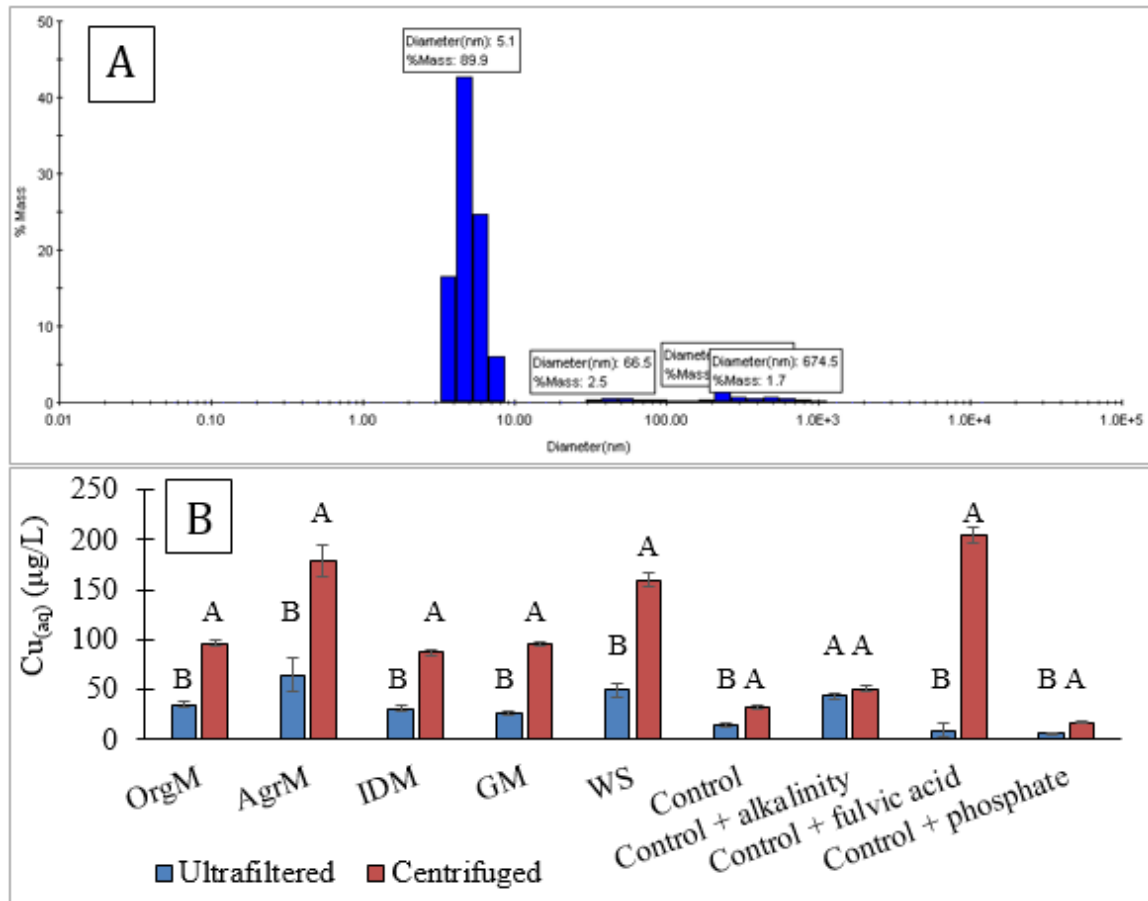
Figure 4-2: Particles detected by DLS in OrgM SPW after incubation with CuO NPs for 240 hours and centrifugation to remove NPs > 10 nm in diameter (A), and effect of NP separation technique on $Cu_{(aq)}$ in all treatments (B). Graph (A) is representative of all SPWs, where > 90% of the mass is in the nano-range. Graph B groups of bars with differing letters (A, B, etc.) are statistically different ($p < 0.05$) by Student's t-test. Graph B bars represent average of 24 independent measurements (48 in control), and error bars are the statistical significance bars. A logarithmic transformation was necessary to maintain normal distribution of the residuals.

between ultrafiltered and centrifuged samples were found in the control and the control + phosphate solutions, which were solutions without DOM. The differences in $Cu_{(aq)}$ were 17.6 and 11.2 µg/L, respectively. Aggregation of the NPs with themselves or other colloids in the control + alkalinity and control + phosphate solutions enhanced NP removal by centrifugation, but only eliminated the difference in the control + alkalinity

solution. Ultrafiltration, however, resulted in $Cu_{(aq)}$ measurements in closer agreement

with geochemical modeling predictions than centrifugation in the inorganic systems only

(Table 4-2). Ultrafiltration was thus the most efficient for separating NPs from solution

in inorganic systems.

Table 4-2: Comparison of steady state $Cu_{(aq)}$ measurements after centrifugation and ultrafiltration in all treatments with geochemically modeled $Cu_{(aq)}$ concentrations in all treatments. Steady state pH and DNOM concentrations are also included.

Treatment	DNOM (mg/L C)	Steady state pH	Steady state $Cu_{(aq)}$ after centrifugation (µg/L)	Steady state $Cu_{(aq)}$ after ultrafiltration (µg/L)	Geochemical modeled $Cu_{(aq)}$ (µg/L)
Control	0	7.80	32.5	14.9	7.45
Control + alkalinity	0	8.79	81.1	77.1	32.2
Control + phosphate	0	8.67	32.7	13.6	6.23
Control + FA	20	8.57	276	13.4	406
OrgM	42.7	8.42	135	48.0	592
AgrM	73.4	8.44	257	88.0	800
IDM	270	8.35	110	36.6	1641
GM	305	8.30	109	31.4	3647
WS	388	8.51	172	63.6	3686

SPWs and the control + FA solution had the largest differences in $Cu_{(aq)}$ between

ultrafiltered and centrifuged samples (Table 4-2). DOC also decreased significantly in

ultrafiltered samples compared to centrifuged samples (Table A-7). As Cu^{2+} has a well-

documented affinity for DNOM, the ultrafiltered samples reduced apparent $Cu_{(aq)}$ by

removing Cu-DNOM complexes, resulting in altered solubility measurements.

Centrifugation was thus most appropriate for separating NPs from solution in systems

with large organic ligands. In the following sections, only centrifugation data will be

reported for SPW and the control + FA, whereas only ultrafiltration data will be reported for the remaining control solutions.

3.4 Effect of time in CuO NP dissolution

$Cu_{(aq)}$ increased in all treatments with time except the control. The control reached equilibrium immediately and did not vary with time. All other solutions increased with time according to the Tukey HSD test. OrgM, AgrM, control + alkalinity, and control + FA displayed typical dissolution kinetics (increase with time to a steady-state condition; Figure 4-3). No microbial contamination was observed except in one replicate of the AgrM SPW (replicate omitted from analysis) and all replicates of IDM SPW (replicates included in analysis). The microbes may have enhanced the solubility of the CuO NPs in the IDM SPW.

First order kinetic dissolution models were chosen to describe the formation of dissolved copper complexes. Fits of the kinetic models were determined by the root mean squared error (RMSE) and residual analysis. Kinetic models were not possible for the WS and the control solution. Dissolved Cu did not change in the control with time (i.e., the system was at steady state at the first sampling time interval). Since only the last two time points in the WS SPW showed an increase over time 0, the WS SPW kinetic model could not be fitted in R because the rate was too low to estimate.

The kinetic model described CuO NP dissolution well (through linear quantile plots excluding outliers and even distribution of residuals) in all solutions (Figure A-7, A-8). The control + alkalinity treatment reached much higher pH after 48 hours than any other treatment and had the poorest linear quantile plot (Figure A-8, A-9). The

Treatment	$C_{Cu,0}$ (µg/L)	$C_{Cu,eq}$ (µg/L)	k (hr^{-1})	RMSE (µg/L)
OrgM	40.7	166	2.23×10^{-2}	21.7
AgrM	83.6	313	2.24×10^{-2}	20.4
IDM	55.2	119	3.53×10^{-2}	21.3
GM	81.8	153	5.04×10^{-3}	10.2
WS	N/A	N/A	N/A	N/A
Control	N/A	N/A	N/A	N/A
Control + alkalinity	3.1	75.6	8.83×10^{-2}	21.7
Control + fulvic acid	53.3	359	3.39×10^{-2}	48.8
Control + phosphate	2.7	16.2	7.50×10^{-3}	2.5
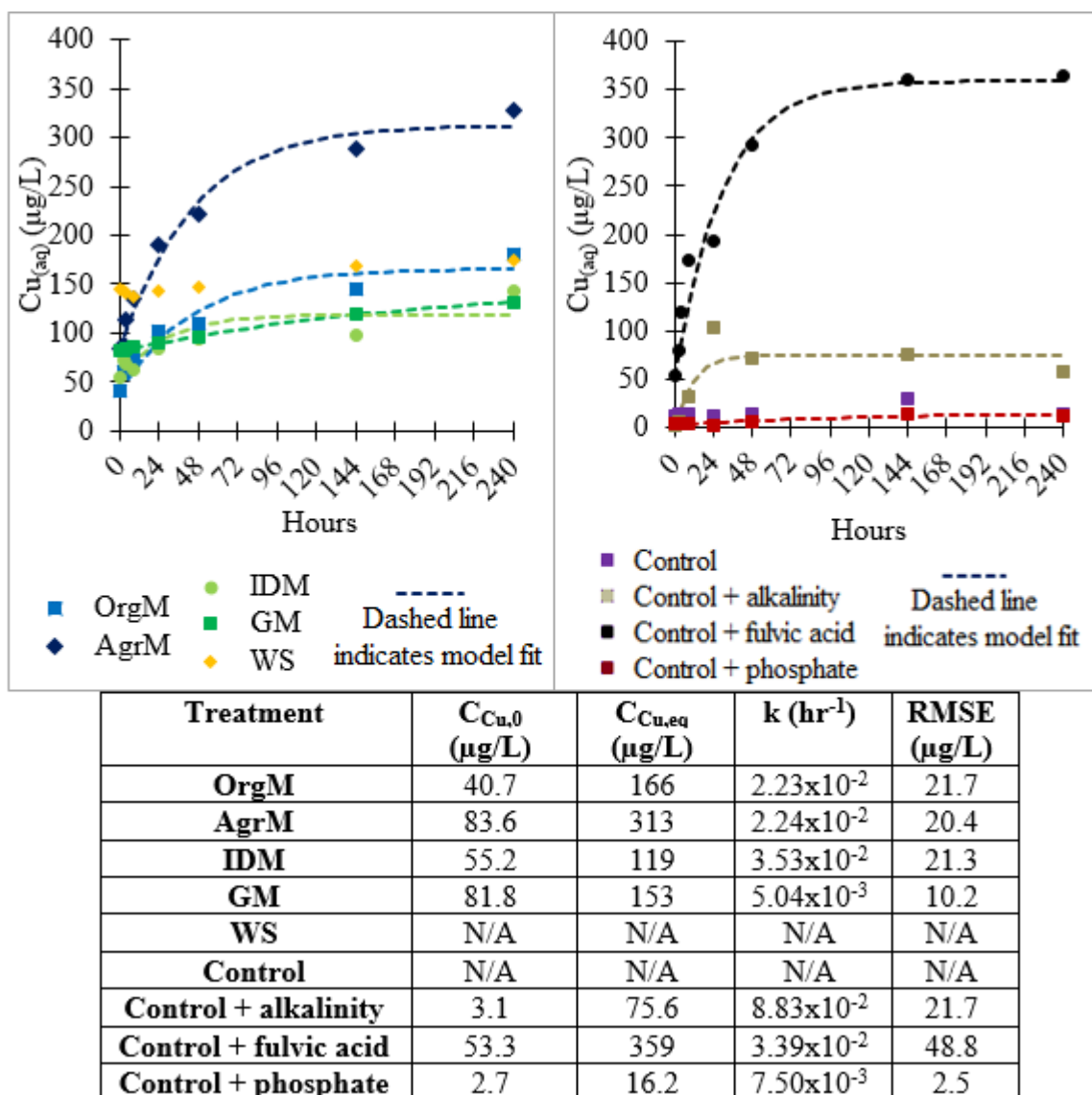
Figure 4-3: Measured Cu$_{(aq)}$ and calculated first order kinetic models of Cu$_{(aq)}$ and parameters in all treatments as a function of time. Points are average of independent sample measurements (n = 3). The dashed lines are the modeled results. SPWs and control + FA are centrifugation data, while control, control + alkalinity, and control + phosphate are ultrafiltration data. $C_{Cu,eq}$ = estimated dissolved Cu equilibrium concentration, $C_{Cu,0}$ = initial dissolved Cu, k = Cu dissolution rate constant, and RMSE = root mean squared error of the model, i.e. the average error of the model to the measured data points.

increasing pH may have limited CuO NP solubility, shifting equilibrium in this sample

which the first order model did not account for. Despite the shifting pH, the Tukey HSD

test did not determine a difference between any of the last four data points in this treatment, suggesting equilibrium was attained.

The rates observed in this study were mixed compared to those observed in other studies. Goa et al (2017) added 10 and 100 mg/kg Cu/soil of CuO NPs to a purchased standard soil incubating the samples for up to 30 days. At selected time intervals they extracted soluble Cu using 0.01 M $CaCl_2$. The first order rate constants were 4.58 and 5.42×10^{-3} hr^{-1} during 30 days for the two doses,[33] which encompassed the GM SPW (5.04×10^{-3} hr^{-1}). Three SPWs however had rate constants an order of magnitude higher than GM SPW, as did the control + alkalinity and control + FA. In the presence of 10 mM NaCl, alginate, bovine serum albumin, and extracellular polymeric substances, first order rate constants were 2.9×10^{-1}, 4.5×10^{-1}, 4.4×10^{-1}, and 6.4×10^{-1} hr^{-1}, respectively,[34] larger by an order of magnitude than the rate constants observed in this study.

All solutions reached steady state conditions, defined by no statistical difference between measured Cu data points with time in at least the final two sampling points. Cu steady state was reached at 0, 48, 48, 144, 144, 144, 24, 144, and 144 hours in the control, control + alkalinity, control + FA, control + phosphate, OrgM, AgrM, IDM, GM, and WS treatments, respectively. Many studies in artificial media (like the controls) also reach equilibrium or constant maximal concentrations within a few days.[17,18,35] The SPWs, more complex media, tended to reach steady states later (> 144 hours), like studies which observed slow dissolution (on the time scale of weeks to months) in natural waters.[23,36] Similarly, dissolution rate constants were lowest in the GM SPW (high DNOM), the control + phosphate (highest mineral precipitation), and unable to be

modeled in the WS SPW (highest DNOM). The complexity of the medium may partly determine the rate to $Cu_{(aq)}$ equilibrium.

pH partially controls solubility and is important to consider in parallel with the dissolved Cu measurements. Despite initial adjustment of pH, pH rapidly increased in all treatments (by one-way ANOVA on each treatment with factor time, followed by Tukey HSD) from 7.5 to 8.3-8.8 during the first 8-48 hours, except the control (pH 7.8, which never statistically changed during 240 hours) (Figure A-9). pH steady state (as defined by statistically unchanging pH conditions by one-way ANOVA) was achieved at 48, 24, 24, 8, 4, 4, 8, and 24 hours in control + alkalinity, control + FA, control + phosphate, OrgM, AgrM, IDM, GM, and WS treatments, respectively. The control + alkalinity, control + FA, and control + phosphate took 24-48 hours to stabilize in pH, while the SPWs took 4-8 hours (except WS). The minimal background in the control solutions provided little buffering capacity, and atmospheric CO_2, production of hydroxide by dissolution of CuO NPs,[37] and conversion of bicarbonate to carbonate caused the pH to remain unstable in the controls for longer than the SPWs. The pH of the SPWs after 24 hours matched the natural pH of the SPWs. Modeled solubility with SPWs over this pH range only changed ±1-26% (Figure A-6) and so pH was not expected to impact $Cu_{(aq)}$ more than 25%.

3.5 Role of DNOM in CuO NP dissolution

Only the control, control + alkalinity, and control + phosphate treatments reached or exceeded the geochemically predicted values in $Cu_{(aq)}$ at some point during 240 hours (Table 4-2). The $Cu_{(aq)}$ in all other treatments remained below modeled concentrations.

Free Cu^{2+} ion activity measurements in the SPWs (a subset of $Cu_{(aq)}$) were low (0.034-0.049 µg/L) but were within 80-124% of MINTEQ predictions (0.037-0.041 µg/L). Free Cu^{2+} ion activity measurements in the control and control with FA/alkalinity/phosphate were higher than the SPWs (0.050-0.247 µg/L). The control free Cu^{2+} was below MINTEQ predictions (36% of predicted) but the remaining three control variations were above (573%, 682%, and 1170% of predicted for FA, phosphate, and alkalinity controls, respectively). It is unknown why free Cu^{2+} activities did not match well in the simpler controls. The predicted free Cu^{2+} activities were extremely low (0.007-0.020 µg/L) in the control + FA, control + phosphate, and control + alkalinity solutions, near the detection limit of the ion selective electrode (approximately 0.012 µg/L). The pH of the three control solutions were the highest of all measured. It is possible that the ion selective electrode had problems at the extreme limits of its range and the high pH.

As $Cu_{(aq)}$ did not reach predicted concentrations in the SPWs, the SPWs at 240 hours were further investigated to explain the lack of dissolution from CuO NPs. DNOM in the SPWs and control + FA, as well as mineral phases in the control + alkalinity and control + phosphate, aggregated CuO NPs more than the control as observed by particles visible to the naked eye at and before 240 hours; larger, more visible pellets after centrifugation; and SEM imaging (Figure A-10 to A-18). The aggregation of NPs increased the average diameter, leading to greater removal efficiencies with centrifugation over the control. Unfortunately, DLS could not resolve NP aggregate diameters from other precipitates. DNOM (including FA) and alkalinity/phosphate promoted aggregation by differing mechanisms. SEM/EDS showed no precipitates in the

control + FA treatment, but instead an even layer of C on the NPs (Figure A-16), meaning that instead FA was associated with the NP surfaces. FA has been previously observed to aggregate CuO NPs,[22] especially when Ca^{2+} is present at neutral to high pH and provides bridging-flocculation of coated NPs.[38] Calcium was present in all solutions as the control was a calcium nitrate solution and the soils were calcareous.

In the phosphate and alkalinity treatments (Figure A-17, A-18), mineral phases (predicted to be hydroxyapatite and calcite, respectively, from MINTEQ) precipitated from solution and induced heteroaggregation with the CuO NPs. Aqueous phosphate decreased in solution over time (Figure A-19), and SEM/EDS showed the presence of calcium and phosphate in the structures as well as the CuO NPs, supporting the modeling results showing hydroxyapatite presence (Figure A-17). SEM/EDS of NPs from the alkalinity treatment showed the presence of calcium, carbon, and oxygen together, supporting modeling results suggesting calcite precipitation (Figure A-18). No heteroaggregation was observed in the control (Figure A-10).

In GM and WS SPWs incubated with CuO NPs, amorphous, particle-containing gel-like structures were observed by light microscopy, but particle identities could not be confirmed with only light microscopy (Figure 4-4A). The amorphous structures were not seen in other SPWs or the $Ca(NO_3)_2$ controls; however, there was evidence that the NPs may be acting as nucleation points for crystalline formation, such as calcite (only in the control and alkalinity treatment; Figure A-20).

FTIR analysis of NPs extracted from solution by centrifugation after 240 hours confirmed the presence of hydrocarbon functional groups associated with the NPs,
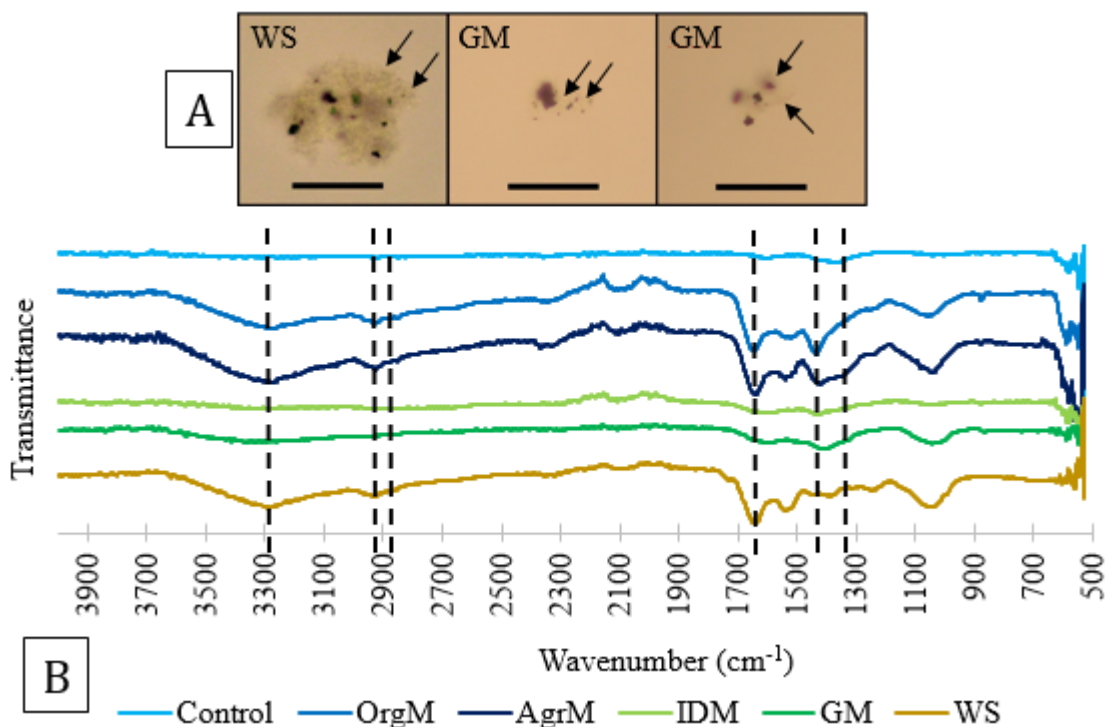
Figure 4-4: Amorphous, translucent structures containing opaque particles seen under light microscopy in GM and WS SPWs incubated with CuO NPs (A) and FTIR scans of CuO NPs incubated in SPWs compared to CuO NPs incubated in the control (B). The translucent structures in (A) are predicted to be precipitated organic matter, and the opaque particles are predicted to be CuO NP aggregates. Bar = 250 microns. Dashed lines in (B) indicate important wavelengths at 2962, 2872, 1450, 1375 (aliphatic methyl), ~3300 (hydroxyl), and ~1650 cm^{-1} (other carbon bonds, possibly aromatic).

which varied by SPW; however, it was unclear whether the hydrocarbons were bonded to the NPs on the basis of these data alone. Control samples of the unaltered organic matter would be required to determine if peaks related to bonding with CuO were diminished in the NP samples, which would indicate coating of the NPs.[39]

Copper is reported to have affinities, from greatest to smallest, for carboxyl (1260 and 1720 cm^{-1}), polysaccharide (1042 and 1100 cm^{-1}), phenolic (1400 cm^{-1}), aromatic (1620 cm^{-1}), amide (1660 cm^{-1}), and aliphatic groups.[40] Carboxyl and aromatic groups, which should have been present in FA, were not seen in any NP sample from the SPWs

(Figure 4-4B). It is possible that these groups were present but their vibrations were quenched by bonding to the NPs, but spectra of the unaltered organic matter must be collected to prove this point. NPs from all SPWs showed broad polysaccharide groups (1042 cm^{-1})[39-40] to varying degrees (IDM had the smallest peak, but this may be due to the unusually large LMWOA portion of the DNOM). OrgM, AgrM, and WS SPWs had aliphatic methyl (2962, 2872, 1450, 1375 cm^{-1}), aliphatic methylene (2926, 2853, 1465 cm^{-1}), and intermolecular-bonded hydroxyl (broad peak near 3300 cm^{-1})[41] groups present.

Soil DNOM (such as FA or HA) complexes Cu^{2+} ions, promoting CuO dissolution by removing Cu^{2+} ions from solution. However, DNOM seemed to suppress NP dissolution in SPWs; a similar effect was seen for silver NPs in soil extracts, which was attributed to the dissolved organic fraction coating.[42] From the suppression of Cu$_{(aq)}$ and association of DNOM with the NPs, it was theorized that Cu$_{(aq)}$ was controlled by either 1) concentration-driven coating of the NPs, and/or 2) sorption of Cu$_{(aq)}$ to precipitated natural organic matter, if present.

CuO NP dissolution experiments were performed in a range of diluted SPWs while maintaining a constant ionic strength to test for a suppressing effect. The dilutions also reduced the concentration of inorganic ions, but only the dilution of DNOM was expected to be significant in CuO NP dissolution, based on sensitivity analyses in MINTEQ (Section 3.2).

DNOM suppressed Cu$_{(aq)}$, especially at high concentrations (Figure 4-5A-E). Across all SPWs, the Cu$_{(aq)}$ measurements at 48 hours (time chosen based on pH

stability) as a function of organic ligand concentration showed relatively low dissolution at 0 mg/L C and at >100 mg/L C (Figure 4-5F). As previously shown in Figure 4-1B, the geochemical models in Figure 4-5 predicted that the majority of dissolved Cu should be complexed primarily to FA, followed by HA (if present), followed by $CuCO_{3(aq)}$. $Cu_{(aq)}$ reasonably matched modeled equilibrium values in OrgM and AgrM at 8.5 mg/L C in OrgM and 15-29 mg/L C in AgrM (Figure 4-5A, B). The other SPWs, at their lowest dilutions, were not diluted so low as OrgM and AgrM SPWs, and thus never matched model predicted $Cu_{(aq)}$ values. However, the largest dilutions yielded the highest $Cu_{(aq)}$ values, even though the predicted $Cu_{(aq)}$ was not met. Low dissolution at 0 mg/L C was due to the lack of Cu-DNOM complexes, while low dissolution at high DOC concentrations was likely due to coating of the NPs.

Batch experiments similar to the solubility experiments were conducted with Cu^{2+} ions instead of CuO NPs in the SPWs to test for sorption of Cu^{2+} ions to colloidal organic matter. Sorption of Cu^{2+} ions to colloidal organic matter and subsequent removal through centrifugation/ultrafiltration would result in lower apparent solubility of the CuO NPs. However, there was no statistically significant loss of Cu^{2+} ions with the SPW after 48 hours except in the control (Table 4-3). The loss of Cu^{2+} ions in the control was likely due to precipitation of CuO, as the control solution was shown to have a maximum solubility of 12.2 μg/L Cu^{2+} under the conditions by geochemical modeling, as no complexing ligands existed to hold Cu^{2+} in solution at pH 7.5. These data show that Cu ions were not sorbing to colloidal DNOM under these conditions, meaning that
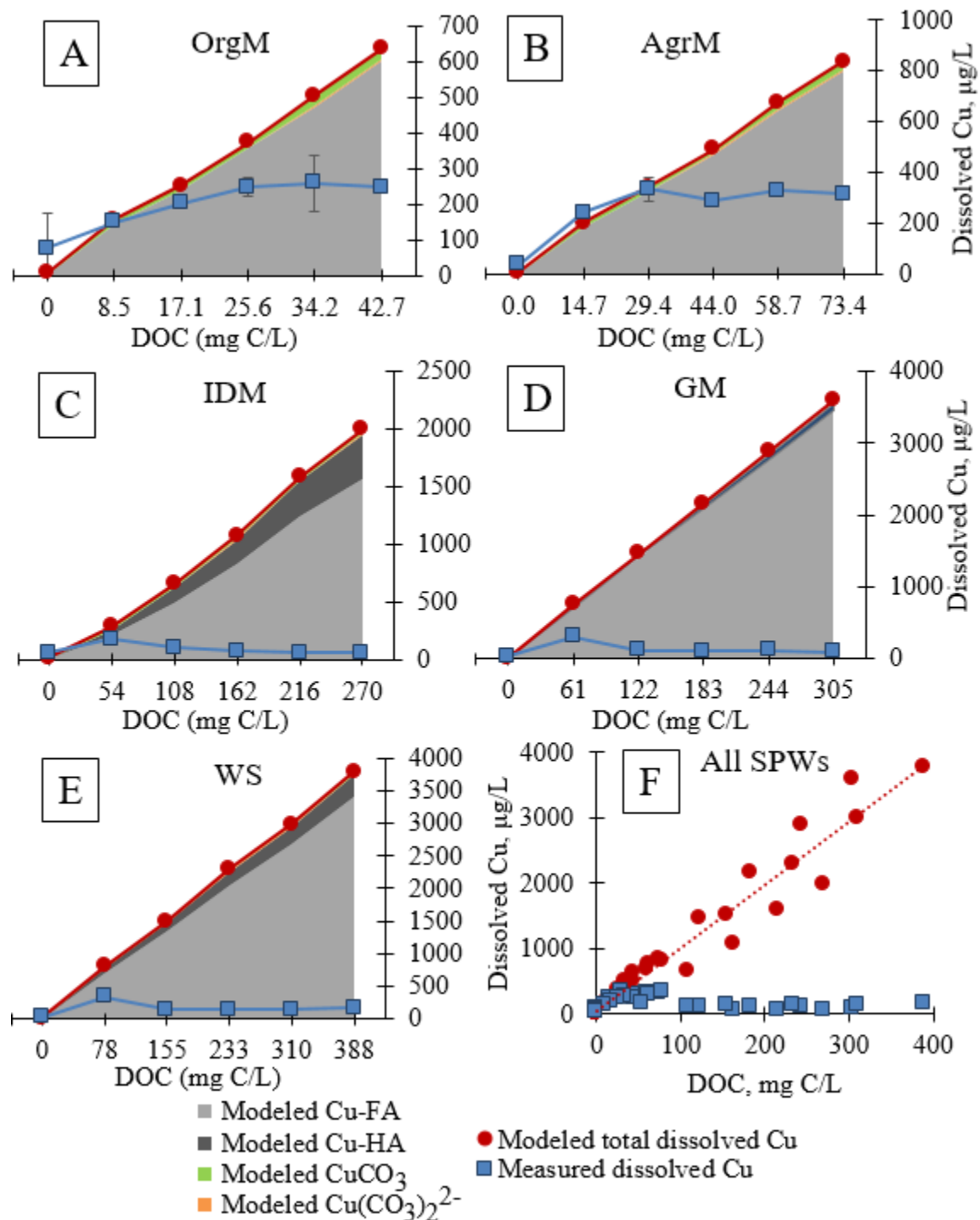
Figure 4-5: Cu(aq) concentration (blue squares) in individual SPWs (A-E) and all SPWs combined (F) at 48 hours using the centrifugation NP separation method, as a function of dilution of SPWs at constant ionic strength, compared to modeled forms of dissolved Cu (stacked areas and red circles). Data points represent the average of three independent replicates, and error bars represent the standard deviation.

the suppression of $Cu_{(aq)}$ from CuO NPs at high DNOM was truly due to coating of the

NPs instead of loss of Cu^{2+} to colloidal organic matter.

Table 4-3: Comparison of $Cu_{(aq)}$ immediately after addition of Cu^{2+} ions in all SPWs to $Cu_{(aq)}$ measured in all SPWs 48 hours later. Numbers are average of independent triplicates ± standard deviation. Sorption of Cu ions to glass walls, centrifuge tubes, or colloidal organic matter is shown to be negligible except in the control.

Soil pore water	Initial $Cu_{(aq)}$ concentration immediately after ion addition (μg/L)	$Cu_{(aq)}$ concentration at 48 hours (μg/L)
Control	26.2 ± 2.0	16.1 ± 2.2
OrgM	243 ± 4.7	240 ± 3.3
AgrM	314 ± 20	299 ± 7.2
IDM	67.8 ± 2.8	72.6 ± 17
GM	109 ± 2.2	128 ± 14
WS	170 ± 8.8	155 ± 8.8

3.6 Applications to the soil environment

Microbes, such as bacteria or fungi, may increase the dissolution of CuO NPs.

This was seen in two of the SPWs (AgrM, IDM), in which individual samples from the

triplicate set became contaminated by common laboratory bacteria, turning the

suspensions cloudy compared to sterile, clear suspensions. DOC and anions changed in

contaminated samples (Figure A-21, A-22), showing metabolism of the SPW

components by bacteria. The sample of AgrM that became contaminated was excluded

from the previous analysis, whereas the IDM samples were included because

contamination occurred in all the triplicates to differing degrees. As all replicates of

IDM were contaminated, the source of contamination was likely not from sample

handling, but rather from a microbe in the soil able to pass the 0.2-micron filter.

In the triplicate AgrM samples, contamination was observed in sample three at and after eight hours. The bacteria increased the dissolution of the CuO NPs relative to the other two samples (Figure 4-6). The increase of dissolution may be attributed to the release of extracellular polymeric substances which have previously been shown to increase CuO NP dissolution, even at high pH.[34,43] Exudates which bacteria may produce to scavenge elements from their environment, such as organic acids[19] or iron-chelating siderophores (such as pyoverdines), also may increase CuO NP solubility. Siderophores are produced by microbes, may be found in soil environments, and have high affinities for complexing Fe^{3+}. Siderophores may have high or higher stability constants with Cu^{2+} than Fe^{3+}, which would increase CuO NP solubility but interfere with iron nutrition for bacteria relying on siderophores. A review of siderophore functions lists enterobactin, schizokinen, yersiniabactin, pyoverdine, pyochelin, and pdtc as potential Cu-complexing siderophores.[44] On the other hand, CuO NPs have been observed to suppress pyoverdine production in the bacteria *Pseudomonas chlororaphis* O6,[45] which may cancel their enhanced solubility in the presence of siderophores. Alterations of siderophore production were also observed in *Pseudomonas aeruginosa* exposed to Cu, which increased production of pyoverdine (a siderophore less specific to Cu) and decreased production of pyochelin (a siderophore more specific to Cu) to protect from Cu toxicity.[46]

Cu^{2+} ions may participate in redox reactions when complexing with organic matter, reducing to Cu^+. FA, for example, can reduce Cu^{2+} to Cu^+ even in the presence of oxygen.[47] What effect, if any, this transformation has on the toxicity of the ions was not
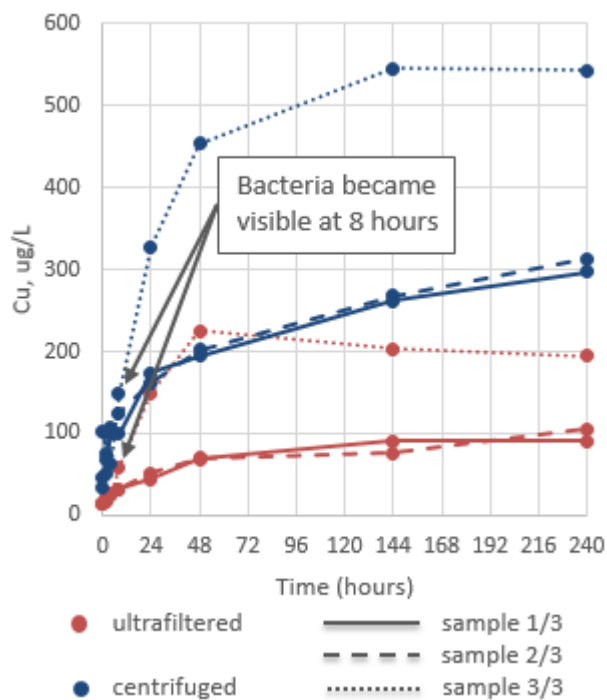
Figure 4-6: Increase of Cu dissolution in microbially contaminated sample three compared to sterile samples one and two in the AgrM SPW triplicate treatment. Each data point is an individual measurement; no error bars are given. Red points are ultrafiltered measurements, and blue points are centrifuged measurements. The solid line is sample 1, the medium dash line is sample 2, and the fine dash line is sample 3.

assayed in this experiment. In another simple experiment, the Suwannee River FA in the control treatment was assayed using a Pierce BCA protein assay kit (ThermoFisher Scientific). The BCA assay measures proteins colorimetrically with Cu^+ ions formed by the reduction of excess Cu^{2+} ions by certain peptides in proteins. Despite a lack of proteins in the FA solution, a strong false positive registered showing that FA reduced Cu^{2+} ions even in the presence of oxygen. Therefore, a significant portion of $Cu_{(aq)}$ in the SPW treatments was likely reduced by FA. Unfortunately, Cu^+ could not be directly assayed in the SPW samples because of difficulty with the sensitivity of the colorimetric

method at the suppressed $Cu_{(aq)}$ values. Future studies should consider the redox transformations of dissolved Cu, and potential effects on ion toxicity.

CuO NPs may have potential as a fertilizer in soil at low doses or for other slow-release applications. However, high doses may stunt plant growth.[13] In CuO NP contaminated soils, DNOM may serve as suppressants on CuO NP dissolution[23] or reduce contact between NPs and cells.[20,22] At lower concentrations, DNOM may increase CuO NP dissolution through formation of soluble Cu-DNOM complexes; these complexes may or may not be bioavailable. Further research is needed because the effects of a solid matrix on the NPs may counteract the suppressing influence of organic matter on the dissolution of CuO NPs, and some organisms may not be shielded from toxicity even when Cu ions are complexed with organic ligands.[48-49]

4. Associated content

<u>Supplemental information</u>

Supplemental information includes figures and tables of full characterization of CuO NPs, geochemical equilibrium modeling parameters, graphs and Tukey's test analyses of individual treatments, and FTIR graphs and SEM images of selected treatments.

Abbreviations

      NP(s), nanoparticle(s); SPW(s), soil pore water(s); HA(s), humic acid(s); FA(s), fulvic acid(s); LMWOA(s), low molecular weight organic acid(s); DOC, dissolved organic carbon; SEM, scanning electron microscopy; EDS, energy-dispersive X-ray spectroscopy; FTIR, Fourier transform infrared spectroscopy; XRD, X-ray diffraction; ICP-MS, inductively coupled plasma mass spectrometry; DLS, dynamic light scattering; ANOVA, analysis of variance; USEPA, United States Environmental Protection Agency; AgrM, GM, IDM, OrgM, WS, soil abbreviations.

5. References

1. Servin, A.; Elmer, W.; Mukherjee, A.; De la Torre-Roche, R.; Hamdi, H.; White, J. C.; Bindraban, P.; Dimkpa, C. A review of the use of engineered nanomaterials to suppress plant disease and enhance crop yield. *J. Nanopart. Res.* **2015**, *17* (2).
2. Elmer, W. H.; White, J. C. The use of metallic oxide nanoparticles to enhance growth of tomatoes and eggplants in disease infested soil or soilless medium. *Environ. Sci.: Nano* **2016**, *3* (5), 1072-1079.
3. Dimkpa, C. O; Bindraban, P. S.; Fugice, J.; Agyin-Birikorang, S.; Singh, U.; Hellums, D. Composite micronutrient nanoparticles and salts decrease drought stress in soybean. *Agron. Sustainable Dev.* **2017**, *37* (5), 1-21.

4. Otero-Gonzalez, L.; Field, J. A.; Sierra-Alvarez, R. Inhibition of anaerobic wastewater treatment after long-term exposure to low levels of CuO nanoparticles. *Water Res.* **2014**, *58*, 160-168.

5. Keller, A. A.; McFerran, S.; Lazareva, A.; Suh, S. Global life cycle releases of engineered nanomaterials. *J. Nanopart. Res.* **2013**, *15* (1692), 1-17.

6. Kim, S.; Sin, H.; Lee, S.; Lee, I. Influence of metal oxide particles on soil enzyme activity and bioaccumulation of two plants. *J. Microbiol. Biotechnol.* **2013**, *23* (9), 1279-1286.

7. Frenk, S.; Ben-Moshe, T.; Dror, I.; Berkowitz, B.; Minz, D. Effect of metal oxide nanoparticles on microbial community structure and function in two different soil types. *PLoS One* **2013**, *8* (12), e8441.

8. Dimkpa, C. O.; Calder, A.; Britt, D. W.; McLean, J. E.; Anderson, A. J. Responses of a soil bacterium, *Pseudomonas chlororaphis* O6 to commercial metal oxide nanoparticles compared with responses to metal ions. *Environ. Pollut.* **2011**, *159* (7), 1749-1756.

9. Xu, C.; Peng, C.; Sun, L.; Zhang, S.; Huang, H.; Chen, Y.; Shi, J. Distinctive effects of TiO2 and CuO nanoparticles on soil microbes and their community structures in flooded paddy soil. *Soil Biol. Biochem.* **2015**, *86*, 24-33.

10. Rousk, J.; Ackermann, K.; Curling, S. F.; Jones, D. L. Comparative toxicity of nanoparticulate CuO and ZnO to soil bacterial communities. *PLoS One* **2012**, *7* (3), e34197.

11. Concha-Guerrero, S. I.; Brito, E. M. S.; Pinon-Castillo, H. A.; Tarango-Rivero, S. H.; Caretta, C. A.; Luna-Velasco, A.; Duran, R.; Orrantia-Borunda, E. Effect of CuO nanoparticles over isolated bacterial strains from agricultural soil. *J. Nanomater.* **2014**, *2014*, 1-13.

12. Ko, K. S.; Kong, I. C. Toxic effects of nanoparticles on bioluminescence activity, seed germination, and gene mutation. *Appl. Microbiol. Biotechnol.* **2014**, *98* (7), 3295-3303.

13. Dimkpa, C. O.; McLean, J. E.; Latta, D. E.; Manangon, E.; Britt, D. W.; Johnson, W. P.; Boyanov, M. I.; Anderson, A. J. CuO and ZnO nanoparticles: Phytotoxity, metal speciation, and induction of oxidative stress in sand-grown wheat. *J. Nanopart. Res.* **2012**, *14* (1125), 1-15.

14. Dimkpa, C. O.; McLean, J. E.; Britt, D. W.; Anderson, A. J. Nano-CuO and interaction with nano-ZnO or soil bacterium provide evidence for the interference of nanoparticles in metal nutrition of plants. *Ecotoxicology* **2015**, *24* (1), 119-129.

15. APHA. *Standard methods for the examination of water and wastewater*. 22nd, ed.; American Public Health Association: Washington, D.C., 2012.

16. Misra, S. K.; Dybowska, A.; Berhanu, D.; Luoma, S. N.; Valsami-Jones, E. The complexity of nanoparticle dissolution and its importance in nanotoxicological studies. *Sci. Total Environ.* **2012**, *438*, 225-232.

17. Wang, Z. Y.; von dem Bussche, A.; Kabadi, P. K.; Kane, A. B.; Hurt, R. H. Biological and environmental transformations of copper-based nanomaterials. *ACS Nano* **2013**, *7* (10), 8715-8727.

18. Gunawan, C.; Teoh, W. Y.; Marquis, C. P.; Amal, R. Cytotoxic origin of copper(II) oxide nanoparticles: Comparative studies with micron-sized particles, leachate, and metal salts. *ACS Nano* **2011**, *5* (9), 7214-7225.

19. Zabrieski, Z.; Morrell, E.; Hortin, J.; Dimkpa, C.; McLean, J.; Britt, D.; Anderson, A. Pesticidal activity of metal oxide nanoparticles on plant pathogenic isolates of pythium. *Ecotoxicology* **2015**, *24* (6), 1305-1314.

20. Peng, C.; Zhang, H.; Fang, H. X.; Xu, C.; Huang, H. M.; Wang, Y.; Sun, L. J.; Yuan, X. F.; Chen, Y. X.; Shi, J. Y. Natural organic matter-induced alleviation of the phytotoxicity to rice (*Oryza sativa* L.) caused by copper oxide nanoparticles. *Environ. Toxicol. Chem.* **2015**, *34* (9), 1996-2003.

21. Jiang, C.; Castellon, B. T.; Matson, C. W.; Aiken, G. R.; Hsu-Kim, H. Relative contributions of copper oxide nanoparticles and dissolved copper to Cu uptake kinetics of Gulf Killifish (*Fundulus grandis*) embryos. *Environ. Sci. Technol.* **2017**, *51*(3), 1395-1404.

22. Zhao, J.; Wang, Z. Y.; Dai, Y. H.; Xing, B. S. Mitigation of CuO nanoparticle-induced bacterial membrane damage by dissolved organic matter. *Water Res.* **2013**, *47* (12), 4169-4178.

23. Conway, J. R.; Adeleye, A. S.; Gardea-Torresdey, J.; Keller, A. A. Aggregation, dissolution, and transformation of copper nanoparticles in natural waters. *Environ. Sci. Technol.* **2015**, *49* (5), 2749-2756.

24. Morris, D. F. C.; Short, E. L. Stability constants of copper (II) chloride complexes. *J. Chem. Soc. (Resumed)* **1962**, 2672-2675.

25. Bilinski, H.; Huston, R.; Stumm, W. Determination of the stability constants of some hydroxo and carbonato complexes of Pb(II), Cu(II), Cd(II) and Zn(II) in dilute solutions by anodic stripping voltammetry and differential pulse polarography. *Anal. Chim. Acta* **1976**, *84* (1) 157-164.

26. Rhoades, J. D., Salinity: Electrical conductivity and total dissolved solids. In *Methods of soil analysis: Part 3-chemical methods*; Sparks, D. L., Ed.; Soil Science Society of America, Inc. & American Society of Agronomy, Inc.: Madison, WI, 1996; pp. 417-435.

27. Guo, L.; Santschi, P. H., Ultrafiltration and its applications to sampling and characterisation of aquatic colloids. In *Environmental colloids and particles: Behaviour, separation and characterisation, volume 10*, Wilkinson, K. J.; Lead, J. R., Eds.; John Wiley & Sons: Hoboken, NJ, 2007; pp. 170.

28. Rachou, J.; Gagnon, C.; Sauve, S. Use of an ion-selective electrode for free copper measurements in low salinity and low ionic strength matrices. *Environ. Chem.* **2007**, *4* (2), 90-97.

29. Sigma-Aldrich Co. Procedures for preparing and using columns of Amberlite XAD, Diaion, Dowex, MCI GEL, Sepabeads, and Supelite DAX adsorbent resins. **1998**, SUPELCO: Bellefonte, PA.

30. Gustaffson, J. P. *Visual MINTEQ*, version 3.1 beta; 2013.

31. Kliche, G.; Popovic, Z. V. Far-infrared spectroscopic investigations on CuO. *Phys. Rev B* **1990**, 42(16), 10060-10066.

32. Sousa, V. S.; Teixeria, M. R. Aggregation kinetics and surface charge of CuO nanoparticles: the influence of pH, ionic strength, and humic acids. *Environ. Chem.* **2013**, 10, 313-322.

33. Gao, X.; Spielman-Sun, E.; Rodrigues, S. M.; Casman, E. A.; Lowry, G. V. Time and nanoparticle concentration affect the extractability of Cu from CuO NP-amended soil. *Environ. Sci. Technol.* **2017**, *51*(4), 2226-2234.

34. Miao, L. Z.; Wang, C.; Hou, J.; Wang, P. F.; Ao, Y. H.; Li, Y.; Lv, B. W.; Yang, Y. Y.; You, G. X.; Xu, Y. Enhanced stability and dissolution of CuO nanoparticles by extracellular polymeric substances in aqueous environment. *J. Nanopart. Res.* **2015**, *17* (404), 1-12.

35. Chusuei, C. C.; Wu, C. H.; Mallavarapu, S.; Hou, F. Y. S.; Hsu, C. M.; Winiarz, J. G.; Aronstarn, R. S.; Huang, Y. W. Cytotoxicity in the age of nano: The role of fourth period transition metal oxide nanoparticle physicochemical properties. *Chem.-Biol. Interact.* **2013**, *206* (2), 319-326.

36. Hanna, S. K.; Miller, R. J.; Zhou, D. X.; Keller, A. A.; Lenihan, H. S. Accumulation and toxicity of metal oxide nanoparticles in a soft-sediment estuarine amphipod. *Aquat. Toxicol.* **2013**, *142-143*, 441-446.

37. Lindsay, W. L., *Chemical equilibria in soils*; John Wiley & Sons: New York, 1979; p 449.

38. Philippe, A.; Schaumann, G. E. Interactions of dissolved organic matter with natural and engineered inorganic colloids: A review. *Environ. Sci. Technol*. **2014**, *48* (16), 8946-8962.

39. Wang, L.; Habibul, N.; He, D.; Li, W.; Zhang, X.; Jiang, H.; Yu, H. Copper release from copper nanoparticles in the presence of natural organic matter. *Water Res.* **2015**, *68*, 12-23.

40. Chen, W.; Habibul, N.; Liu, X.; Sheng, G.; Yu, H. FTIR and synchronous fluorescence heterospectral two-dimensional correlation analyses on the binding characteristics of copper onto dissolved organic matter. *Environ. Sci. Technol.* **2015**, *49*(4), 2052-2058.

41. Silverstein, R. M.; Bassler, G. C.; Morrill, T. C. *Spectrometric identification of organic compounds*; John Wiley & Sons: New York, 1963, pp. 83-139.

42. Klitzke, S.; Metreveli, G.; Peters, A.; Schaumann, G. E.; Lang, F. (2015). The fate of silver nanoparticles in soil solution - sorption of solutes and aggregation. *Sci. Total Environ.* **2015**, *535*, 54-60.

43. Adeleye, A. S.; Conway, J. R.; Perez, T.; Rutten, P.; Keller, A. A. Influence of extracellular polymeric substances on the long-term fate, dissolution, and speciation of copper-based nanoparticles. *Environ. Sci. Technol*. **2014**, *48* (21), 12561-12568.

44. Johnstone, T. C.; Nolan, E. M. Beyond iron: non-classical biological functions of bacterial siderophores. *Dalton Trans.* **2015**, *44*, 6320-6339.

45. Dimkpa, C. O.; McLean, J. E.; Britt, D. W.; Johnson, W. P.; Arey, B.; Lea, A. S.; Anderson, A. J. Nanospecific inhibition of pyoverdine siderophore production in Pseudomonas chlororaphis O6 by CuO nanoparticles. *Chem. Res. Toxicol.* **2012**, *25* (5), 1066-1074.

46. Teitzel, G. M.; Geddie, A.; De Long, S. K.; Kirisits, M. J.; Whiteley, M.; Parsek, M. R. Survival and growth in the presence of elevated copper: Transcriptional profiling of copper-stressed Pseudomonas aeruginosa. *J. Bacteriol.* **2006**, *188* (20), 7242-7256.

47. Pham, A. N.; Rose, A. L.; Waite, T. D. Kinetics of Cu(II) reduction by natural organic matter. *J. Phys. Chem. A* **2012**, *116* (25), 6590-6599.

48. McLean, J. E.; Pabst, M. W.; Miller, C. D.; Dimkpa, C. O.; Anderson, A. J. Effect of complexing ligands on the surface adsorption, internalization, and bioresponse of copper and cadmium in a soil bacterium, Pseudomonas putida. *Chemosphere* **2013**, *91* (3), 374-382.

49. Wang, Z. Y.; Li, J.; Zhao, J.; Xing, B. S. Toxicity and internalization of CuO nanoparticles to prokaryotic alga Microcystis aeruginosa as affected by dissolved organic matter. *Environ. Sci. Technol.* **2011**, *45* (14), 6032-6040.

CHAPTER 5

AGRICULTURAL SOIL PORE WATERS REDUCE TOXICITY OF COPPER OXIDE

NANOPARTICLES TO WHEAT (TRITICUM AESTIVUM) SEEDLINGS

Abstract

As CuO nanoparticles (NPs) may be applied on or near soils under agricultural conditions, the interactions of CuO NPs with soils, crops, and microbes must be further studied. One sub-lethal dose of CuO NPs, 100 mg/kg Cu/sand, was tested against wheat in a sand and soil pore water (SPW) matrix to mimic the solution phase of soils without the mineral surface complexities. A soil bacterium, *Pseudomonas chlororaphis* O6 (*Pc*O6), was added to half of treatments to test the effects of microbes in this matrix. After 10 days of growth, the wheat was harvested, indicators of plant health were recorded, and the pore water (PW) was analyzed for dissolved copper, pH, and root exudates. NP dissolution was increased with increasing dissolved natural organic matter (DNOM) content of the SPWs. SPWs protected wheat seedlings from some of the root shortening compared to the no-DNOM 3.34 M $Ca(NO_3)_2$ control, but did not fully remediate the seedlings. Two of the SPWs also decreased shoot copper uptake compared to the control despite increased soluble copper, but had no effect on root copper accumulation. CuO NPs increased dissolved organic carbon (a measure of DNOM and/or root exudates), malate, citrate, gluconate, 2'-deoxymugineic acid (DMA), and dissolved copper. Cu-DMA complexes were associated with toxicity symptoms in wheat. *Pc*O6 enhanced root shortening in the wheat seedlings in the presence of CuO

NPs, and degraded malate, citrate, and DOC which reduced the total dissolved copper concentrations in planted samples. *Pc*O6 did not degrade DMA, instead increasing DMA from wheat roots, possibly via resource competition between *Pc*O6 and wheat for iron. *Pc*O6 decreased soluble copper but did not decrease shoot copper uptake, although CuO NP contact with roots was diminished.

Introduction

Nanoparticles (NPs, particles less than 100 nm in at least one dimension) have potential uses in agriculture (Anderson et al. 2017). CuO NPs in particular have strong potential as a foliar fungicide (Elmer & White 2016) or fertilizers (Monreal et al. 2016; Dimkpa and Bindraban, 2017), and may find uses as drought treatments (Dimkpa et al. 2017). CuO NPs in these applications will inevitably contact soils through overspray/leaf litter of foliar applications or intentional application to soil. CuO NPs may also partition into biosolids in wastewater treatment plants and be applied to soils post-biological treatment (Keller et al. 2013; Cornelis et al. 2014; Otero-Gonzalez et al. 2014). Thus, the fate, transformations, and interactions of CuO NPs with soil, microbes, and plants must be further studied.

Toxicological studies show that CuO NPs have dose-dependent toxicity to many soil microbes and crops, but these studies typically test the challenge (CuO NPs) against the target organism in a well-defined system (Dimkpa et al. 2011a; Dimkpa et al. 2012b; McManus 2016; Peng et al. 2016). For example, CuO NPs have dose-dependent toxicity to wheat, an important global crop, when tested in simple sand and water systems with and without a background electrolyte (Dimkpa et al. 2012b, McManus 2016). However,

the soil solution environment contains a rich mixture of microbes, dissolved natural organic matter (DNOM), and dissolved minerals and gases among other components. Relatively few studies investigate the toxicity of CuO NPs in whole soils (Schlich et al. 2016; Singh and Kumar 2016; Anderson et al. 2017b; Peng et al. 2017) or similar systems. Fewer still investigate how whole soil affects the NPs. Complexes of Cu with organic and inorganic ligands, changes in speciation with pH and ionic strength, and surface coatings of the NPs change the behavior of the NPs and the plant and bacteria response. As soils inherently contain bacteria and DNOM, the dissolution of Cu from CuO and subsequent uptake into the plant may be affected. In semi-arid soils with alkaline pH, the higher pH limits solubility of CuO (Palmer and Bénézeth 2004) and uptake of the NPs. Complexation reactions of dissolved Cu with inorganic or organic ligands may also alter Cu uptake into wheat plants. Even in semi-arid soils, sufficient DNOM may exist to bind dissolved Cu ions, which may protect seedlings from the NPs' influence.

CuO NPs may also stimulate and/or interact with exudation of organic molecules from roots and bacteria. In wheat, sand, water (with a background salt) and CuO NP systems, the roots increased exudation of organic compounds, including citrate, malate, and the phytosiderophore 2'-deoxymugineic acid (DMA) (McManus 2016). The increased exudation also increased soluble Cu from the CuO NPs, and Cu uptake into the shoot was positively correlated with increased exudation (McManus 2016). Bacteria increase solubility of CuO NPs through similar mechanisms of release of extracellular polymeric substances (Adeleye et al. 2014; Miao et al. 2015) and possibly iron

siderophores such as pyoverdines, which complex with Cu (Dimkpa et al. 2011b; Dimkpa et al. 2012b).

The objectives of this study were to examine the toxicity, uptake, solubility, and distribution of Cu in plant, sand, or liquid phases of CuO NPs as affected by differing soil pore water (SPWs) chemistries, soil bacteria, and wheat. Replicated growth studies were performed in a factorial design with four factors: presence/absence of wheat seedlings, CuO NPs, a soil bacterium, *Pseudomonas chlororaphis* O6 (*Pc*O6), and three SPWs (plus a control salt solution). The SPWs varied primarily in DNOM, but also cations (calcium, magnesium, sodium, and potassium) and anions (chloride, sulfate, and nitrate). A Cu mass balance was conducted on the entire system after wheat growth to study Cu distribution. The dissolved Cu in the pore waters (PWs) was measured after exposure to the wheat and SPWs to examine NP solubility. Finally, wheat growth was examined to determine NP toxicity and uptake with and without *Pc*O6. The results showed that CuO NPs partially dissolved in the PWs, and that SPWs remediated some of the toxic effects of CuO NPs on the wheat seedlings, dependent on the SPW, compared to the control PW and previous experiments. *Pc*O6 decreased CuO NP solubility overall, but increased damage to root length from CuO NPs.

Materials and Methods

Experimental design

The experiments were designed to test the mixed effects of SPWs, bacteria, and plant growth on CuO NPs. Silica sand supplemented with either a 3.34 M $Ca(NO_3)_2$ PW solution or SPW was the growth matrix; the SPW matrix is more complex than previous

experiments by including soluble soil components without the complexity of the soil solid phase. The concentration of the 3.34 M $Ca(NO_3)_2$ solution was chosen because the ionic strength was in the range of the SPWs tested. One dose of CuO NPs (100 mg/kg Cu/sand) was chosen as this dose has been previously shown to be sub-lethal to wheat while causing substantial root-shortening and increased root exudation (McManus 2016).

All experiments were conducted with independent triplicate samples. The factors used were the presence/absence of wheat plants, the presence/absence of a well-studied root-colonizing bacteria (Dimkpa 2011a) previously isolated from a wheat field soil, *Pseudomonas chlororaphis* O6 (*Pc*O6), the presence/absence of CuO NPs, and type of PW (one control solution and three SPWs; Table B-1 and B-2). The entire experiment was repeated after the first run to test the reproducibility of the results.

Preparation of soil pore waters and root-colonizing bacteria

Five soils were collected from agricultural and grassland sites in Northern Utah Cache County, UT, USA in late summer 2016 as previously described (Chapter 3). Two out of the five soils collected were eliminated from this experiment because the Warm Springs soil (WS) was an outlier in terms of almost every variable, and the iron-deficient Millville soil (IDM) was not an agricultural soil. The three selected soils (Millville series, coarse-silty, carbonatic, mesic *Typic Haploxerolls*) had similar pH but varied crop management practices, altering NOM characteristics. Characteristics of the soils (predominant crops, cultivation techniques) are given in the Chapter 4 supporting information (Table A-1). SPWs were generated per standard methods (Rhoades 1996) as

previously described (Chapter 4). Characteristics of the SPWs, such as pH, EC, soluble cations, anions, and organic matter are given in Chapter 4 (Table 4-1, Table A-4).

Stock cultures of *Pc*O6 were stored frozen at -80 °C in 15% glycerin until use. Stocks were placed onto minimal medium agar plates to grow overnight into the log phase, at which time sterile water was added to the agar plate to create a suspension of cells. The cells were diluted to ~1x10^7 CFU/mL before addition to the SPWs.

Preparation of wheat seeds, growth boxes and growth conditions

Wheat (*Triticum aestivum*) seeds (Dolores variety, hard red winter wheat) were sterilized in 3% bleach for 10 minutes, then rinsed at least five times in sterile deionized water. The seeds were sown onto Luria-Bertani agar (LB) petri dishes at approximately 25 seeds per dish according to the methods of McManus (2016). The petri dishes were sealed with parafilm and incubated for four days at 25 ºC.

Silica sand (UMINIC Corp, ID) was washed by hand in deionized water three times, then placed in a 550 ºC muffle furnace to volatilize organic matter. After removal of organic matter, the sand was washed with deionized water again and set to dry in a 100 ºC oven (McManus 2016).

One hundred milligrams Cu/kg sand (as CuO NPs) was added to the dry sand, shaken by hand, and then shaken at high speed on a reciprocal shaker for 30 minutes (McManus 2016). The NPs were previously characterized (Chapter 4). Three hundred grams of sand with the CuO NPs was dosed into acid-rinsed magenta boxes (Sigma-Aldrich, V8505, 10x7x7 cm). The magenta boxes were closed, autoclaved at 121 ºC for 2 hours, and allowed to cool to room temperature.

The PW was 45 mL of sterile 3.34 mM $Ca(NO_3)_2$ (control) or 0.2 micron-filter sterilized SPWs (OrgM, AgrM, GM), which was added to the sand in triplicate boxes and mixed with a sterile spatula in a laminar-flow hood. The ratio of water to sand was 1.5 times field capacity (McManus 2016). Twenty-five germinated wheat seeds from the agar plates which showed no signs of microbial infection were spread evenly into each box and then covered with one-half cm of sand (McManus 2016). The boxes were closed again and wrapped in parafilm to minimize water losses and air exchange during the growth period. If PcO6 needed to be present in the boxes (as per the experimental design), a 250 µL aliquot of about $1x10^7$ CFU/mL of PcO6 was added to each 45 mL aliquot of soil pore water prior to watering the sterile boxes.

Boxes were set under fluorescent lamps generating a photosynthetic photon flux density of 144 pmol m^{-2} s^{-1} at the box surface for 10 days under a 16-hour light/8-hour dark cycle (Dimkpa et al. 2012a) in a constant temperature room set at 25 ℃ (Figure B-1). The boxes were randomly rotated daily to minimize light gradient effects.

Harvesting and analytical procedures

On the 10th day of growth, the boxes were opened at 3-6 hours after the beginning of the light cycle to ensure maximum root exudation (Oburger et al. 2014). Forty-five mL of sterile deionized water was added to each box and allowed to sit for 15 minutes (McManus 2016). If wheat seedlings were present, they were gently pulled from the sand, shaken to remove loose sand, and one root was placed on a sterile LB petri dish to test for microbial colonization. The sand was mixed and placed in a sterile, acid-rinsed glass funnel to extract the PW by vacuum. Fifteen µL of PW was immediately

placed on an LB petri dish to test for bacterial contamination and/or verify the presence of *Pc*O6 (if present in the boxes initially). The roots of the plants were rinsed with deionized water to remove attached sand, the root length was measured, and then the shoots and roots were sectioned and placed into clean plastic bags while the coleoptile portion (about 3 cm of shoot above the seed) was discarded due to potential NP contamination (McManus 2016).

The pH and EC of the PW were measured by standard methods (APHA 2012). Aliquots of PW (approximately 4.5 mL) were centrifuged at ~17,800 x g for 15 minutes, a time and speed calculated by the Stokes-Einstein equation to pellet CuO NPs larger than 10 nm, and the supernatant was collected (about 3 mL). Four mL of PW was filtered by a 3 kDa ultrafilter to partition dissolved Cu complexed to DNOM < 3 kDa from dissolved Cu complexed to DNOM > 3 kDa. Both techniques were characterized previously (Chapter 3) to remove CuO NPs > 10 nm (centrifugation) or 1.3 nm (ultrafiltration). Ultrafiltration also removes a portion of the DNOM (Chapter 4). Dissolved metals and DNOM in both the centrifuged and ultrafiltered portions were measured by ICP-MS with USEPA method 6020 and carbon analyzer as dissolved organic carbon (DOC) with standard methods (APHA 2012), respectively. Low molecular weight organic acids (LMWOAs) and inorganic anions were measured by ion chromatography (Dionex method 123) after centrifugation. The root exudate DMA was measured using liquid chromatography triple quadrupole mass spectrometry as outlined by McManus (2016), and the bacterial siderophore pyoverdine was measured by fluorescence as outlined by Dimkpa et al. (2011b). Free Cu^{2+} was measured with an ion-

selective electrode (Rachou 2007). Metal contents in the roots, shoots, and sand were measured by ICP-MS after hot nitric acid digestion (Jones and Case 1990; EPA 1996). A geochemical equilibrium model (MINTEQ v 3.1; Gustaffson 2013) was used to compare theoretical dissolved Cu to actual measurements (see Chapter 4 for more details).

To back-calculate the concentrations of constituents in the pore waters, the boxes were weighed at the beginning and end of the growth period (10 days). Boxes typically lost amounts of water between 0-2 grams (mL). Roots and shoots were weighed before and after drying to measure the water taken into the plant. The following formula was applied to calculate a dilution factor:

$$Dilution\ factor_{box\ \#x} = \frac{1}{\frac{(45\ mL - (water\ loss\ from\ box, plant\ in\ g\ or\ mL))}{(90\ mL - (water\ loss\ from\ box, plant\ in\ g\ or\ mL))}}$$

The concentration of each detected PW constituent was multiplied by the calculated dilution factor for each box to obtain the true concentrations. Dilution factors ranged from 2.01-2.05 (for unplanted boxes) and 2.15-2.30 (for planted boxes).

Statistical analysis

Principal components analysis (PCA) was used to determine relationships among variables in wheat and in PWs. PCAs use linear combinations of all included variables to reduce variability to fewer dimensions than the original dataset. Variables included in the PCA were only included if < 50% of the measurements were censored (i.e., the censored data could be imputed). Censored data were imputed from a normal distribution of the non-censored data. To confirm relationships among variables, the significance and magnitude of the pairwise Pearson's correlations was considered.

A chi-squared test (p = 0.05) was used to determine if microbial contamination was evenly distributed across all treatments.

Analysis of variance (ANOVA) was used to determine if significant differences existed between samples under varied tested conditions. The variables DOC, dissolved Cu, free Cu^{2+}, and Cu size distribution (above or below 3 kDa) were analyzed with a four-way ANOVA with factors presence/absence wheat, presence/absence PcO6, presence/absence of CuO NPs, and PW type (three SPWs and one control calcium nitrate solution). Root and shoot length, and root and shoot Cu contents were analyzed by three-way ANOVA with factors presence/absence PcO6, presence/absence of CuO NPs, and PW type. Post-hoc testing was performed using the Tukey honestly significant difference (HSD) test to determine significant differences among the factors (main effects) and factor interactions in the samples (p = 0.05). Censored data were imputed from a normal distribution of the non-censored data only if at least 50% of the data points were not censored. The data for each measured variable is presented by first identifying the significance and magnitude (if applicable) of each main effect, followed by the significant interactions. A main effect is the average of all data points with the factor (i.e., presence of PcO6) versus the average of data points without the factor (i.e., absence of PcO6). An interaction indicates that the impact of one factor depends on the level of other factors. Interactions split the data into $2^{(n+m)}$ subgroups, where n = number of factors and m = 1 if PW type is one of the main factors (m = 0 otherwise). Square root and logarithmic transformations were necessary in some variables to maintain normal distribution of the residuals. Measurements shown in graphs and in the text are the

average of the two independent studies with triplicate samples ± the Tukey HSD or Student's t-test statistical significance bar.

Results and Discussion

Quality control: Bacterial contamination

Before the objectives were examined, the quality control of the study was first established through bacterial contamination. Bacterial contamination in planted systems, particularly for aseptic conditions, is not commonly reported in the literature. Other standard quality control data, such as analytical blank samples, spikes, and calibration concentration verification samples, were satisfactory for all reported analyses.

Overall, 60 out of 192 boxes (31%) tested positive for foreign bacteria (Table 5-1) by culture on LB agar. *Pc*O6 formed wet, orange colonies whereas contaminating bacteria took many differing forms. Under these conditions, contamination in the growth boxes could not be completely avoided, even with autoclaving of the boxes and sand before use, thorough surface sterilization of the seeds and initial growth on sterile LB plates, and aseptic techniques. The contamination was spread evenly across PW types (29-35%), but were primarily found in planted samples compared to unplanted samples (48% versus 15%), non-*Pc*O6 samples compared to *Pc*O6 samples (61% versus 1%), and non CuO NP samples compared to CuO NP samples (39% versus 24%) (Table 5-1). By a chi-squared test, PW type did not significantly impact contamination rates, but the presence of wheat ($p < 0.0001$), the lack of CuO NPs ($p = 0.0287$), and the lack of *Pc*O6 ($p < 0.0001$) increased contamination rates.

Table 5-1: Number of contaminated boxes by wheat, CuO NPs, and *Pc*O6 treatments. Each cell contains a maximum of six boxes.

| | Planted | | | | Unplanted | | | | |
| | CuO NPs | | Non-CuO NPs | | CuO NPs | | Non-CuO NPs | | |
PW	*Pc*O6	Non-*Pc*O6	*Pc*O6	Non-*Pc*O6	*Pc*O6	Non-*Pc*O6	*Pc*O6	Non-*Pc*O6	**Totals**
Control	0	5	0	6	0	0	0	3	14
OrgM	0	6	0	6	0	0	0	4	16
AgrM	0	5	1	5	0	0	0	3	14
GM	0	6	0	6	0	1	0	3	16
Totals	0	22	1	23	0	1	0	13	60

Contamination almost always occurred in planted, non-*Pc*O6, non-CuO NP growth boxes and occasionally in unplanted, non-*Pc*O6/non-CuO NPs boxes. Given the even distribution of infection across all SPWs, the SPWs were not the likely source. Most likely, endophytes living inside the seed grew after transplanting despite the described precautions. Endophytes are common in wheat and are associated with different genera but often isolates have biocontrol activity (Díaz Herrera et al. 2016; Comby et al. 2017). The toxicity of CuO NPs to a variety of microbes (as seen in soils by Frenk et al. 2013, for example) and the competitive native *Pc*O6 against the microbes explains the lower rates of infection in treatments with each of those two variables.

Ultimately, the impact of the contaminating bacteria was likely small compared to the *Pc*O6, but cannot be quantified because no sterile control exists. However, three lines of evidence show that the influence of the endophytic bacteria was minimal. First, citrate and malate were detectable in contaminated, planted boxes, but they were not in *Pc*O6 planted boxes. The lack of metabolism of the LMWOAs shows that the contaminating bacteria were not very active compared to *Pc*O6. Second, when contaminated unplanted, non-*Pc*O6, non-CuO NP samples were compared to sterile

unplanted, non-*Pc*O6, non-CuO NP samples (the only data points which can be compared to each other because of the ~50% contamination rate) by one-way ANOVAs, no SPW significantly changed in DOC or pH (Figure B-2). *Pc*O6 did alter DOC and pH when it was present, however. Third, although a one-way ANOVA showed significant differences in gluconate, DOC, DMA, and dissolved Cu between contaminated and non-contaminated samples, the exact same measurements were similarly affected by *Pc*O6 in a one-way ANOVA (Figure B-3). As contaminated samples aligned very well with non-*Pc*O6 samples (i.e., all but one contaminated box were non-*Pc*O6 samples, due to the aggressiveness of *Pc*O6), these changes were likely due to the presence of *Pc*O6, not the presence of contaminating bacteria.

PCA Results

To guide discussion of the results, two PCAs were performed to discover related variables according to the two objectives of this study. First, dissolved Cu was examined in CuO NP samples with all detectable potential complexing anions and pH/EC. The samples grouped into two main clusters: The GM PW separated from the other three PWs along both principle components one and two (Figure 5-1A). The variable loading showed four main variable groupings: Nitrite/DMA, EC/nitrate, pH/sulfate, and dissolved Cu/DOC (Figure 5-1B). GM SPW contains higher concentrations of salts than the other SPWs (Table A-4) which is what separates GM from the other cluster.

Relationships shown in the PCA were confirmed by Pearson's correlations. Significant Pearson's correlations existed between dissolved Cu and every component
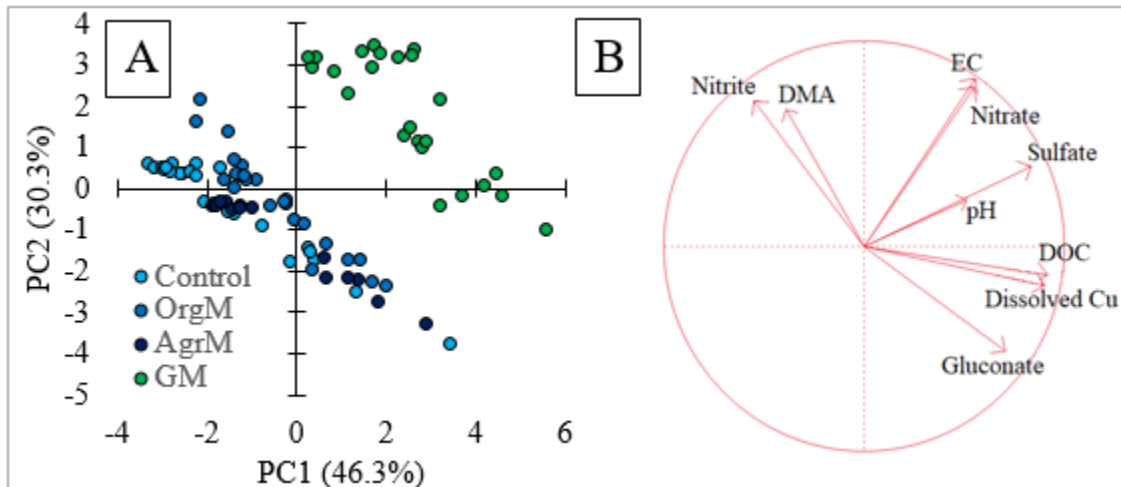
Figure 5-1: Score plot (A) and loading plot (B) of PCA of NP samples in study. Variables (9) included gluconate, nitrite, nitrate, sulfate, DMA DOC, pH, EC, and dissolved Cu. Chloride and other low molecular weight organic acids were not included because they were below detection > 50% of samples.

in the PCA. The magnitude of R was also considered; a cutoff of R = 0.5 was chosen arbitrarily to help identify correlations with less scatter. Gluconate (R = +0.719), DOC (R = +0.916), and sulfate (R = +0.8081) correlated with dissolved Cu and had R values above 0.5. All remaining correlations fell below R = 0.4. However, while dissolved Cu and gluconate/DOC had continuous, linear relationships over both the x and y plane, sulfate and dissolved Cu had two distinct clusters of points connected by the correlation line. The GM PW had high sulfate concentrations (~ 160 mg/L) but the other PWs had far lower sulfate concentrations (below detection to ~30 mg/L). From these results, sulfate was not considered important to dissolved Cu, and it was determined that dissolved Cu should be examined in concert with DOC and gluconate.

A PCA of all planted samples was also performed to elucidate relationships between root/shoot lengths and root/shoot Cu and other variables. The samples with CuO NPs were separated from non-CuO NP samples mainly along the first principal

component axis (Figure 5-2A). The GM SPW samples also separated from the other

three PWs, as in Figure 5-1A, along the second principal component axis. Two main

variable loadings were observed: a group with pH, EC, and shoot length, and a group

with dissolved Cu, root/shoot Cu, citrate, gluconate, and DMA (Figure 5-2B). The latter

group was inversely associated with root length. In other words, increasing

concentrations of dissolved Cu, root/shoot Cu, gluconate, citrate, and DMA were

associated with shorter root lengths.
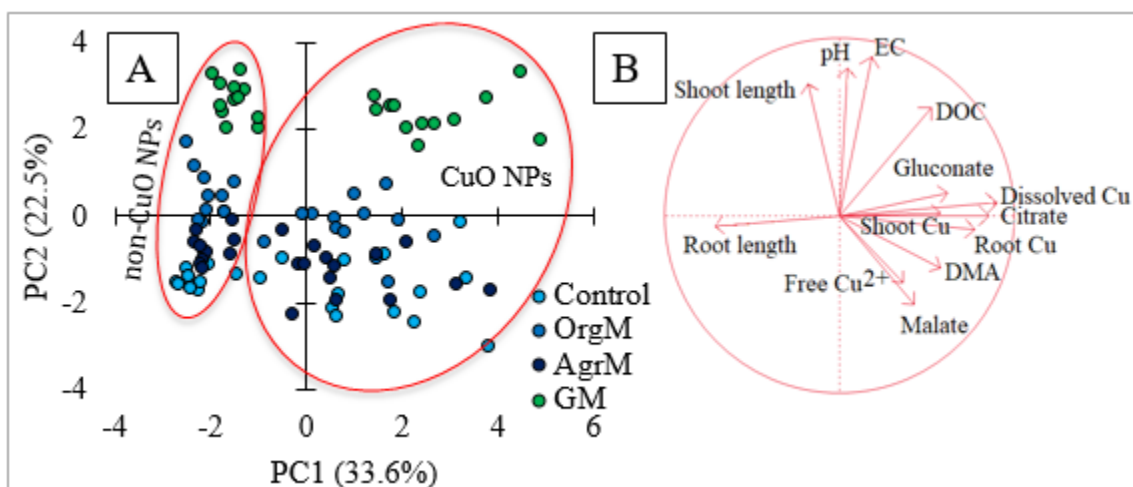
Figure 5-2: PCA score plot (A) and loading plot (B) of all planted samples in study. Variables included (13) were gluconate, malate, citrate, DMA, DOC, pH, EC, dissolved Cu, free Cu^{2+}, root Cu, shoot Cu, root length, and shoot length.

Pearson's correlations showed that shoot Cu only had one correlation with an R

value greater than 0.5 (shoot Cu and root length, R = -0.5416). Root Cu had several

correlations with an R value greater than 0.5: Root Cu and gluconate (R = +0.520),

citrate (R = +0.522), dissolved Cu (R = +0.7621), and root length (R = -0.517). Shoot

length only correlated above R = 0.5 with EC (R = +0.572). Finally, root length had four

correlations above R = 0.5: Root length and DMA (R = -0.6109), dissolved Cu (R = -

0.560), shoot Cu (previously listed), and root Cu (previously listed). In summary, root Cu and root length were the variables with the greatest number of important correlations. Dissolved Cu was important to both root Cu and root length. Gluconate, citrate, and DMA appeared to play important roles in root Cu and root length as well.

In the second PCA, dissolved Cu again correlated above R = 0.5 with DOC and gluconate, but also with citrate (R = +0.720), showing that citrate should also be considered with dissolved Cu in planted samples.

Dissolved Cu: Relationship with DOC, gluconate, and citrate

An objective of this study was to determine how the solubility of the CuO NPs was affected by different PWs, and the presence/absence of wheat and *Pc*O6. The dissolution of Cu was expected to be partially dependent on DOC, gluconate, and citrate from Figure 5-1. Dissolved Cu, DOC, and gluconate were evaluated by four-way ANOVA, while citrate was evaluated only in planted, non-*Pc*O6 samples by two-way ANOVA (presence/absence of CuO NPs, and differing PWs).

Gluconate was elevated in the SPWs compared to the control (Figure 5-3A), increased by CuO NPs (Figure 5-3B) and wheat (Figure 5-3C), and decreased by *Pc*O6 (Figure 5-3D). Gluconate was always present with or without wheat, NPs, or *Pc*O6 in the PWs and had no obvious source. *Pc*O6 seemed to partially metabolize the gluconate, while CuO NPs and wheat provoked an elevated gluconate response, perhaps as a stress response. The SPWs, which had low levels of gluconate at the start (OrgM = 1.9 mg/L, AgrM = 3.9 mg/L, GM = below detection) seemed to promote formation of gluconate better than the control.
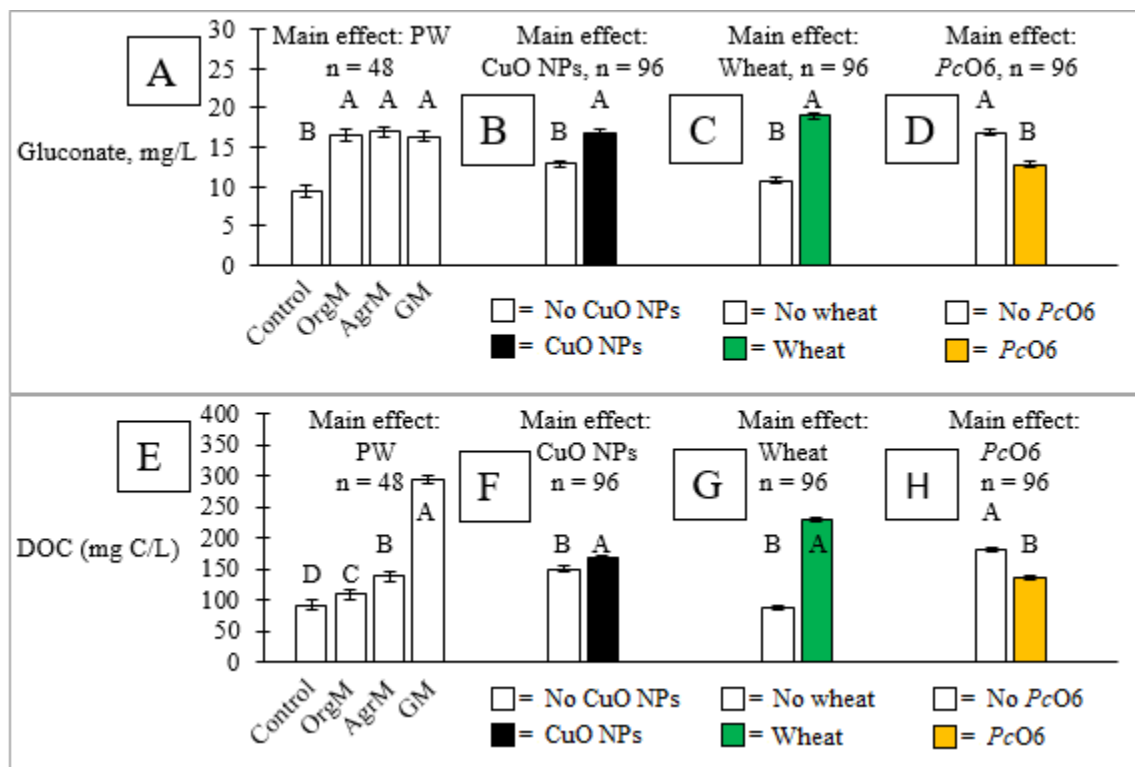
Figure 5-3: Gluconate concentrations by main effects PW (A), CuO NPs (B), wheat (C), and *Pc*O6 (D) and DOC concentrations by main effects PW (E), CuO NPs (F), wheat (G), and *Pc*O6 (H). Main effect bars contain all samples with the factor listed below the bars, regardless of whether other factors differ; i.e., PW bars contain all samples with the PW indicated regardless of whether wheat, *Pc*O6, or CuO NPs were present or not. Bars = average of independent sample measurements, and error bars = Tukey HSD or Student's t-test statistical significance. Bars with differing letters (A, B, etc.) are statistically different ($p < 0.05$). Gluconate and DOC required a square root transformation for ANOVA to maintain normal distribution of residuals.

DOC increased in the SPWs above the control (Figure 5-3E), was increased by CuO NPs (Figure 5-3F) and wheat (Figure 5-3G) and was decreased by *Pc*O6 (Figure 5-3H). The SPWs naturally had variations in DOC, explaining the differences seen between PWs. Wheat produced root exudates, increasing DOC, whereas *Pc*O6 metabolized root exudates. CuO NPs increased DOC by stimulating wheat to produce more root exudates, though this effect was the smallest of all main effects.

Dissolved Cu was increased in the SPWs compared to the control (Figure 5-4A) in the same pattern as DOC (Figure 5-3E). Dissolved Cu increased in the presence of CuO NPs (Figure 5-4B) and wheat (Figure 5-4C) due to production of root exudates (Figure 5-3G). Dissolved Cu decreased with *Pc*O6 (Figure 5-4D) due to *Pc*O6's metabolism of root exudates (Figure 5-3H), removing many of the plant produced ligands that potentially complex Cu in solution, despite possibly simultaneously producing new Cu ligands or stimulating the release of differing root exudates. As an example, *Pc*O6 stimulated the release of more DMA from wheat roots than without *Pc*O6.
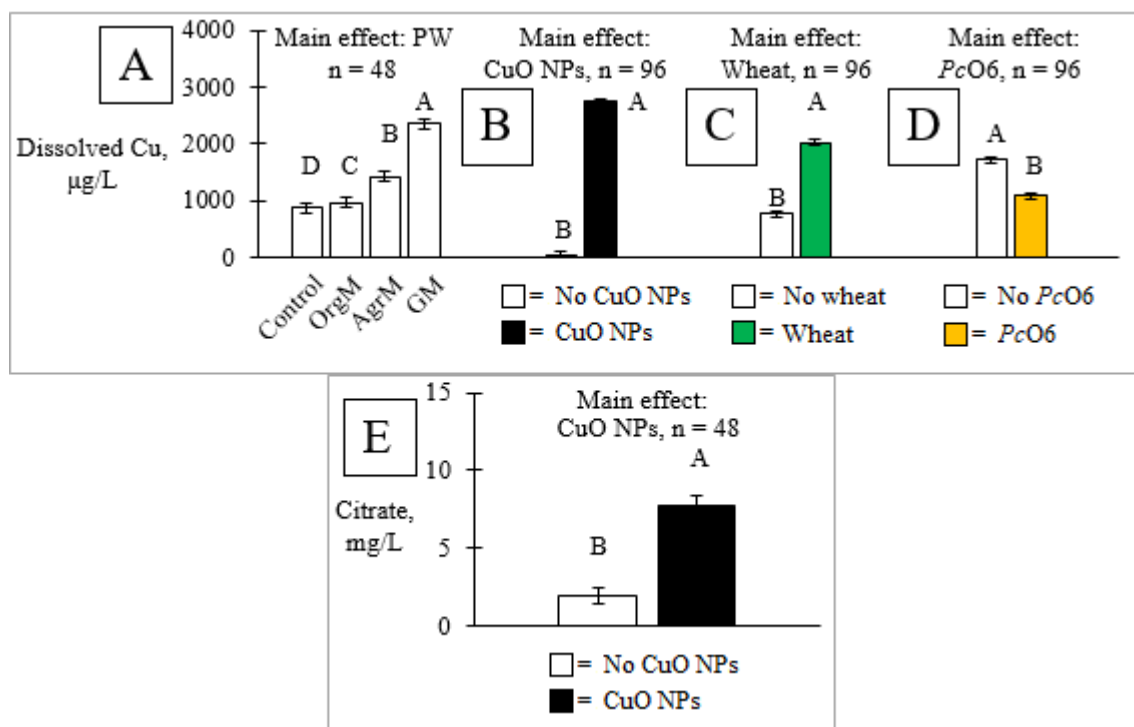
Figure 5-4: Dissolved Cu by main effects PW (A), CuO NPs (B), wheat (C), and *Pc*O6 (D), and citrate by main effect CuO NPs (E). Bars = average of independent sample measurements, and error bars = Student's t-test or Tukey HSD statistical significance. Bars with differing letters (A, B, etc.) are statistically different (p < 0.05). Dissolved Cu required a square root transformation for ANOVA to maintain normal distribution of residuals.

Citrate could only be analyzed by a two-way ANOVA because there was no citrate detected without wheat (due to citrate being a root exudate of wheat) or with PcO6 (because PcO6 metabolized citrate when present). Citrate was not altered by PW (Figure 5-4E), but was increased by CuO NPs (Figure 5-4F) like gluconate and DOC.

Interactions of the test parameters were important to gluconate, DOC, dissolved Cu, and citrate. All combinations of interactions were significant to dissolved Cu (with the exception of PW/PcO6), including the four-way interaction of PW, PcO6, CuO NPs, and wheat (the highest interaction; Figure 5-5A). Dissolved Cu levels in samples without CuO NPs were low (≤ 121 µg/L) and were not statistically different, so they are not shown in the figure (though still included in the four-way ANOVA). The four-way interaction was not significant for DOC, but the three way-interaction of PW, PcO6, and wheat was (Figure 5-5B). CuO NPs did not change DOC in combination with PW/PcO6/wheat, so the data for samples with and without CuO NPs are grouped together in Figure 5-5B.

In the control PW with no wheat or PcO6, dissolved Cu reached ~270 µg/L with ~73 µg/L activity of free Cu^{2+}. DOC was similarly low (Figure 5-5B). Geochemical modeling of the control system at the measured average pH, 6.51, predicts that ~431 µg/L Cu with 265~ µg/L activity of free Cu^{2+} will dissolve. The results indicate that the predicted Cu solubility was not met. Furthermore, ~197 µg/L Cu (the difference between the total dissolved Cu and the activity of free Cu^{2+}) was complexed or otherwise did not generate a response from the ion selective electrode. A geochemical model of this system predicted that gluconate, formate, acetate, nitrate, alkalinity (from atmospheric
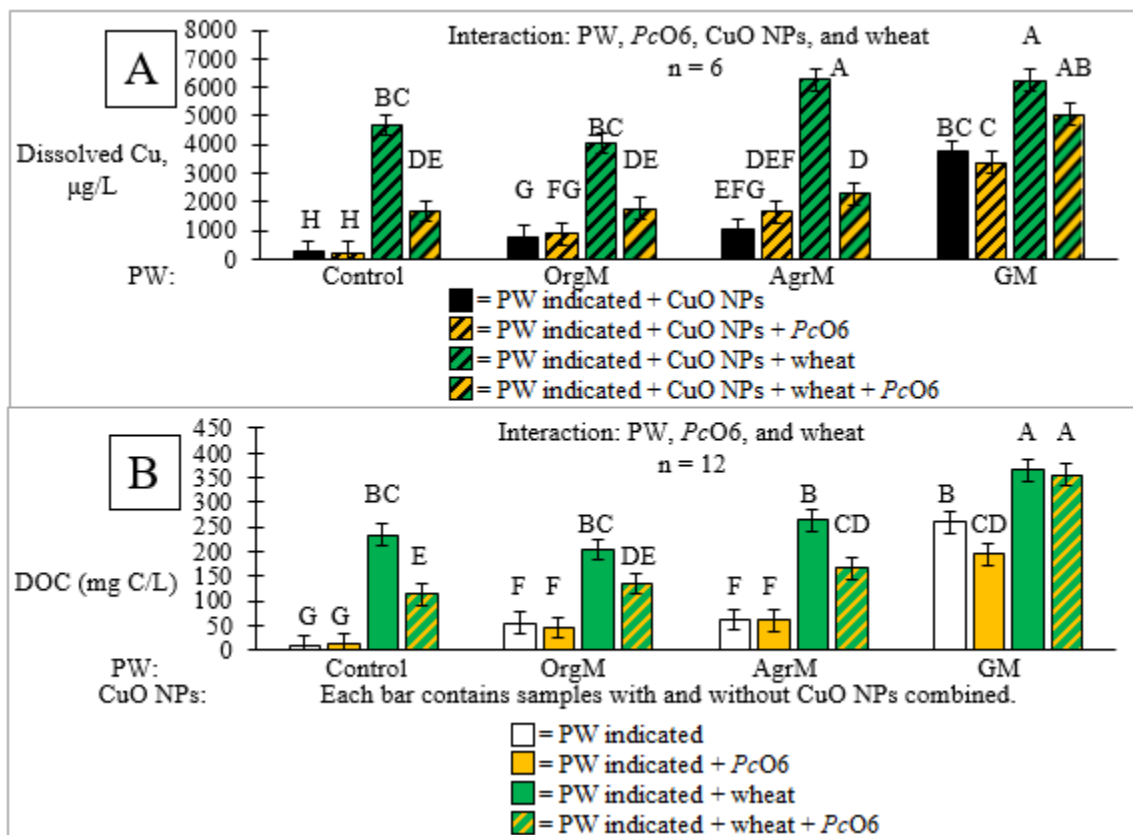
Figure 5-5: Dissolved Cu by interaction of PW, *Pc*O6, CuO NPs, and wheat (A) and DOC by interaction of PW, *Pc*O6, and wheat (B). Bars = average of independent sample measurements, and error bars = Student's t-test or Tukey HSD statistical significance. Bars with differing letters (A, B, etc.) are statistically different (p < 0.05). Dissolved Cu required a square root transformation for ANOVA to maintain normal distribution of residuals.

CO_2) and hydroxide in the control PW provided the complexing anions for the dissolved Cu.

The SPWs with CuO NPs but without wheat/*Pc*O6 (Figure 5-5A) dissolved more Cu (800-3,800 µg/L) than the control PW under the same conditions (Figure 5-5A, 270 µg/L), likely due to the humic and fulvic acids components of the SPWs (Table 4-1) complexing Cu ions. Geochemical models of the PWs without wheat/*Pc*O6 confirmed that FA and HA were the major drivers (~75-95%) of Cu complexation. DOC in the

PWs without wheat/*Pc*O6 (Figure 5-5B) increased in the same order as dissolved Cu

(Figure 5-5A). The dissolved Cu measurements matched well with geochemical

modeling predictions. The OrgM, AgrM, and GM SPWs dissolved 133%, 107%, and

71% of the predicted dissolved Cu concentrations, respectively (Figure 5-6) compared

with 62% for the control. The measured free Cu^{2+} ion activities compared to the model

were less satisfactory, at 28%, 272%, 146%, and 179% for the control, OrgM, AgrM,

and GM SPWs, respectively.
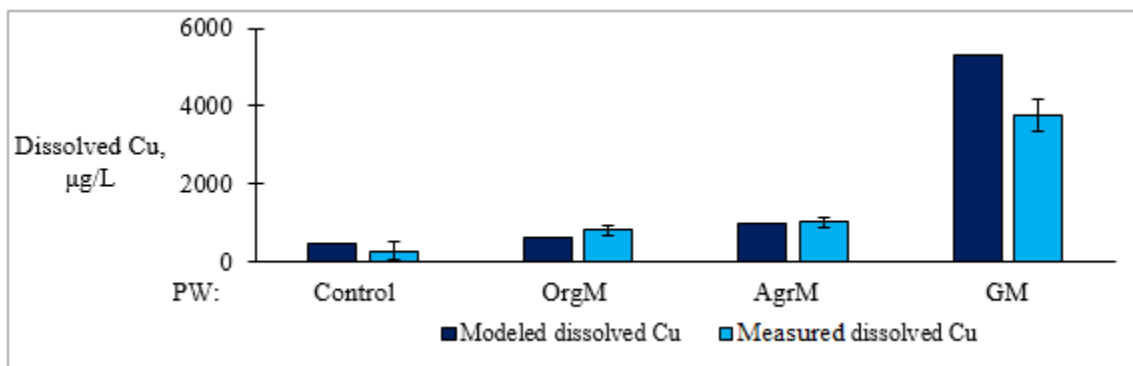
Figure 5-6: Modeled vs. measured dissolved Cu in the four PWs with CuO NPs, but without wheat/*Pc*O6. Bars for "Measured dissolved Cu" represent the average of six independent measurements and error bars represent the standard deviation of the measurements. Bars for "Modeled dissolved Cu" represent the model output of the sum of all forms of dissolved Cu.

These results contrasted with Chapter 4 results, in which the CuO NPs in the same

SPWs (but in an Erlenmeyer flask rather than a sand matrix) dissolved 41%, 31%, and

3.6% of the predicted dissolved Cu concentrations for the OrgM, AgrM, and GM SPWs,

respectively, despite similar incubation lengths (10 days). The differences which could

have contributed between these two studies were likely 1) differences in pH and changes

in solution chemistry, 2) the presence of sand, which may have provided more surface

area for the FA/HA to coat (rather than coating only the NPs as in Chapter 4 and

suppressing dissolution), and 3) the increased surface area from higher concentration of

CuO NPs in this study (equivalent to 667 mg/L Cu from CuO NPs when accounting for

300 g sand and 45 mL PW per box) versus Chapter 3 (10 mg/L Cu). The changes in pH

in the PWs were previously shown to impact dissolved Cu by no more than 26% (Figure

4-1D, Figure A-6). Changes in solution chemistry between the original SPWs (Table 4-

1) and the PWs from the sand (primarily decreases in DOC of 0-20 mg/L, increases in

gluconate, and small fluctuations in major cations/anions which occurred in the PWs +

sand compared to just the SPWs) were not large enough to result in major differences in

geochemical model output. Rather, the sand and higher concentration of CuO NPs likely

provided greater surface area for the humic and fulvic acids to coat, resulting in lesser

coatings, faster kinetics of dissolution, and overall greater NP dissolution during 10

days.

Without wheat the addition of *Pc*O6 with the control or the SPWs did not affect

the dissolution of Cu over that observed in the absence of *Pc*O6 (Figure 5-5A). DOC in

the PWs without wheat was also unaffected by *Pc*O6 (Figure 5-5B) except for GM

which decreased with *Pc*O6. Geochemical modeling indicated the PWs with *Pc*O6 but

without wheat dissolved 140%, 213%, and 84% of the modeled dissolved Cu in the

OrgM, AgrM, and GM PWs, respectively, compared to 815% in the control. In general,

more Cu dissolved than was predicted, suggesting that the *Pc*O6 produced exudates not

included in the geochemical model which complexed additional Cu than PWs with no

*Pc*O6. Pyoverdines were never detected in solution, however. CuO NPs decrease

pyoverdine production from *Pc*O6 (Dimkpa et al. 2012a), which may explain the lack of pyoverdines. The Cu-complexing exudates *Pc*O6 produced remain unknown and must await future studies, but may include extracellular polymeric substances or additional siderophores.

With wheat, the control and all SPWs dissolved significantly more Cu than without wheat; dissolved Cu concentrations ranged from 4,000 µg/L (OrgM) to 6,300 µg/L (AgrM) (Figure 5-5A) and were elevated due to enhanced root exudate production by the wheat (Figure 5-5B), as also seen by McManus (2016). Overall, the PWs with wheat dissolved 641%, 510%, and 149% of the modeled dissolved Cu for the OrgM, AgrM, and GM PWs, respectively, compared to 1089% in the control. These results suggest that many Cu-complexing plant exudates are unknown in this study and missing from the model. Missing model components are confirmed to exist because the known exudates combined with the original DOC in the PWs do not add up to the total DOC measured after wheat growth. The total DOC, as well as individual components malate, citrate, and DMA, were increased in planted samples by CuO NPs (Fig 5-7). Increased wheat root exudation by CuO NPs has been seen before in hydroponic systems (Michaud et al. 2008) and sand and water matrices (McManus 2016). Wheat production of malate and citrate increased in the presence of Cu ions (Nian et al. 2002). As citrate dissolves CuO NPs and complexes Cu (Zabrieski et al. 2015), the stimulation of citrate production by the NPs or ions may have resulted in a feedback mechanism (McManus 2016) dissolving more Cu and stimulating more exudate production.
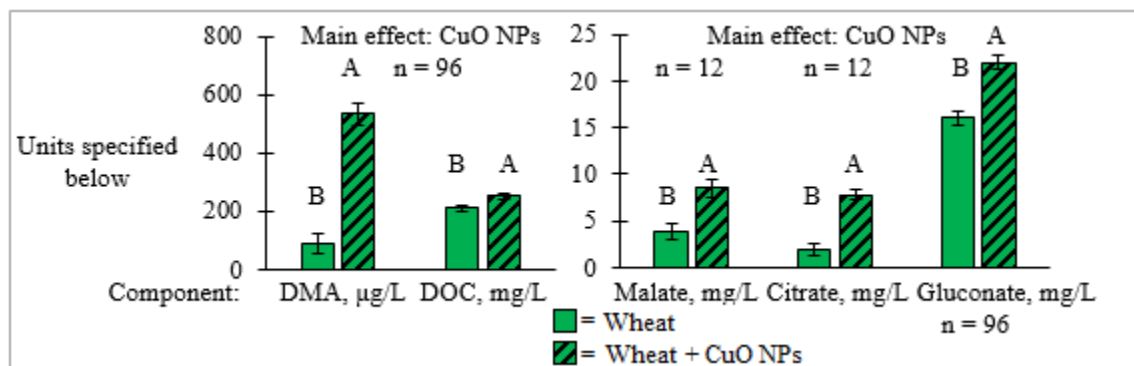
Figure 5-7: DMA, DOC, malate, citrate, and gluconate in planted samples with and without CuO NPs. Bars = average of independent sample measurements, and error bars = Student's t-test statistical significance. Bars with differing letters (A, B, etc.) are statistically different ($p < 0.05$).

When *Pc*O6 was present in planted systems (Figure 5-5A), dissolved Cu concentration decreased to values between those observed for the planted and unplanted systems without *Pc*O6 (in the control, OrgM, and GM SPWs) or back to the original unplanted system concentration without *Pc*O6 (AgrM SPW), consistent with results seen by Wright et al. (2016). DOC followed a similar trend (Figure 5-5B), suggesting that the root exudates were being metabolized by the *Pc*O6, removing potential chelators from solution. Overall, the PWs with wheat and *Pc*O6 dissolved 140%, 214%, and 128% of the modeled dissolved Cu in the OrgM, AgrM, and GM SPWs, respectively, compared to 691% in the control. These values are closer to 100% (except for the control) likely because *Pc*O6 metabolized many of the unknown components of the wheat root exudates. In the control, despite *Pc*O6 metabolism, there were likely many unknown metabolites remaining, as an elevated concentration of DOC remains in this PW (Figure 5-5B).

Citrate and malate, two LMWOAs and root exudates which were specifically measured, were below the detection limit (0.5 mg/L) when *Pc*O6 was present. Although *Pc*O6 metabolized citrate and malate, DMA was increased by *Pc*O6 (Figure B-4). Persistence of DMA in the presence of *Pc*O6 and the wheat endophytes, or even increasing DMA concentrations, has not been observed before. These results suggest that DMA, or the metal-DMA complex, was not bioavailable to the *Pc*O6. DMA is broken down in bulk soil environments primarily by Gram-negative bacteria (such as *Pc*O6) and has a half-life similar to other LMWOAs of 3-8 hours (Oburger et al. 2016). Wheat and root-colonizers/endophytes may have co-evolved to avoid metabolism of the phytosiderophores.

Overall, wheat exudates increased dissolved Cu, but *Pc*O6 metabolized root exudates and decreased dissolved Cu. Kent and Vikesland (2016) noted that CuO NPs could dissolve completely in short time frames if the system remained undersaturated with respect to Cu, even at high pH. This suggests that in soils, the dissolution of CuO NPs will be controlled by the saturation level of Cu (which is dependent on pH and available ligands), the rate at which dissolved Cu is removed from the system, and the rate at which new ligands enter the system. In the sand and PW systems, solubility of the CuO NPs would have increased indefinitely if the rooting zone were regularly flushed by PW free of Cu.

Dissolved Cu: Size distribution

The size distribution of Cu was determined by ultrafiltration with a 3 kDa filter and a Cu ion selective electrode, and gives information about whether dissolved Cu is

complexed to large molecules (> 3 kDa molecules) or small molecules (< 3 kDa molecules) or is uncomplexed. Soils, for example, tend to have large molecules of humic and fulvic acids, whereas plants and bacteria tend to utilize smaller molecules (amino acids, low molecular weight organic acids). The size distribution of Cu was only examined in boxes with CuO NPs, as low Cu levels prevailed in non-CuO NP boxes.

Dissolved Cu distribution depended on main effects PW and wheat (Figure 5-8). The control PW had more Cu free or complexed to molecules < 3 kDa than the AgrM PW (Figure 5-8A). Wheat overall increased the proportion of Cu complexed to molecules < 3 kDa through root exudates (Figure 5-8B). The interaction of wheat and PW was also significant (Figure 5-8C). Nearly 92% of Cu in the unplanted control, which had DOC levels below detection, was smaller than 3 kDa due to the lack of large complexing molecules, whereas the addition of wheat decreased the percentage of Cu < 3 kDa to 66% (Figure 5-8C) due to exudation of primarily small but also large DOC molecules. Cu in the three SPWs without wheat, by contrast, was mostly larger than 3 kDa (75-83%) due to complexation with FA/HA in the SPWs. The addition of wheat increased the proportion of Cu complexed to smaller molecules (< 3 kDa) from 18-25% to 41-60% (Figure 5-8C). These results showed that the SPWs, before planting, naturally contained Cu-complexing molecules in both size ranges, but primarily > 3 kDa, as FA/HA. While plants may have produced some Cu-complexing molecules > 3 kDa such as proteins (as shown by the 34% of dissolved Cu > 3 kDa in the control PW with wheat, Figure 5-8C), most Cu-complexing molecules produced were < 3 kDa. This result confirms that organic exudates from the roots are the driver behind the increase of

soluble Cu in planted samples. Geochemical modeling of the PW Cu speciation agreed, as the proportion of FA/HA complexing Cu in the PWs always decreased in the planted models compared to the unplanted models.
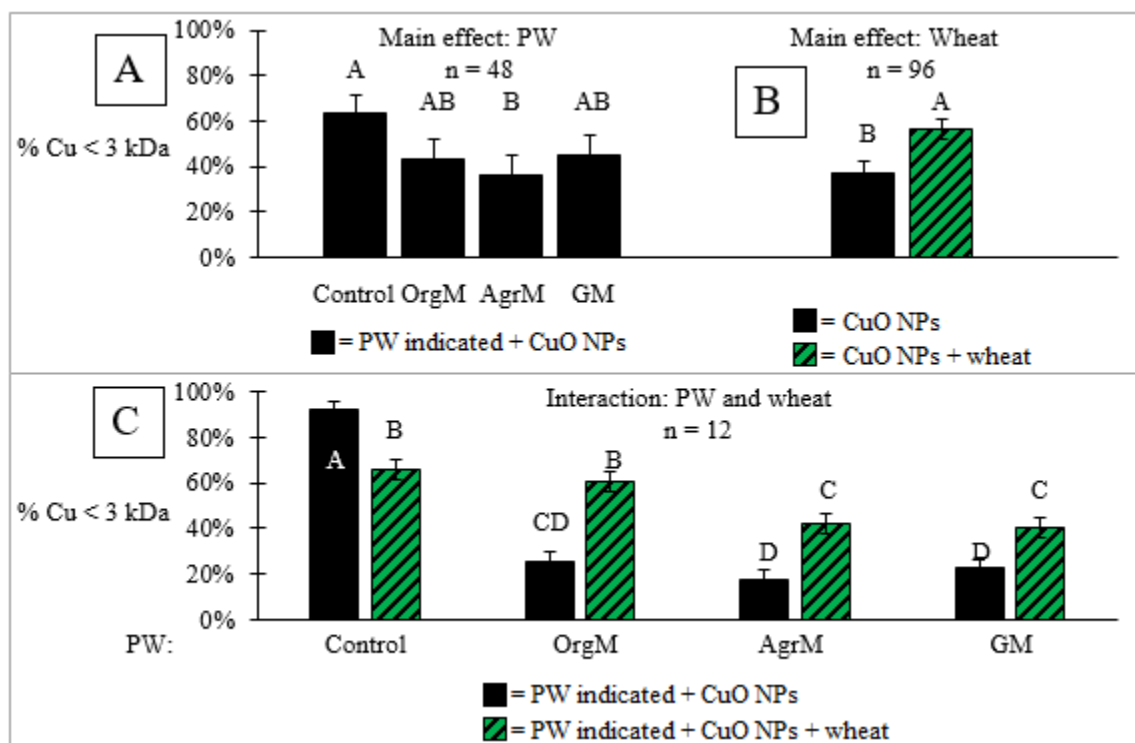
Figure 5-8: Dissolved Cu size distribution by main effects PW (A), wheat (B), and the interaction of PW/wheat (C). Bars = average of independent sample measurements, and error bars = Student's t-test or Tukey HSD statistical significance. Bars with differing letters (A, B, etc.) are statistically different ($p < 0.05$).

Uncomplexed ("free") Cu^{2+} ions (those ions not bound to any ligands) were detectable in all solutions with or without CuO NPs, but were altered by PW (Figure 5-9A), increased by CuO NPs (Figure 5-9B), and reduced by $PcO6$ (Figure 5-9C). Free Cu^{2+} was highest in the control PW (17.3 µg/L) because there was little to complex with the Cu ions. Free Cu^{2+} decreased in all SPWs in the order OrgM = AgrM > GM (Figure 5-9A). CuO NPs increased free Cu^{2+} concentrations from (Figure 5-9B) while $PcO6$, on

the other hand, reduced average free Cu^{2+} concentrations probably through exudation of ligands (Figure 5-9C). Wheat did not alter free Cu^{2+} (data not shown), despite the production of Cu-complexing root exudates.
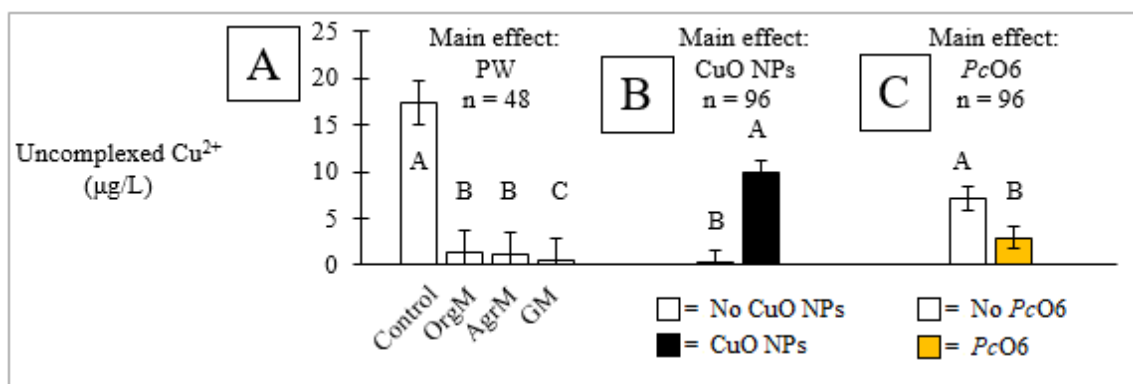

Figure 5-9: Uncomplexed ("free") Cu^{2+} concentrations in rooting zone extractions by main effects PW (A), CuO NPs (B), and *Pc*O6 (C). Bars represent the average of independent sample measurements, and error bars represent the standard deviation. Bars with differing letters (A, B, etc.) are statistically different ($p < 0.05$). A logarithmic transformation was utilized for free Cu^{2+} in order to maintain normal distribution of the residuals.

NP toxicity: Root and shoot length

Another objective of the study was to examine how differing PWs and *Pc*O6 altered CuO NP toxicity. Variables in this section were analyzed by a three-way ANOVA (presence/absence of CuO NPs, presence/absence of *Pc*O6, and PW).

Toxicity of the NPs to the wheat was determined through four symptoms: root and shoot length, and root and shoot Cu uptake. Longer roots and shoots and lower root and shoot uptakes were assumed to be healthier plants, indicating less NP bioavailability. Toxicity of the NPs to the *Pc*O6 was determined through culturability on LB medium after incubation. The PCA (Figure 5-2) suggested that shoot Cu, root Cu,

and dissolved Cu were associated together, and were all inversely associated to root length, and these relationships are examined here.

Root length was altered by PW and decreased by CuO NPs (Figure 5-10). While the control, OrgM, and GM root lengths were statistically the same (6.4-6.9 cm), AgrM root lengths were longer (7.8 cm, Figure 5-10A). CuO NPs reduced root lengths 37% overall (8.6 m to 5.4 cm) across all PWs (Figure 5-10B).
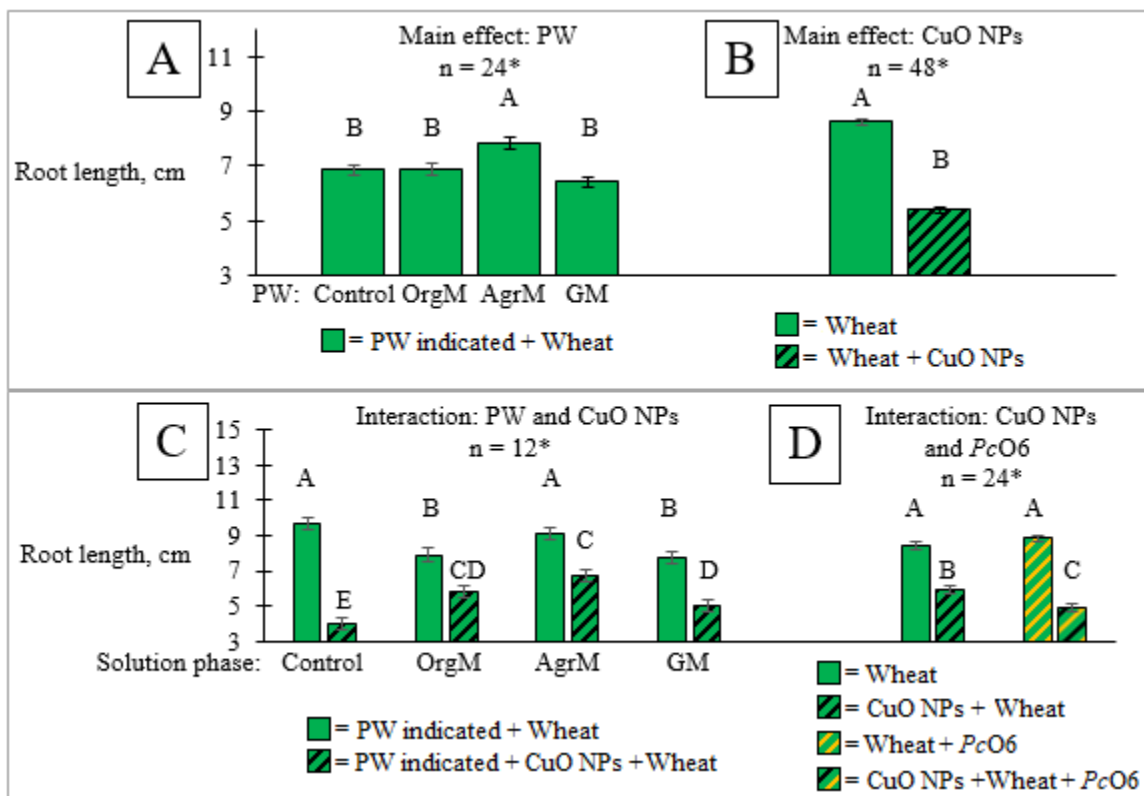
Figure 5-10: Root length in planted samples by main effects PW (A) and CuO NPs (B) and interactions of PW/CuO NPs (C) and CuO NPs/*Pc*O6 (D). Bars = average of independent sample measurements (n indicated on graphs), and error bars = Tukey HSD statistical significance. Bars with differing letters (A, B, etc.) are statistically different (p < 0.05). *The bars AgrM (A), -CuO NPs (B), AgrM -CuO NPs (C) and -CuO NPs - *Pc*O6 (D) contain 2 less in n than indicated, due to a measurement error.

The interactions of PW/CuO NPs (Figure 5-10C) and CuO NPs/*Pc*O6 (Figure 5-10D) were also significant to root length. Root length was visibly shortened (19-20%) without CuO NPs by growth in GM and OrgM SPWs compared to the control (Figure 5-10C). Greater nutrient availability as well as higher salt content (Table A-4) may partially explain root shortening in GM SPW. Wheat root shortening of 29% has been observed at a salinity of 4 mS/cm in an artificial soil (Alom et al. 2016), a salinity comparable to the GM SPW (at ~3.2 mS/cm). With CuO NPs, root lengths were reduced 59%, 26%, 27%, and 35% in the control, OrgM, AgrM, and GM PWs, respectively (Figure 5-10C). Root shortening which occurred in wheat exposed to CuO NPs and SPWs was remediated above the control, suggesting that SPW components mitigated the toxicity of the NPs or their ions to the wheat. Root shortening after wheat exposure to Cu has been observed previously with both CuO NPs (Dimkpa et al. 2012b; McManus 2016) and Cu ions (Michaud et al. 2008; Dimkpa et al. 2012b). The root shortening in the control at the dose of 100 mg/kg Cu/sand from CuO NPs with 3.34 mM $Ca(NO_3)_2$ was 59%, nearly double that seen by McManus (2016) at the same dose in 0.7 mM $Ca(NO_3)_2$ of 33%, but near equal with that seen by Wright et al. (2016) at the same dose in deionized water (65%). Cu from CuO NPs also changes root morphology by proliferating root hairs nearer to the root tip (Adams et al. 2017). Root hairs were not measured in this study, but the proliferation of root hairs may have a protective effect for wheat.

*Pc*O6 without CuO NPs had no effect on root length, but *Pc*O6 with CuO NPs caused shorter roots than CuO NPs alone. CuO NPs without *Pc*O6 reduced root length

30%, but the addition of *Pc*O6 with CuO NPs reduced root length 42% (Figure 5-10D). *Pc*O6 enhanced damage of CuO NPs to the wheat roots, despite lowering the soluble Cu concentrations (Figure 5-5A). Wright et al. (2016) observed that there was a non-significant trend of *Pc*O6 to elongate roots exposed to CuO NPs, thus the results from these two studies differ. The differences between this study and Wright et al. (2016) were the use of SPW in this study, the method of inoculation (seed inoculation by Wright et al. (2016) versus suspension in SPW in this study), and the statistical significance of the results. It is possible that these differences between studies altered how the *Pc*O6 distributed throughout the growth box and thus how the *Pc*O6 interacted with the CuO NPs, increasing NP damage rather than decreasing damage. Geochemical modeling may also help partially explain the increased damage. DMA, which is increased by *Pc*O6, complexed 213, 139, 86, and 153 µg Cu/L in the control, OrgM, AgrM, and GM PWs, respectively, which matches the order of root shortening observed.

All SPWs remediated root length to a degree. In order to find the mechanism of remediation, toxicity models may be useful. Free Cu^{2+} ions are the main mode of toxicity under the biotic ligand model (BLM), a commonly used toxicity model, which has been previously applied successfully to wheat roots for Cu toxicity (Luo et al. 2008). Rising pH, complexation of Cu with DOC, and competition with cations Ca^{2+}/Mg^{2+} for root sorption sites (Luo et al. 2008) would limit the bioavailability and thus toxicity of the free Cu^{2+} ion. Under the BLM, roots should be longest at high pH/high DOC/high Ca^{2+}, Mg^{2+} (for equal concentrations of total dissolved Cu). The PCA (Figure 5-2) and Pearson's correlations did not fully support the hypotheses of the BLM, however.

Competing cations and DOC were not associated with lengthening roots. In contrast, some forms of DOC (gluconate, citrate, DMA) were associated with shortening roots and increasing root Cu, failing to provide the predicted protections and suggesting that some complexes were bioavailable to the wheat. Free Cu^{2+} was significantly (although poorly) associated with shortening roots by Pearson's correlation; however, the wheat responses seen were more exaggerated than past studies. Michaud et al. (2008) saw a 50% and 25% reduction of wheat root length after eight days at 0.6 μM free Cu^{2+} (~38 μg/L) and 0.2 μM free Cu^{2+} (~13 μg/L), which were both higher concentrations than this study's measured values (59% and 26-35% root length reduction in 26 μg/L and 0.6-4 μg/L free Cu^{2+} in control and SPWs, respectively). Thus the damage seen in this study could not be fully explained by free Cu^{2+}.

Cu complexes likely were bioavailable and played a role in root shortening. DMA, an iron phytosiderophore of wheat, is intended to solubilize iron in iron-deficient environments such as high-pH calcareous soils. However, Cu binds stronger to DMA than iron (Murakami et al. 1989). Geochemical modeling of the PWs showed that DMA was always 100% complexed to Cu when present. Citrate, by contrast, was only bound to significant portions of Cu in the control (14.7% of citrate as Cu-citrate) and AgrM (5.5% of citrate as Cu-citrate) in the PWs, and malate was never bound to Cu in an appreciable portion. As Fe-DMA is bioavailable to wheat, it is possible that Cu-DMA is as well. Likewise, an increase of toxicity in the form of a Cu-citrate complex has been observed before against a bacterium, *Pseudomonas putida* (McLean et al. 2013), and Cu-citrate increased superoxide dismutase and peroxidase in wheat while a Cu-acetate

complex did not (Olteanu et al. 2013). It is likely that both Cu-DMA and Cu-citrate complexes were bioavailable to wheat, resulting in additional toxicity.

As with root length, the main effects of PW and the presence/absence of NPs were significant to shoot length (Figure 5-11) but not the presence/absence of PcO6. Shoot length was increased 9.5% by GM SPW (Figure 5-11A); the increased nutrients available in GM SPW, i.e., nitrate, phosphate, and DOC (Table 4-1) were the most likely source of increased shoot length. Although shoot length was inhibited 3.3% by CuO NPs (Figure 5-11B), the difference was likely not important to the overall growth of the plant during the two-week growth period. CuO NPs have been observed to decrease shoot length before (Dimkpa et al. 2012b) and a downward, but insignificant, trend in shoot length was seen by McManus (2016) between increasing CuO NP dose and shoot length. Shoot length was mainly correlated with EC (Figure 5-2B) rather than any form of Cu.

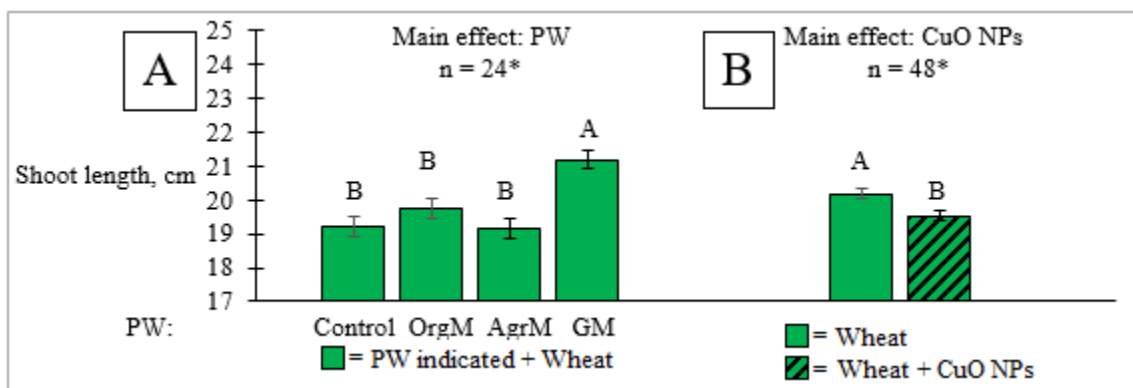Figure 5-11: Shoot length in planted samples by main effects PW (A) and CuO NPs (B). Bars = average of independent sample measurements (n indicated on graphs), and error bars = Tukey HSD or Student's t-test statistical significance. Bars with differing letters (A, B, etc.) are statistically different ($p < 0.05$). *The bars AgrM and no CuO NPs contain two less in n than indicated, due to a measurement error.

CuO NP bioavailability: Shoot and root metals

Shoot Cu concentrations were altered by main effects of PWs (Figure 5-12A) and increased by CuO NPs (Figure 5-12B). The PW shoot Cu increased in the order of AgrM = OrgM < Control = GM (Figure 5-12A). Average shoot Cu concentration also increased with the presence of CuO NPs (Figure 5-12B) from an overall average of 14.4 mg/kg dry weight to 29.5 mg/kg dry weight. The shoot Cu concentration in wheat from OrgM and AgrM PWs was lower than the control, despite equivalent or higher soluble Cu (Figure 5-6A), showing that the SPWs offered protection to the wheat. GM PW had the highest soluble Cu levels (Figure 5-5A), yet remained at the same shoot Cu concentration as the control, also showing the SPW offered protection against the CuO NPs.
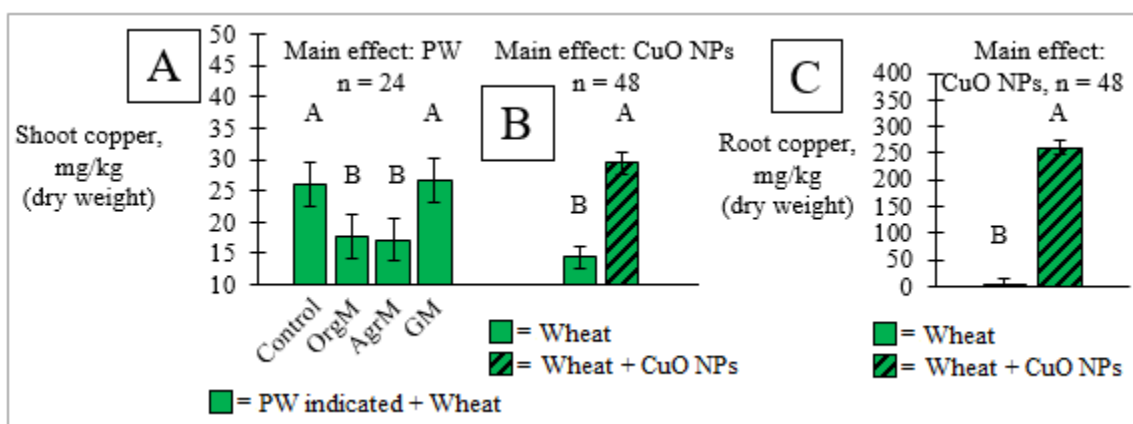
Figure 5-12: Shoot Cu in planted samples by main effects PW (A) and CuO NPs (B), and root Cu in planted samples by main effect CuO NPs (C). Bars = average of independent sample measurements (n indicated on graphs), and error bars = Tukey HSD statistical significance. Bars with differing letters (A, B, etc.) are statistically different ($p < 0.05$). Logarithmic transformations were applied to shoot and root Cu to maintain normal distributions of the residuals.

The PCA (Figure 5-2) and Pearson's correlations showed that shoot Cu overall was mainly associated with root length. As roots become shorter due to Cu toxicity and

more loaded with Cu, shoot concentrations increase. Associations of shoot Cu with other components, such as citrate and DMA, were weaker than the association with root length. Low molecular weight organic acids (citrate, DMA) may transport Cu from the root into the shoot, as seen in a review determining that citrate (as well as asparagine and histidine) was a primary complexer of Cu and Zn in soybean and tomato xylem (Rauser 1999), and Cu-DMA has been detected in rice xylem (Ando et al. 2013), but this area needs more research.

Root Cu concentration was only affected by addition of the CuO NPs, increasing from < 1 mg/kg dry weight to 261 mg/kg dry weight (Figure 5-12C). It is known that some of the root Cu was actually adsorbed NPs (whether to the roots or root-associated sand), as there was no attempt (besides deionized water rinsing) to remove adsorbed NPs/sand. The average wheat root Cu concentration of this study (261 mg/kg) aligned between the wheat root Cu concentrations seen by Zhou et al. (2011) for doses of 50 and 100 mg/L CuO NPs in suspension. Under the conditions of Zhou et al. (2011), about 29-34% of the root Cu was adsorbed NPs, meaning that about 76-89 mg/kg Cu in the root was potentially due to adsorbed CuO NPs in this present study.

Contamination of the root surfaces (i.e. physical attachment) by CuO NPs may lead to incorrect associations of root Cu with other variables in this study. However, Zhou et al. (2011) observed that the adsorption rate of CuO NPs to wheat roots remained fairly constant even with large variations in dose (uptake:adsorption ratio always ranging from 1.4-2.5 over the range 5-200 mg/L CuO NPs). The important associations of root Cu are the positive associations with gluconate, DOC, DMA, and dissolved Cu, and the

negative associations with shoot and root length. These correlations were confirmed as significant by both PCA and Pearson's correlations.

Bioconcentration (uptake) and bioaccumulation (uptake and contact) factors (BCF and BAF, respectively) were calculated for the shoot and root, respectively, for each treatment condition, with and without PcO6 (Table 5-2). A BCF could not be calculated for roots as some of the root Cu was adsorbed NPs. The BCF for shoots was calculated as shoot Cu divided by soluble Cu, and the BAF for roots was calculated as root Cu divided by NP dose, 100 mg/kg. BCFs/BAFs were meaningless in non-CuO NP treatments, as the concentrations of Cu were very low and the seedling received Cu nutrition from the seed during this time. In the CuO NP treatments however, root and shoot uptake was observed (Figure 5-12B, C) outside of the seed nutrition.

Table 5-2: Shoot Cu bioconcentration factors and root Cu bioaccumulation factors by treatment. Shoot BCFs and root BAFs with differing letters are statistically different by two-way ANOVA followed by the Tukey HSD test.

PW	PcO6	Shoot BCF	Root BAF
Control	N	8.81^{bcd}	3.21^a
Control	Y	19.0^a	1.58^a
OrgM	N	6.37^{bcd}	2.68^a
OrgM	Y	14.3^{ab}	2.60^a
AgrM	N	2.80^d	3.84^a
AgrM	Y	12.3^{abc}	1.38^a
GM	N	7.91^{bcd}	3.25^a
GM	Y	5.44^{cd}	2.33^a

The main effect PcO6 increased shoot BCFs because soluble Cu decreased, yet the shoot Cu content remained elevated. Main effect PW was also important as AgrM/GM PWs had lower shoot BCFs compared to the control. Finally, the interaction

of PW and *Pc*O6 was important in shoot BCF (Table 5-2). Shoot BCFs were highest in

the control, OrgM, and AgrM PWs with *Pc*O6, and lowest in the remaining treatments.

Only the control and AgrM PWs showed a significant difference between the *Pc*O6 and

non-*Pc*O6 shoot BCFs.

Root BAFs were highest in the non-*Pc*O6 treatments, which was the only

significant main effect (Table 5-2). The interaction of PW and *Pc*O6 was not significant.

From these results, it appears that *Pc*O6 overall decreased contact between roots and

NPs (Table 5-2), even though *Pc*O6 shortened roots exposed to CuO NPs more than

roots exposed to CuO NPs without *Pc*O6.

CuO NP toxicity: *Pc*O6

The concentration of NPs in this study, 100 mg/kg Cu/sand (equivalent to 667

mg/L Cu from CuO NPs when accounting for 300 g sand and 45 mL PW per box) was

above the previously determined lethal concentration to *Pc*O6 grown in liquid culture of

500 mg/L Cu from CuO NPs (Dimkpa et al. 2011a), but did not eliminate culturability of

the *Pc*O6 in any PW after 10 days. Sorption of the NPs to the sand and/or alteration by

the SPWs may have reduced contact between NPs and the cells, decreasing their toxicity

to *Pc*O6.

CuO NP mass balance

Mass balance for Cu in the sand, plant, and water was 87% of the added dose

across all treatments. Of the 87% recovered, 99.4% was associated with the sand, 0.4%

was dissolved, and about 0.3% was associated with wheat (root or shoot Cu). Neither the

Cu mass balance nor the sand recovery was significantly associated with any main effect or interaction.

The NPs primarily remained in the solid phase associated with the sand. Approximately 86% of the Cu was retained this way. Even at the highest dissolved concentrations (~8 mg/L Cu), less than 1.5% of the CuO NPs were in the aqueous phase, and fewer still (~0.3%) were located with the plant. These results suggest that CuO NPs, at high doses in a solid matrix, will persist and remain for long periods of time, dissolving as ligands become available. The remaining 13% of Cu was likely suspended CuO NPs in the PW or due to error. A portion of the NPs were mobile (i.e., able to move through the sand; evidence seen through dark-colored extracts), and may also be mobile in whole soils.

Mechanism of SPW protection against NPs

The mechanism by which the PWs originating from soils protected the wheat seedlings remains unclear. Previous studies have seen coating of the NPs by humic and fulvic acids or other organic matter (Conway et al. 2015, Sousa and Teixeira 2013) and steric repulsion of the NPs and rice roots (Peng et al. 2016) or *E. coli* (Zhao et al. 2013). Coating of the NPs was not specifically investigated in this study, but based on results from NP solubility, significant coating of NPs was unlikely due to the surface area of the sand surface area removing some of the humic/fulvic acids from solution and the significant NP dissolution observed.

Complexation of Cu by soil components, such as humic and fulvic acids, did occur in the SPWs which increased solubility of the CuO NPs; in geochemical models of

the planted PWs after harvest, humic and fulvic acids (assumed to be recalcitrant and modeled at the full pre-harvest concentration) complexed 74-82%, 78-89%, and 96-98% of the dissolved Cu for OrgM, AgrM, and GM SPWs, respectively. Despite equivalent or higher solubility levels in the SPWs compared to the control PW, each SPW provided protection in root length and shoot uptake compared to the control, likely through humic and fulvic acid complexation. DMA, however, was associated with toxicity symptoms in the wheat. More research should be performed to understand the connections between DNOM, root exudates, and susceptibility to or protection from Cu toxicity. As soils contain differing mixtures of organic molecules, the types of DNOM and variations in functional groups may also explain some of the variation in level of protection offered by DNOM.

Conclusion

The objectives of this study were to examine the toxicity, uptake, solubility, and distribution of Cu in plant, sand, or liquid phases of CuO NPs as affected by differing soil pore water (SPWs) chemistries, soil bacteria, and wheat. SPWs decreased the toxicity of Cu ions to wheat as seen by partially remediated root lengths and lower Cu shoot bioconcentration factors, but did not affect root bioaccumulation factors. *Pc*O6 decreased Cu root bioaccumulation factors, but increased Cu shoot bioconcentration factors and increased damage caused by CuO NPs to wheat roots, possibly by promoting higher DMA concentrations.

SPWs increased the solubility of CuO NPs above the solubility observed in 3.34 mM $Ca(NO_3)_2$. Wheat also increased CuO NP solubility through exudation of organic

compounds. *Pc*O6 did not alter CuO NP solubility except by metabolizing root exudates, partially canceling the increased dissolution of CuO NPs seen in the presence of wheat. Cu distribution in the sand was not affected by SPW, wheat, or *Pc*O6; however, soluble Cu and plant Cu uptake was altered by these factors.

As CuO NPs were less toxic defined by root length to wheat seedlings in the presence of SPWs than in simpler solutions, CuO NPs will likely be less toxic to crops and bacteria in whole soils than these sand and SPW systems through processes such as sorption of NPs and Cu ions to mineral surfaces and exclusion from the rooting zone. Relatively rapid dissolution of CuO NPs in soil will likely occur per the DNOM content of the soil, as seen in this study. CuO NPs may persist and provide long-term soluble Cu, particularly if the system is undersaturated with respect to Cu (Kent and Vikesland 2016), perhaps through high rainfall/irrigation which consistently flushes the rooting zones of accumulated Cu or continued complexation by root or bacterial exudates. Coating of NPs with organic matter and complexation of Cu ions with DNOM reduces their toxicity to wheat and other organisms as seen in this study and others (Pradhan et al. 2016; Peng et al. 2016; Zhao et al. 2013). Further research should identify the roles of soil organic matter in the behavior of CuO NPs in whole soils to accurately perform risk assessment.

References

Adams, J., Wright, M., Wagner, H., Valiente, J., Britt, D., and Anderson, A. (2017). "Cu from dissolution of CuO nanoparticles signals changes in root morphology." *Plant Physiol. Biochem.*, 110, 108-117.

Adeleye, A. S., Conway, J. R., Perez, T., Rutten, P., and Keller, A. A. (2014). "Influence of extracellular polymeric substances on the long-term fate, dissolution, and

speciation of copper-based nanoparticles." *Environ. Sci. Technol.*, 48(21), 12561-12568.

Alom, R., Abu Hasan, M., Rabiul Islam, M, and Wang, Q. (2016). "Germination characters and early seedling growth of wheat (*Triticum aestivum* L.) genotypes under salt stress conditions." *J. Crop Sci. Biotechnol.*, 19(5), 383-392.

Anderson, A. J., McLean, J. E., Jacobson, A. R., and Britt, D. W. (2017a). "CuO and ZnO nanoparticles modify interkingdom cell signaling processes relevant to crop production." *J. Agric. Food Chem.*, DOI 10.1021/acs.jafc.7b01302

Anderson, A., McLean, J., McManus, P., and Britt, D. (2017b). "Soil chemistry influences the phytotoxicity of metal oxide nanoparticles." *Int. J. Nanotechnol.*, 14(1-6), 15-21.

Ando, Y., Nagata, S., Yanagisawa, S., and Yoneyama, T. (2013). "Copper in xylem and phloem saps from rice (*Oryza sativa*): The effect of moderate copper concentrations in the growth medium on the accumulation of five essential metals and a speciation analysis of copper-containing compounds." *Funct. Plant Biol.*, 40(1), 89-100.

APHA. (2012). *Standard methods for the examination of water and wastewater*. 22nd ed.; American Public Health Association: Washington, D.C.

Comby, M., Gacoin, M., Robineau, M., Rabenoelina, F., Ptas, S., Dupont, J., Profizi, C., and Baillieul, F. (2017). "Screening of wheat endophytes as biological control agents against fusarium head blight using two different in vitro tests." *Microbiol. Res.*, 202, 11-20.

Conway, J. R., Adeleye, A. S., Gardea-Torresdey, J., and Keller, A. A. (2015). "Aggregation, dissolution, and transformation of copper nanoparticles in natural waters." *Environ. Sci. Technol.*, 49(5), 2749-2756.

Cornelis, G., Hund-Rinke, K., Kuhlbusch, T., Van den Brink, N., and Nickel, C. (2014). "Fate and bioavailability of engineered nanoparticles in soils: A review." *Crit. Rev. Environ. Sci. Technol.*, 44(24), 2720-2764.

Díaz Herrera, S., Grossi, C., Zawoznik, M., and Groppa, M. D. (2016). "Wheat seeds harbour bacterial endophytes with potential as plant growth promoters and biocontrol agents of *Fusarium graminearum.*" *Microbiol. Res.*, 186-187, 37-43.

Dimkpa, C. O., and Bindraban, P. S. "Nanofertilizers: New products for the industry?" *J. Agric. Food Chem.*, DOI 10.1021/acs.jafc.7b02150

Dimkpa, C. O, Bindraban, P. S., Fugice, J., Agyin-Birikorang, S., Singh, U., and Hellums, D. (2017). "Composite micronutrient nanoparticles and salts decrease drought stress in soybean." *Agron. Sustainable Dev.*, 37(5),

Dimkpa, C. O., Calder, A., Britt, D. W., McLean, J. E., and Anderson, A. J. (2011a). "Responses of a soil bacterium, *Pseudomonas chlororaphis* O6 to commercial metal oxide nanoparticles compared with responses to metal ions." *Environ. Pollut.*, 159(7), 1749-1756.

Dimkpa, C. O., McLean, J. E., Britt, D. W., and Anderson, A. J. (2011b). "CuO and ZnO nanoparticles differently affect the secretion of fluorescent siderophores in the beneficial root colonizer, *Pseudomonas chlororaphis* O6." *Nanotoxicology*, 6(6), 635-642.

Dimkpa, C. O., McLean, J. E., Britt, D. W., Johnson, W. P., Arey, B., Lea, A. S., and Anderson, A. J. (2012a). "Nanospecific inhibition of pyoverdine siderophore production in *Pseudomonas chlororaphis* O6 by CuO nanoparticles." *Chem. Res. Toxicol.*, 25(5), 1066-1074.

Dimkpa, C. O., McLean, J. E., Latta, D. E., Manangon, E., Britt, D. W., Johnson, W. P., Boyanov, M. I., and Anderson, A. J. (2012b). "CuO and ZnO nanoparticles: phytotoxicity, metal speciation, and induction of oxidative stress in sand-grown wheat." *J. Nanopart. Res.*, 14(9).

Elmer, W. H., and White, J. C. (2016). "The use of metallic oxide nanoparticles to enhance growth of tomatoes and eggplants in disease infested soil or soilless medium." *Environ. Sci.: Nano*, 3(5), 1072-1079.

EPA. (1996). *Method 3050B: Acid Digestion of Sediments, Sludges, and Soils*, Revision 2.

Frenk, S., Ben-Moshe, T., Dror, I., Berkowitz, B., and Minz, D. (2013). "Effect of metal oxide nanoparticles on nicrobial community structure and function in two different soil types." *PLoS One*, 8(12).

Gustaffson, J. P. (2013). "Visual MINTEQ", 3.1 beta.

Jones, J. B., and Case, V. W. (1990) "Sampling, handling, and analyzing plant tissue samples." *Soil Testing and Plant Analysis*, American Society of Agronomy, Madison, WI.

Keller, A. A., McFerran, S., Lazareva, A., and Suh, S. (2013). "Global life cycle releases of engineered nanomaterials." *J. Nanopart. Res.*, 15(6).

Kent, R. D. and Vikesland, P. J. (2016). "Dissolution and persistence of copper-based nanomaterials in undersaturated solutions with respect to cupric solid phases." *Environ. Sci. Technol.*, 50, 6772-6781.

Luo, X. S., Li, L. Z., and Zhou, D. M. (2008). "Effect of cations on copper toxicity to wheat root: Implications for the biotic ligand model." *Chemosphere*, 73(3), 401-406.

McLean, J. E., Pabst, M. W., Miller, C. D., Dimkpa, C. O., and Anderson, A. J. (2013). "Effect of complexing ligands on the surface adsorption, internalization, and bioresponse of copper and cadmium in a soil bacterium, *Pseudomonas putida*." *Chemosphere*, 91(3), 374-382.

McManus, P. (2016). "Rhizosphere interactions between copper oxide nanoparticles and wheat root exudates in a sand matrix: Influences on bioavailability and uptake," Utah State University, Logan.

Miao, L. Z., Wang, C., Hou, J., Wang, P. F., Ao, Y. H., Li, Y., Lv, B. W., Yang, Y. Y., You, G. X., and Xu, Y. (2015). "Enhanced stability and dissolution of CuO

nanoparticles by extracellular polymeric substances in aqueous environment." *J. Nanopart. Res*., 17(10).

Michaud, A. M., Chappellaz, C., and Hinsinger, P. (2008). "Copper phytotoxicity affects root elongation and iron nutrition in durum wheat (*Triticum turgidum durum* L.)." *Plant Soil*, 310(1-2), 151-165.

Monreal, C. M., DeRosa, M., Mallubhotla, S. C., Bindraban, P. S., and Dimkpa, C. (2016). "Nanotechnologies for increasing the crop use efficiency of fertilizer-micronutrients." *Biol. Fertil. Soils*, 52(3), 423-437.

Murakami, T., Ise, K., Hayakawa, M., Kamei, S., and Takagi, S. I. (1989). "Stabilities of metal-complexes of mugineic acids and their specific affinities for iron(III)." *Chem. Lett*., (12), 2137-2140.

Nian, H., Yang, Z. M., Ahn, S. J., Cheng, Z. J., and Matsumoto, H. (2002). "A comparative study on the aluminium- and copper-induced organic acid exudation from wheat roots." *Physiol. Plant*., 116(3), 328-335.

Oburger, E., Gruber, B., Schindlegger, Y., Schenkeveld, W. D. C., Hann, S., Kraemer, S. M., Wenzel, W. W., and Puschenreiter, M. (2014). "Root exudation of phytosiderophores from soil-grown wheat." *New Phytol*., 203(4), 1161–74.

Oburger, E., Gruber, B., Wanek, W., Watzinger, A., Stanetty, C., Shindlegger, Y., Hann, S., Schenkeveld, W. D. C., Kraemer, S. M., and Puschenreiter, M. (2016). "Microbial decomposition of ^{13}C-labeled phytosiderophores in the rhizosphere of wheat: Mineralization dynamics and key microbial groups involved." *Soil Biol. Biochem*., 98, 196-207.

Olteanu, Z., Truta, E., Oprica, L., Zamfirache, M. M., Rosu, C. M., and Vochita, G. (2013). "Copper-induced changes in antioxidative response and soluble protein level in *Triticum aestivum* CV. beti seedlings." *Rom. Agric. Res*., 30, 163-170.

Otero-Gonzalez, L., Field, J. A., and Sierra-Alvarez, R. (2014). "Inhibition of anaerobic wastewater treatment after long-term exposure to low levels of CuO nanoparticles." *Water Res*., 58, 160-168.

Palmer, D. A., and Bénézeth, P. (2004). "Solubility of copper oxides in water and steam." *Proc., 14th International Conference on the Properties of Water and Steam in Kyoto*, 491-496.

Peng, C., Duan, D., Xu, C., Chen, Y., Sun, L., Zhang, H., Yuan, X., Zheng, L., Yang, Y., Yang, J., and Zhen, X. (2016). "Translocation and biotransformation of CuO nanoparticles in rice (*Oryza sativa* L.) plants." *Environ. Pollut*., 197, 99-107.

Peng, C., Xu, C., Liu, Q., Sun, L., Luo, Y, and Shi, J. (2017). "Fate and transformation of CuO nanoparticles in the soil-rice system during the life cycle of rice plants." *Environ. Sci. Technol*., 51, 4907-4917.

Pradhan, A., Geraldes, P., Seena, S., Pascoal, C., and Cássio, F. (2016). "Humic acid can mitigate the toxicity of small copper oxide nanoparticles to microbial decomposers and leaf decomposition in streams." *Freshwater Biol*., 61, 2197-2210.

Rachou, J., Gagnon, C., and Sauve, S. (2007). "Use of an ion-selective electrode for free copper measurements in low salinity and low ionic strength matrices.*" Environ. Chem*. 4(2), 90-97.

Rauser, W. E. (1999). "Structure and function of metal chelators produced by plants: The case for organic acids, amino acids, phytin, and metallothioneins." *Cell Biochem. Biophys*., 31, 19-48.

Rhoades, J. D. (1996). "Salinity: Electrical conductivity and total dissolved solids." *Methods of soil analysis: Part 3-chemical methods*, edited by D. L. Sparks, Soil Science Society of America, Inc. & American Society of Agronomy, Inc.: Madison, WI,; pp 417-435.

Schlich, K., Beule, L., and Hund-Rinke, K. (2016). "Single versus repeated applications of CuO and Ag nanomaterials and their effect on soil microflora." *Environ. Pollut*., 215, 322-330.

Singh, D., and Kumar, A. (2016). "Impact of irrigation using water containing CuO and ZnO nanoparticles on *Spinach oleracea* grown in soil media." *Bull. Environ. Contam. Toxicol*., 97, 548-553.

Sousa, V. S., and Teixeira, M. R. (2013). "Aggregation kinetics and surface charge of CuO nanoparticles: The influence of pH, ionic strength and humic acids." *Environ. Chem*., 10(4), 313-322.

Wright, M., Adams, J., Yang, K., McManus, P., Jacobson, A., Gade, A., McLean, J., Britt, D., and Anderson, A. (2016). "A root-colonizing psuedomonad lessens stress responses in wheat imposed by CuO nanoparticles." *PLoS ONE*, 11(10).

Zhao, J., Wang, Z. Y., Dai, Y. H., and Xing, B. S. (2013). "Mitigation of CuO nanoparticle-induced bacterial membrane damage by dissolved organic matter." *Water Res*., 47(12), 4169-4178.

Zhou, D. M., Jin, S. Y., Li, L. Z., Wang, Y., and Weng, N. Y. (2011). "Quantifying the adsorption and uptake of CuO nanoparticles by wheat root based on chemical extractions." *J. Environ. Sci*., 23(11), 1852-1857.

CHAPTER 6

ENGINEERING SIGNIFICANCE

CuO NPs have several agricultural applications, including as fungicides (Elmer and White 2016), micronutrient fertilizers (Monreal et al. 2016; Dimkpa and Bindraban, 2017), and drought treatments (Dimkpa et al. 2017), and thus their behavior in the environment, and especially soils, should be considered before widespread use occurs. CuO NPs have shown toxicity to soil microbial communities and crops (Frenk et al. 2013; Kim et al. 2013; McManus 2016; Xu et al. 2015), when the dose is sufficiently high (generally dose > 0.01% w/w or 100 mg/kg). However, a lower dose may improve crop yield, reduce disease, increase drought tolerance (as previously noted), and/or avoid negative effects to the soil biome. Studies exploring agricultural applications of CuO NPs should include an accounting of unintended effects of the NPs on soil processes and the soil biome.

CuO NPs may be released from paints, coatings, consumer products or other applications and pass through engineered wastewater treatment systems at low levels, posing risks both similar to personal care products and pharmaceuticals (toxicity to aquatic organisms after release) and dissimilar (acute or chronic toxicity to microorganisms and biofilms within the wastewater treatment system) (Clar et al. 2016; Miao et al. 2016). CuO NPs in an anaerobic wastewater system generally deposited into the biosolids, but 20-32% remained in the effluent (Otero-Gonzalez et al. 2014). The biosolids are usually either landfilled or applied to soils, while the effluent is either

discharged or reused (especially with rising water stress around the world). Thus, CuO NPs may contact soils through solid phases or irrigation, and the consequences of both routes of exposure should be considered. For waste streams containing NPs, the wastewater treatment system may be manipulated according to the known properties of NPs to intentionally remove NPs through biosolid deposition so that treated secondary water use for irrigation is done safely.

In some of the first studies on each of these respective topics, Schlich et al. (2016) found that a soil concentration of CuO NPs > 333 mg/kg was necessary to produce toxic effects to soil bacteria, while Singh and Kumar (2016) found that below 10 mg/L CuO NPs, wastewater effluent used to irrigate spinach produced no negative effect compared to the control. Further research should be conducted to confirm these findings, as well as investigate the effects of long-term buildup of nanomaterials in soils from wastewater reuse on soils and crops.

Soil properties will greatly influence the overall behavior of CuO NPs. From these results, pH, alkalinity, and organic matter content and speciation are shown to vary how CuO NPs dissolve and aggregate. Other variables not tested here which may impact the fate and behavior of CuO NPs in soils may include clay minerals, soil texture, carbonates, ionic strength, acidity, sulfides, and differing root exudates or bacterial metabolites. Studies of CuO NPs in a range of soil conditions should be undertaken to identify low- and high-risk soils worldwide.

References

Clar, J. G., Li, X., Impellitteri, C. A., Bennett-Stamper, C., and Luxton, T. P. (2016). "Copper nanoparticle induced cytotoxicity to nitrifying bacteria in wastewater treatment: A mechanistic copper speciation study by X-ray absorption spectroscopy." *Environ. Sci. Technol*., 50, 9105-9113.

Dimkpa, C. O., and Bindraban, P. S. "Nanofertilizers: New products for the industry?" *J. Agricul. Food Chem.*, DOI 10.1021/acs.jafc.7b02150

Dimkpa, C. O, Bindraban, P. S., Fugice, J., Agyin-Birikorang, S., Singh, U., and Hellums, D. (2017). "Composite micronutrient nanoparticles and salts decrease drought stress in soybean." *Agron. Sustain. Dev*., 37(5),

Elmer, W. H., and White, J. C. (2016). "The use of metallic oxide nanoparticles to enhance growth of tomatoes and eggplants in disease infested soil or soilless medium.*" Environ. Sci.: Nano*, 3(5), 1072-1079.

Frenk, S., Ben-Moshe, T., Dror, I., Berkowitz, B., and Minz, D. (2013). "Effect of metal oxide nanoparticles on microbial community structure and function in two different soil types." *PLoS One*, 8(12).

Kim, S., Sin, H., Lee, S., and Lee, I. (2013). "Influence of metal oxide particles on soil enzyme activity and bioaccumulation of two plants." *J. Microbiol. Biotechnol*., 23(9), 1279-1286.

Miao, L., Wang, C., Hou, J., Wang, P., Ao, Y., Li, Y., Geng, N., Yao, Y., Lv, B., Yang, Y., You, G., and Xu, Y. (2016). "Aggregation and removal of copper oxide (CuO) nanoparticles in wastewater environment and their effects on the microbial activities of wastewater biofilms." *Bioresour. Technol*., 216, 537-544.

McManus, P. (2016). "Rhizosphere interactions between copper oxide nanoparticles and wheat root exudates in a sand matrix: Influences on bioavailability and uptake," Utah State University, Logan.

Monreal, C. M., DeRosa, M., Mallubhotla, S. C., Bindraban, P. S., and Dimkpa, C. (2016). "Nanotechnologies for increasing the crop use efficiency of fertilizer-micronutrients." *Biol. Fertil. Soils*, 52(3), 423-437.

Otero-Gonzalez, L., Field, J. A., and Sierra-Alvarez, R. (2014). "Inhibition of anaerobic wastewater treatment after long-term exposure to low levels of CuO nanoparticles." *Water Res*., 58, 160-168.

Schlich, K., Beule, L., and Hund-Rinke, K. (2016). "Single versus repeated applications of CuO and Ag nanomaterials and their effect on soil microflora." *Environ. Pollut.*, 215, 322-330.

Singh, D., and Kumar, A. (2016). "Impact of irrigation using water containing CuO and ZnO nanoparticles on *Spinach oleracea* grown in soil media." *Bull. Environ. Contam. Toxicol*., 97, 548-553.

Xu, C., Peng, C., Sun, L., Zhang, S., Huang, H., Chen, Y., and Shi, J. "Distinctive effects of TiO_2 and CuO nanoparticles on soil microbes and their community structures in flooded paddy soil." *Soil Biol. Biochem*., 86, 24-33.

CHAPTER 7

SUMMARY AND CONCLUSION

Soil pore waters (SPWs) enhance the solubility of CuO nanoparticles (NPs) above the solubility predicted simply as a function of pH. High concentrations of alkalinity (> 100 mg /L $CaCO_3$) in SPWs, particularly when originating from carbonates, play a relatively small role in CuO NP dissolution through complexation of copper ions with carbonate. Dissolved natural organic matter (DNOM, such as humic and fulvic acids) has potential to solubilize up to an order of magnitude more copper (milligrams of copper per liter) than alkalinity. These findings disproved null hypothesis one in the area of solubility for all SPWs, alkalinity, and fulvic acid, but not phosphate. Also, all treatments showed enhanced aggregation of NPs through heteroaggregation or coating, disproving null hypothesis one in the area of surface chemistry.

CuO NPs in a sand matrix with SPW were less toxic (as observed by root length and shoot copper uptake) to wheat than CuO NPs in a sand matrix with a background calcium nitrate solution. The CuO NPs' reduction of toxicity to wheat occurred despite similar or greater solubility of the CuO NPs across all SPWs compared to the control. Furthermore, shoot copper bioconcentration factors decreased in wheat planted in AgrM/GM SPWs compared to the control, although root copper bioaccumulation factors did not change. These results disprove null hypothesis two, as SPWs did partially mitigate toxicity and shoot uptake of Cu from CuO NPs to wheat.

A bacterium, *Pseudomonas chlororaphis* O6 (*Pc*O6), did not protect wheat from CuO NPs, but instead enhanced root shortening. *Pc*O6 did increase Cu shoot bioconcentration factors compared to no *Pc*O6, but reduced Cu root bioaccumulation factors compared to no *Pc*O6. Overall, null hypothesis three was not disproven as *Pc*O6 did not reduce CuO NP toxicity and had mixed effects on Cu uptake.

In addition to the success or failure of the null hypotheses, several other conclusions from the two studies can be drawn:

- At high DNOM concentrations, solubility of CuO NPs is limited below theoretical predictions, while still enhanced above water. The suppression of CuO NP solubility by DNOM was hypothesized to be by coating of the NP surface.

- In the sand and SPW matrix with CuO NPs, the NPs reached their full theoretical solubility, in contrast to results from NPs only in a SPW matrix. In the solid matrix, more of the soluble DNOM may have adsorbed to sand and the excess NPs, allowing dissolution to proceed. These results suggest that saturation of the SPW by soluble copper from CuO NPs may occur in sandy soils.

- Free Cu^{2+} ions were decreased in SPWs below the control, and remained well below the levels that typically cause toxicity in wheat. Calcium, which competes with copper for root sorption sites, did not protect wheat in the control despite having similar dissolved calcium levels to the SPWs. These results suggest that free Cu^{2+} was not wholly responsible for wheat toxicity. Rather, the ligands 2'-

deoxymugineic acid (DMA) and citrate, which are produced by wheat roots particularly during copper stress, were also associated with root shortening and may have been part of the toxicity mechanism. On the other hand, complexation of the soluble copper with DNOM shielded the wheat from dissolved copper and lessened stress responses compared to the control, even with equal or higher concentrations of soluble copper compared to the control. Coating of the NPs with DNOM, as observed during these experiments in solubility studies, may also play a role in the reduction of toxicity from CuO NPs.

- The responses of *Pc*O6 to the NPs was not measured, but the NPs did not eliminate the *Pc*O6. Even though *Pc*O6 did not appear to be significantly impacted by the CuO NPs, other soil bacteria may be, especially those more sensitive to copper.

Overall, these results suggest that solubility of CuO NPs in soils under high-DNOM, sandy conditions could be in the mg/L range, due primarily to DNOM. Toxicity of CuO NPs to crops in soils is mediated compared to toxicological hydroponic studies or other simple systems, but not fully. Application of CuO NPs to soils, whether intentionally as a fungicide, micronutrient fertilizer, or drought protection treatment, or accidentally as from reused wastewater or biosolids, should certainly not exceed 100 mg/kg Cu/soil (0.01% w/w) because toxic effects are seen at this level against wheat in SPW and microbes. Conversely, micronutrient crop nutrition may be manipulated through complexes (such as copper-citrate of copper-DMA) or NPs.

Future research should utilize whole soils (in conjunction with simpler systems to determine individual effects of differing clays, DNOM properties, etc.) and lower concentrations to determine appropriate doses of NPs for agricultural treatments. Unexpected or negative effects of NPs, such as acute and chronic damage to soil microbial communities, crops, soil texture and hydraulic conductivity rates, etc. should also be considered. Finally, transformation to CuO NPs, particularly surface coatings and oxidation/reduction reactions, should be examined more closely in soil environments to determine long-term fate.

APPENDICES

APPENDIX A

CHAPTER 4 SUPPORTING INFORMATION

Table A-1: Dissolved copper from CuO NPs as affected by ligands from several studies.

Author	Solution + pH	Cu concentration (mg/L)
Wang et al. (2013)	50 mM acetate buffer, pH 4	~70
	50 mM acetate buffer, pH 5	~45
	50 mM acetate buffer, pH 6	~10
	PBS buffer, pH 7.4	~2
	50 mM borate buffer, pH 8	<1
	50 mM borate buffer, pH 9	< 1
	PBS buffer + Cys, pH 7.4	~4
	PBS buffer + His, pH 7.4	~30
Gunawan et al. (2011)	Water, pH undefined	6.4
	LB medium, pH 7.2	366.2
Zabrieski et al. (2015)	Water + citrate, pH 6.29	145
Peng et al. (2015)	Water, pH 7	<0.25
	Water + humic acid, pH 7	~1.5
Jiang et al. (2017)	Water, pH 7	~0.05
	Water + humic acid, pH 7	~0.3
	Water + fulvic acid, pH 7	~0.1

Table A-2: Characteristics of soils. Soil samples were collected in 2014 and tested at a laboratory certified under the North American Proficiency Testing Program for Agricultural Labs.

| Soil characteristics					
Soil abbreviation	OrgM	AgrM	IDM	GM	WS
Name origin	Organic farm, Millville	Agricultural field, Millville	Iron deficient, Millville	Community garden, Millville	Warm Springs
Soil series, texture	Millville silt loam	Millville silt loam	Millville loam	Millville silt loam	Warm springs sandy loam
Texture (% sand/silt/clay)	19/56/26	22/56/23	31/46/24	13/59/28	57/26/18
Cultivation	organic certified	commercial production	grassland field	unknown amendments	heavy compost
Crop	continuous green cover	winter wheat	native grasses	varied (community garden)	corn, tomato, squash
pH	7.7	7.8	7.7	7.8	7.3
EC (dS/m)	1.04	0.50	0.37	0.60	3.88
Phosphorus (mg/kg)	52.1	10.1	12.6	19.3	324
Potassium (mg/kg)	434	111	227	369	899
Ammonium (mg/kg N)	2.01	2.43	0.51	< 1.25	6.5
Nitrate (mg/kg N)	31.8	11.5	1.8	10.4	172.0
Sulfate (mg/kg S)	6.5	3.6	1.6	3.3	50.9
Organic matter (% of whole soil)	5.6	3.0	3.1	4.1	8.7
Cation exchange capacity (cmol/kg)	20.0	13.8	21.2	21.0	24.2
Calcium carbonate (%)	14.6	14.1	4.3	16.1	6.2
Saturation point (%)	46.5	41.0	30.7	45.5	38.5
DTPA – Fe (mg/kg)	9.8	8.95	2.98	10.5	24.3
DTPA – Cu (mg/kg)	1.44	1.29	1.31	2.72	7.76
DTPA – Mn (mg/kg)	16.3	14.1	6.7	13.8	22.8
DTPA – Zn (mg/kg)	3.07	1.66	0.7	1.62	22.4
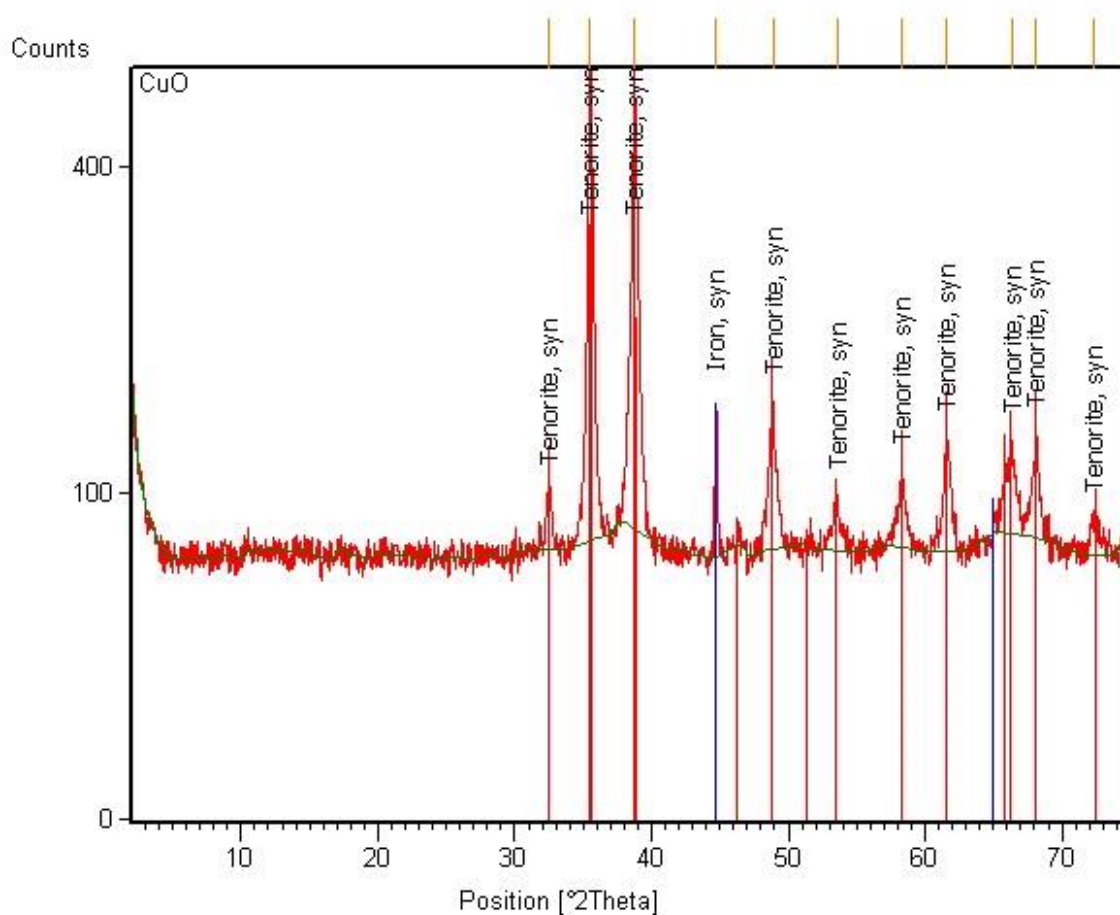
Figure A-1: XRD pattern of CuO NPs.

Table A-3: XRD characterization of CuO NPs.

Pos. [°2Th.]	Height [cts]	FWHM [°2Th.]	d-spacing [Å]	Rel. Int. [%]
32.4910	29.14	0.3936	2.75577	6.40
35.5228	455.35	0.1181	2.52721	100.00
38.7897	398.15	0.3149	2.32157	87.44
44.6955	98.16	0.1771	2.02757	21.56
48.9147	92.91	0.2755	1.86210	20.40
53.5777	28.02	0.3149	1.71052	6.15
58.3120	42.15	0.3149	1.58242	9.26
61.5336	65.81	0.2755	1.50707	14.45
66.3125	54.68	0.3149	1.40959	12.01
68.1128	61.69	0.3149	1.37665	13.55
72.3798	15.90	0.7680	1.30457	3.49
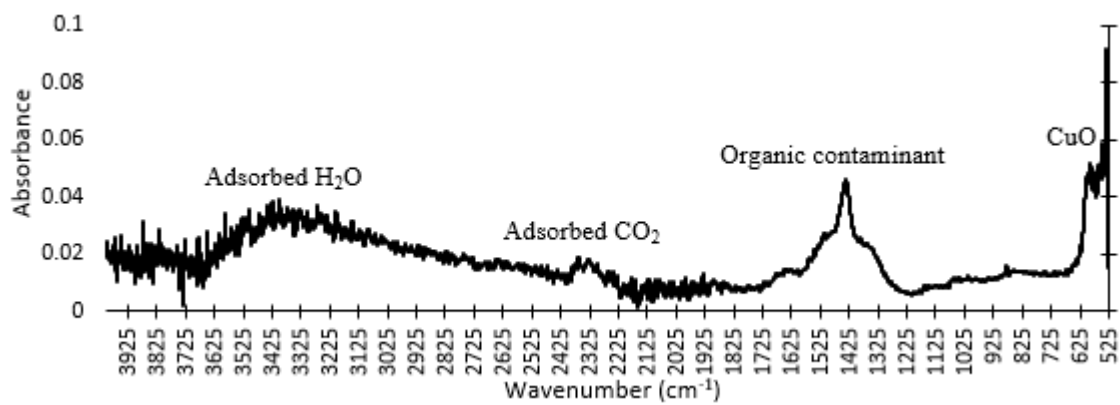
Figure A-2: FTIR spectrum of the unaltered, as-is CuO NPs, with annotation.

Table A-4: Metal concentrations in CuO NPs

Metal	Symbol	Concentration in new batch (mean ± SD, μg/g)	Concentration in old batch (mean ± SD, μg/g) (Dimkpa et al. 2012)	Limit of detection in new batch (mean ± SD, μg/g)
Aluminum	Al	66.5 ± 1.24	216 ± 23.0	0.402 ± 0.007
Antimony	Sb	<0.241	1.99 ± 0.42	0.241 ± 0.004
Arsenic	As	169 ± 2.4	17.5 ± 0.4	0.020 ± 0.0003
Barium	Ba	2.88 ± 0.15	3.05 ± 0.24	0.101 ± 0.002
Beryllium	Be	<0.003	0.13 ± 0.01	0.003 ± 0.00005
Cadmium	Cd	48.2 ± 0.48	0.46 ± 0.01	0.015 ± 0.0003
Calcium	Ca	1,040 ± 22	N/A	8.04 ± 0.14
Chromium	Cr	14.4 ± 0.009	18.5 ± 5.4	0.005 ± 0.00008
Cobalt	Co	205 ± 0.38	86.3 ± 1.5	0.025 ± 0.0004
Copper	Cu	833,000 ± 43,400	694,000 ± 22,000	0.080 ± 0.001
Iron	Fe	147 ± 4.02	814 ± 41	0.704 ± 0.012
Lead	Pb	22.1 ± 0.31	4.43 ± 0.61	0.035 ± 0.0006
Magnesium	Mg	111 ± 1.64	N/A	3.02 ± 0.051
Manganese	Mn	31.1 ± 0.16	130 ± 3	0.015 ± 0.0003
Nickel	Ni	40.2 ± 0.026	18.3 ± 9.0	0.040 ± 0.0007
Potassium	K	<10.1	N/A	10.1 ± 0.17
Phosphorus	P		137 ± 0.65	
Selenium	Se	<0.010	0.76 ± 0.16	0.010 ± 0.0002
Silicon	Si		500 ± 91	
Sodium	Na	6,830 ± 176	N/A	10.1 ± 0.17
Strontium	Sr	6.58 ± 0.078	N/A	0.101 ± 0.002
Thallium	Tl	1.53 ± 0.084	0.13 ± 0.01	0.010 ± 0.0002
Vanadium	V	<0.025	7.45 ± 0.11	0.025 ± 0.0004
Zinc	Zn	23.2 ± 0.73	153 ± 42.4	0.251 ± 0.004

| ☆ | HV | HFW | mag ⊞ | det | WD | pressure | dwell | spot | ——— 200 nm ——— |
| | 30.00 kV | 1.04 µm | 200 000 x | ETD | 7.0 mm | 9.68e-6 Torr | 15 µs | 1.0 | CuO np's |
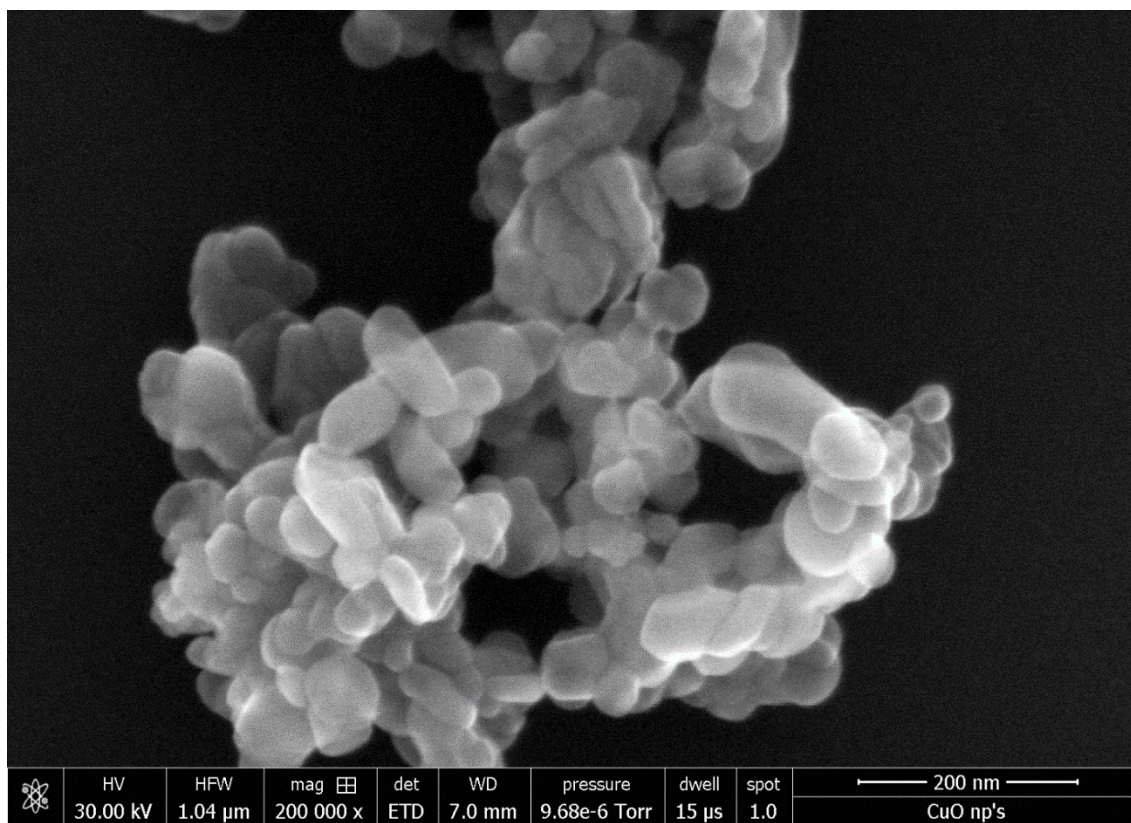
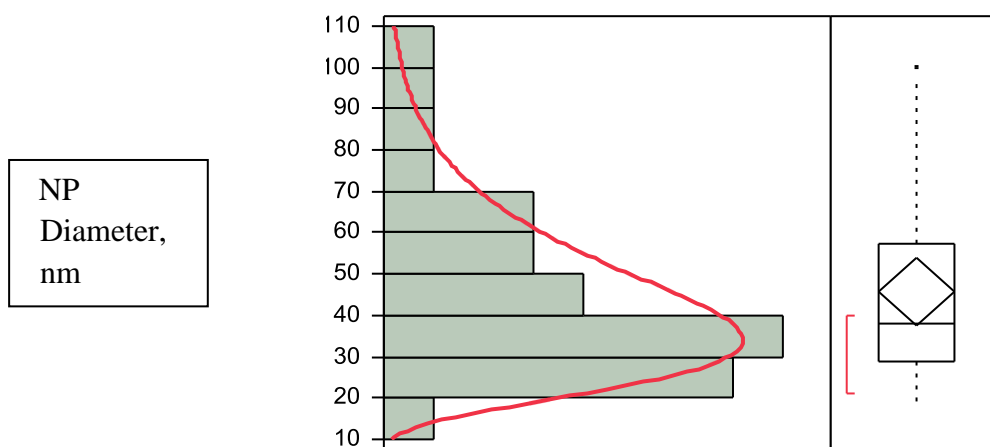Figure A-3: Representative SEM image of CuO NPs.

NP Diameter, nm

Figure A-4: Histogram and quantile boxplot of CuO NP diameters (N = 30 from 3 images). Average NP diameter = 46 nm, median NP diameter = 38 nm.

Table A-5: Full characterization of SPWs. Blank = below detection.

Soil name	OrgM	AgrM	IDM	GM	WS
Na (mg/L)	11.8	9.4	3.4	27.5	54.4
Mg (mg/L)	55.7	17.9	41.1	145.9	76.4
Al (µg/L)	8.3	6.9	7.6		
K (mg/L)	28.7	4.2	30.1	299.1	208.2
Ca (mg/L)	167.6	97.4	186.8	372.3	200.2
V (µg/L)	5.2	5.4	4.3	7.5	5.6
Cr (µg/L)	9.6	1.1	3.1	1.5	2.3
Mn (µg/L)	5.5	12.4	1459.3	118.0	232.9
Fe (µg/L)	67.1	14.6	22.2	53.9	316.5
Co (µg/L)	1.6	1.5	10.0	11.1	5.0
Ni (µg/L)	5.7	6.7	11.0	20.3	17.2
Cu (µg/L)	13.4	22.8	22.7	48.4	122.8
Zn (µg/L)	51.1	34.1	31.4	48.7	74.6
As (µg/L)	7.2	6.1	10.1	18.8	38.4
Se (µg/L)	1.0	4.3	1.6	1.8	7.2
Sr (µg/L)	668.7	97.7	193.7	1124.0	864.5
Ba (µg/L)	402.0	161.6	318.9	640.4	322.1
Gluconate (mg/L)	1.9	3.9			
Lactate (mg/L)			17.9		
Acetate (mg/L)	0.7		244		
Isobutyrate (mg/L)				3.6	
Butyrate (mg/L)			1.4		
Isovalerate (mg/L)			5.2	5.2	
Valerate (mg/L)			0.8		
Chloride (mg/L)	50.2	5.6	12.3		
Nitrite (mg/L N)	5.7	11.8			
Nitrate (mg/L N)	148.6	12.6		574	71.5
Sulfate (mg/L)	36.8	18.4	9.9		
Oxalate (mg/L)			0.7		
Phosphate (mg/L P)			0.9	1.99	8.5
Citrate (mg/L)			0.6		
Alkalinity (mg /L $CaCO_3$)	340	450	1010	490	1270
EC (µS/cm)	735	391	1100	3380	2030
DOC (mg/L C)	42.7	73.4	270	305	388
HA (mg/L C)	<0.8	<0.8	14.2	4.3	16.5
FA (mg/L C)	28.3	38.0	67.5	165	169

Table A-6: MINTEQ modeling parameters

Setting name	Set to:
Cations/anions	As specified in Table A-3
pH	7.5
Ionic strength	Calculated from problem
Temperature	25 ℃
Alkalinity	Turned on, entered as specified in mg/L $CaCO_3$
Atmosphere	None, unless no alkalinity was specified; then, 400 ppm CO_2
Dissolved solids	Not allowed to precipitate
CuO NPs	Entered as infinite solid, tenorite(c)
Fulvic and humic acid	Entered as mg/L DOC (Table A-3) with NICA-Donnan model
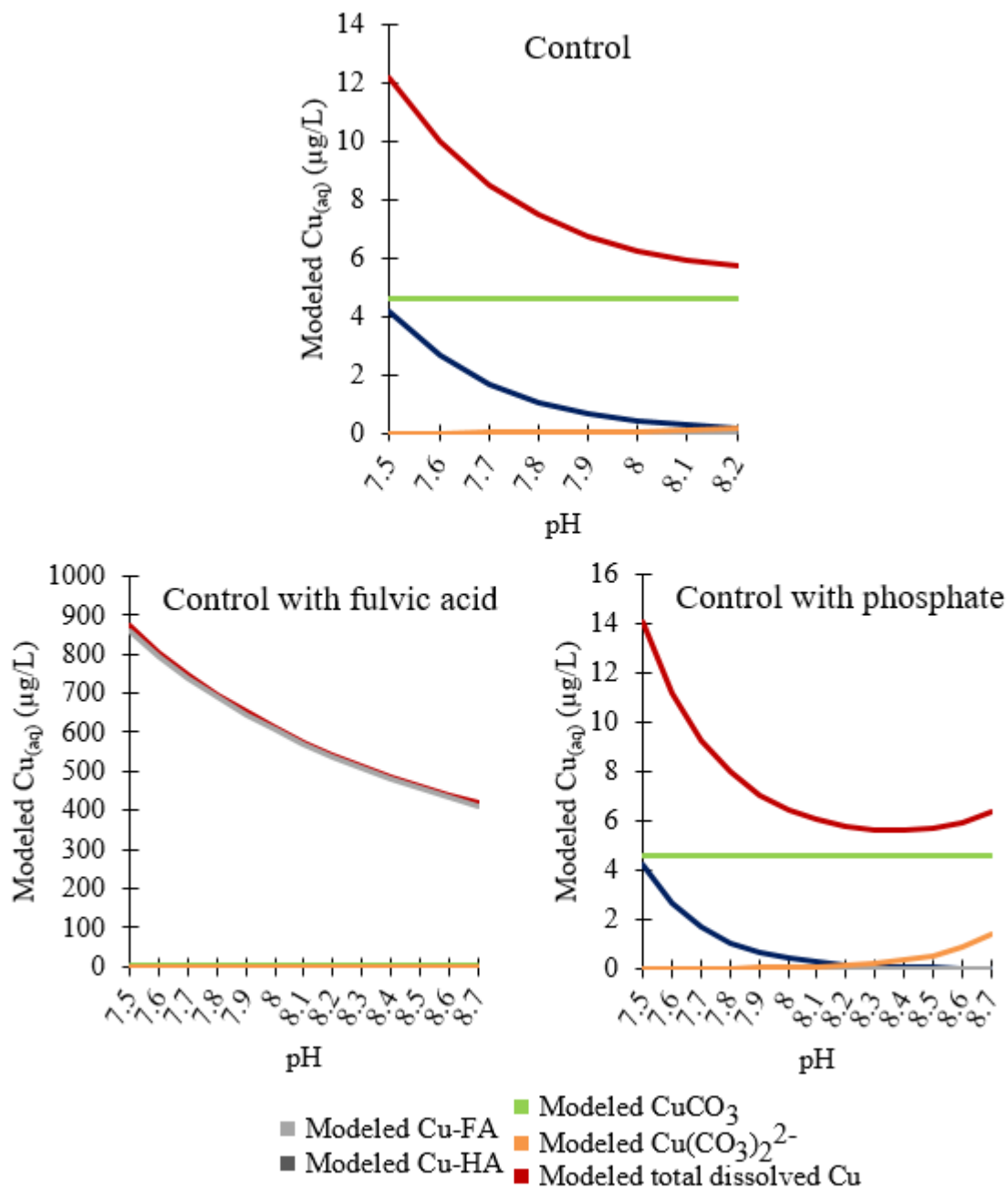
Figure A-5: MINTEQ modeled predictions of speciation of $Cu_{(aq)}$ with increasing pH (to maximum measured pH) in control and control with fulvic acid/phosphate. Red line (total modeled dissolved Cu) is sum of all other lines. Note changing axis values in each graph.
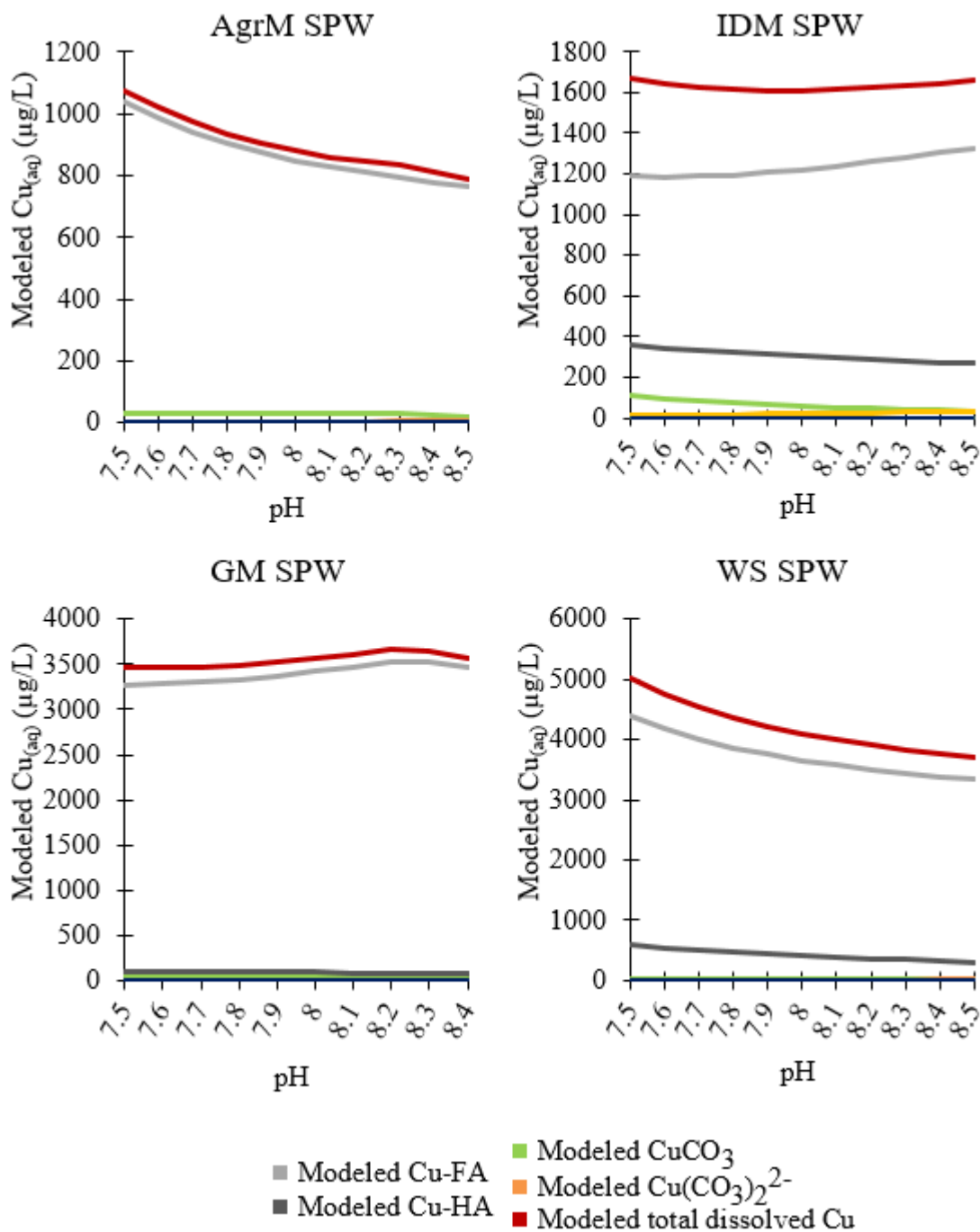
Figure A-6: MINTEQ modeled predictions of speciation of $Cu_{(aq)}$ with increasing pH (to maximum measured pH) in all SPWs. Red line (total modeled dissolved Cu) is sum of all other lines. Note changing axis values in each graph.

Table A-7: Dissolved organic carbon after centrifugation vs. after ultrafiltration. Values given are average of independent triplicates ± standard deviation (coefficient of variation). Value marked with * was affected by microbial contamination.

Sample	Original DOC (mg/L C)	DOC after 10-day incubation, centrifugation (mg/L C)	DOC after 10-day incubation, ultrafiltration (mg/L C)
Control + FA	20	23.9 ± 2.8 (0.12)	12.8 ± 1.2 (0.09)
OrgM	42.7	41.1 ± 2.0 (0.049)	18.0 ± 1.5 (0.083)
AgrM	73.4	70.0 ± 6.3 (0.090)	23.5 ± 1.8 (0.077)
IDM	270	161 ± 33* (0.20)	200 ± 3.7 (0.019)
GM	305	295 ± 3.2 (0.011)	167 ± 9.1 (0.054)
WS	388	356 ± 21 (0.059)	98.3 ± 19 (0.19)
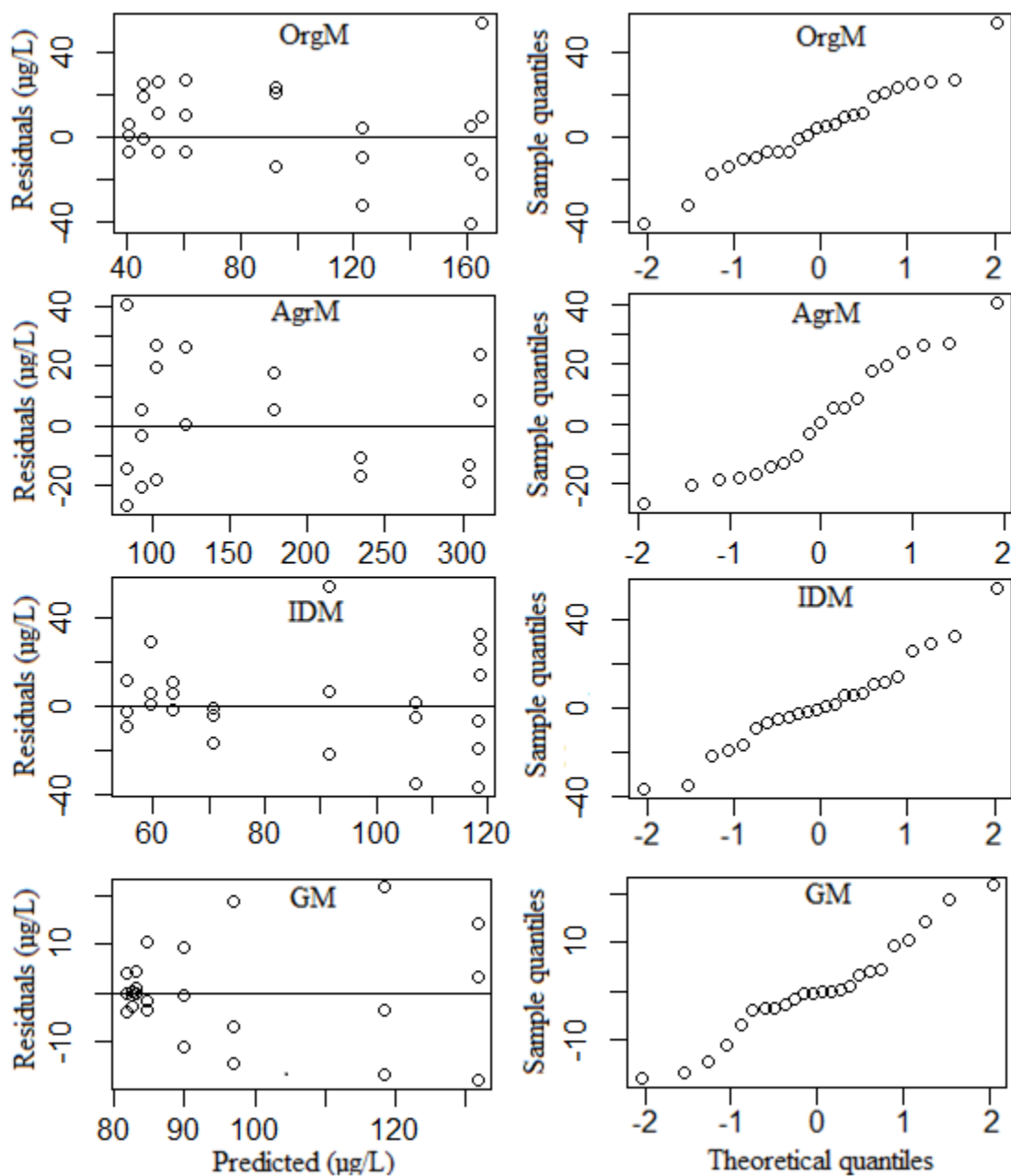
Figure A-7: Residuals (left) and normal quantile plots (right) from all SPW first order kinetics models.
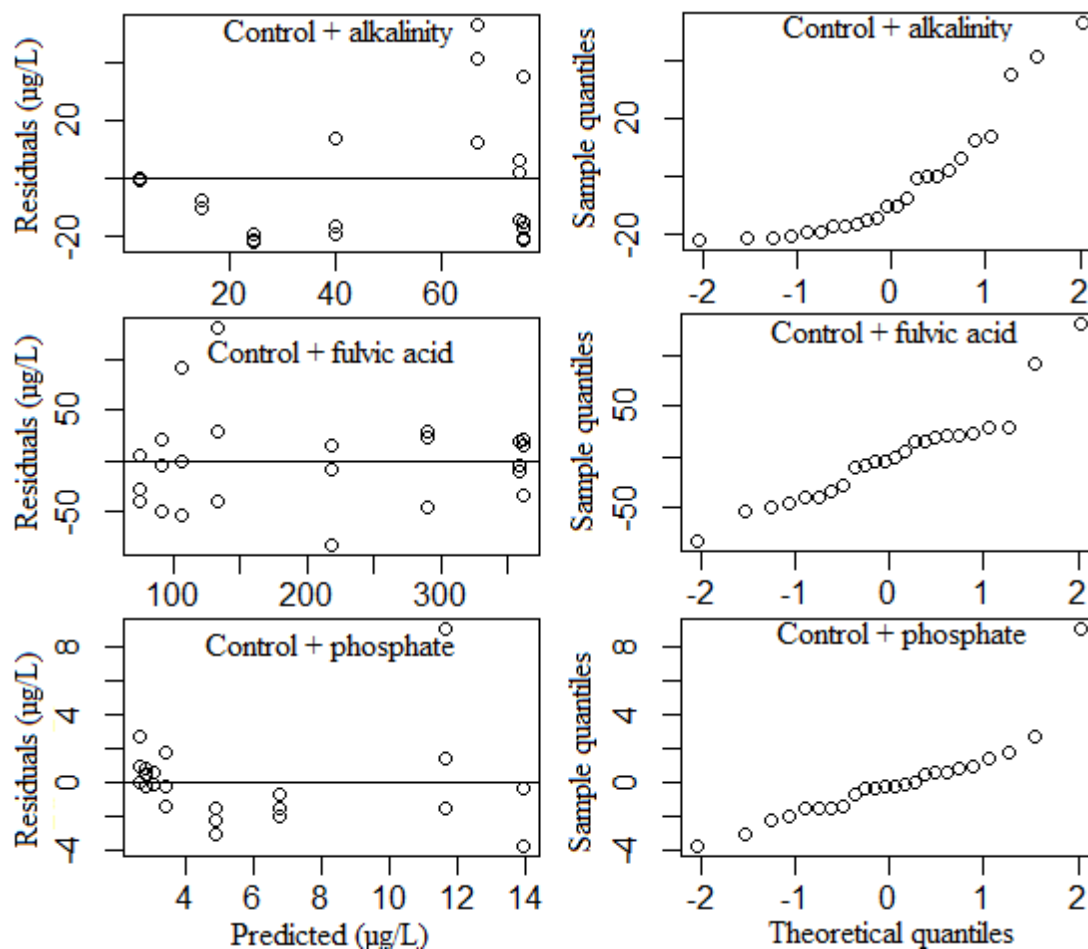
Figure A-8: Residuals (left) and normal quantile plots (right) from all control + additions first order kinetics models.
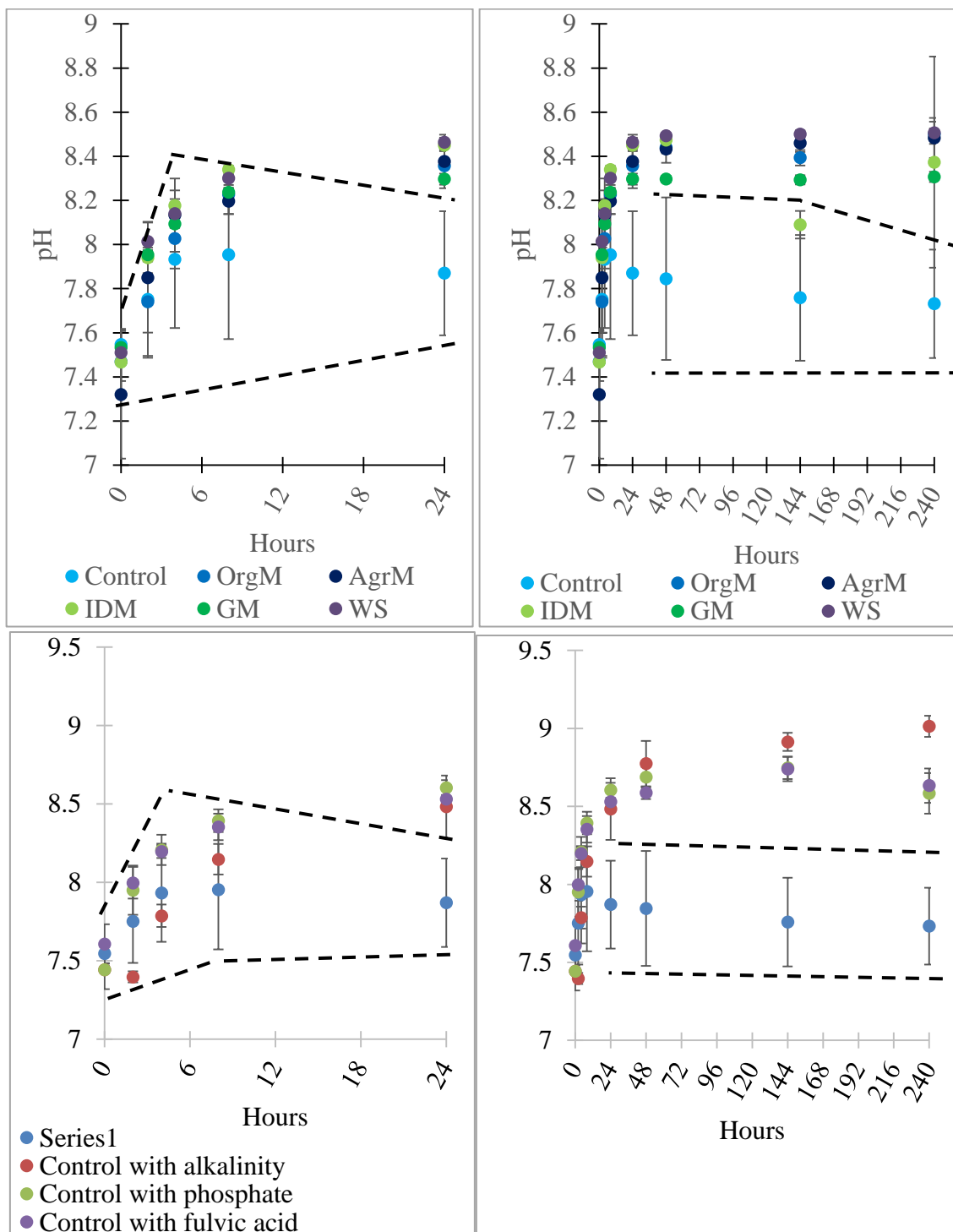
Figure A-9: pH in all SPWs (A) and controls (B) with time. Data points represent average of triplicate measurements, error bars represent standard deviation. Data points outside of dashed lines are significantly different from the control with no additions (blue) by Dunnett's test (p<0.05). Left graphs are expansion of right graph from 0-24 hours.
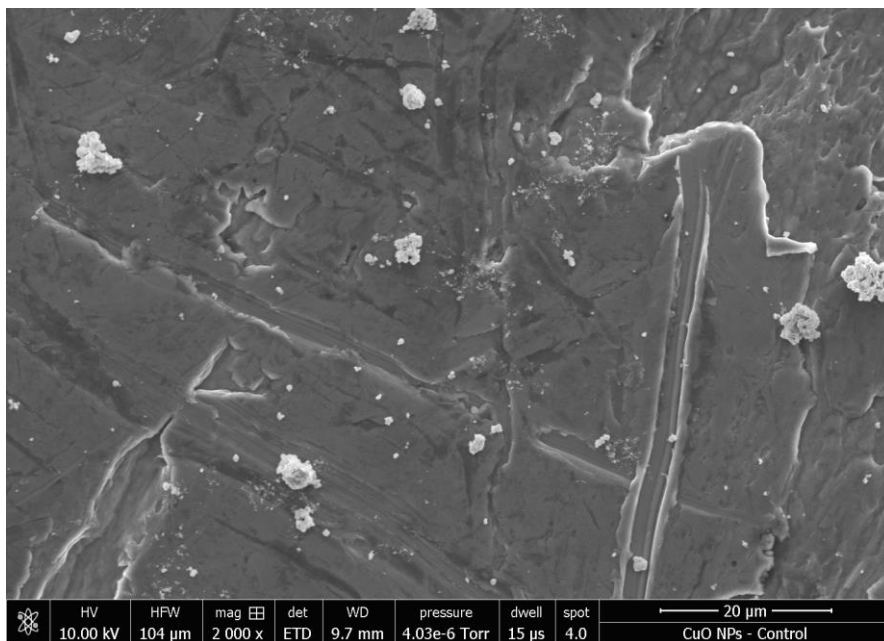
Figure A-10: SEM image of aggregated NPs exposed to 3.34 mM $Ca(NO_3)_2$. Note few large aggregates (4-5 microns) and many smaller aggregates.
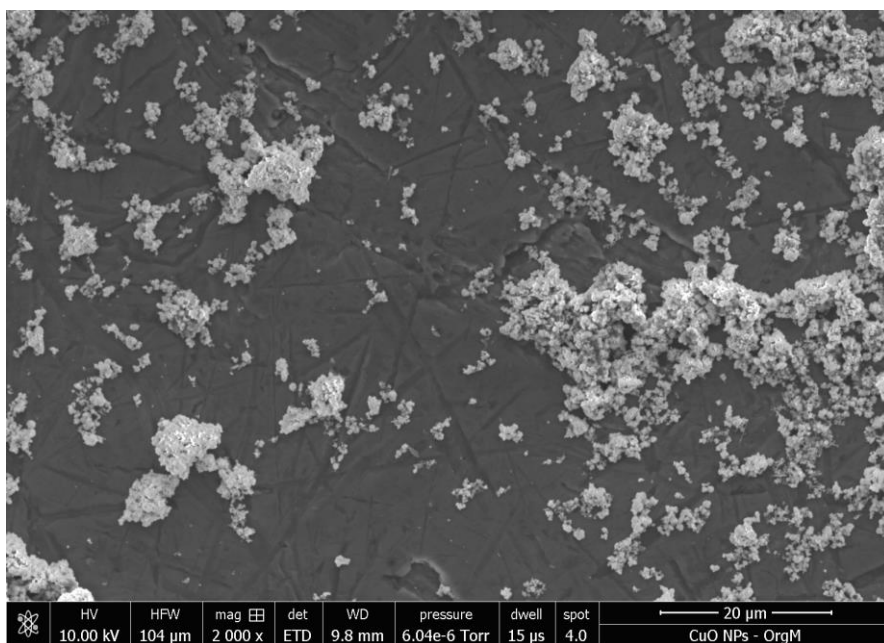
Figure A-11: SEM image of aggregated NPs exposed to OrgM SPW. Note many large aggregates (4-5 microns) and few smaller aggregates.
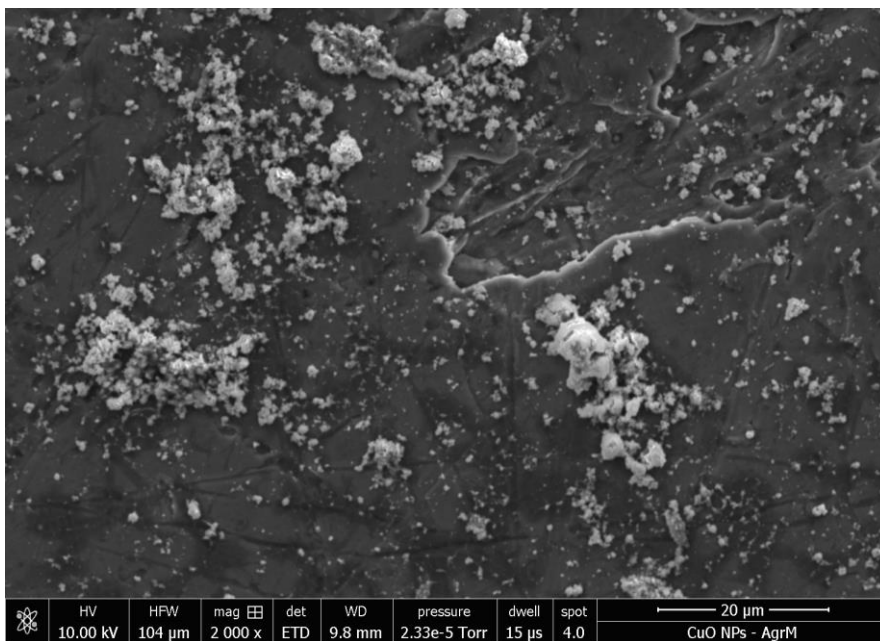
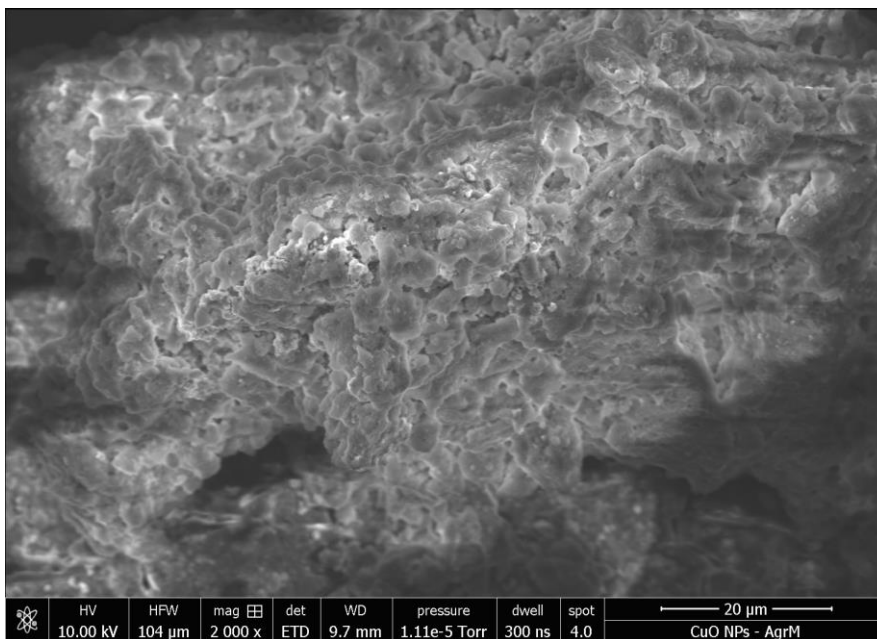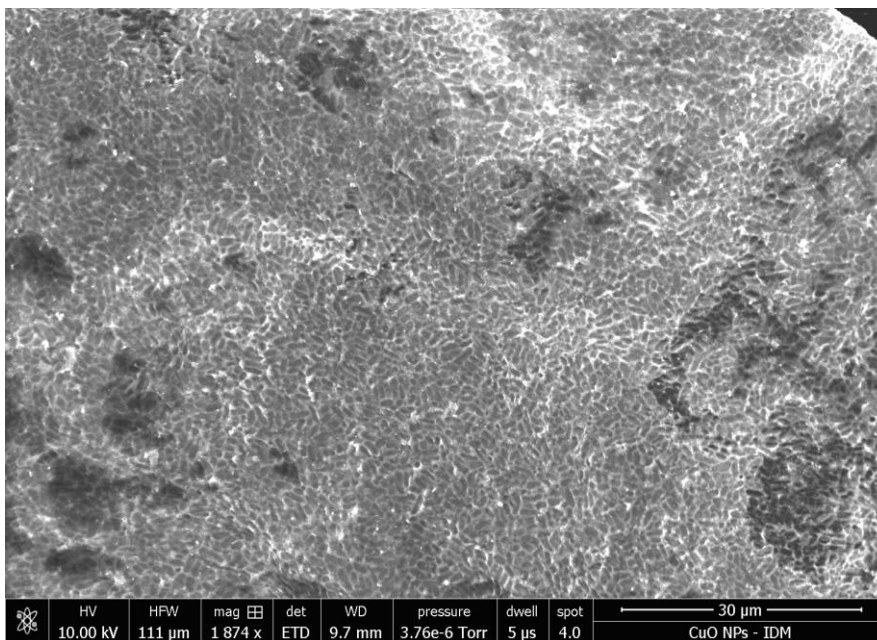Figure A-12: SEM image of aggregated NPs exposed to AgrM SPW. Note large aggregates and few smaller aggregates.
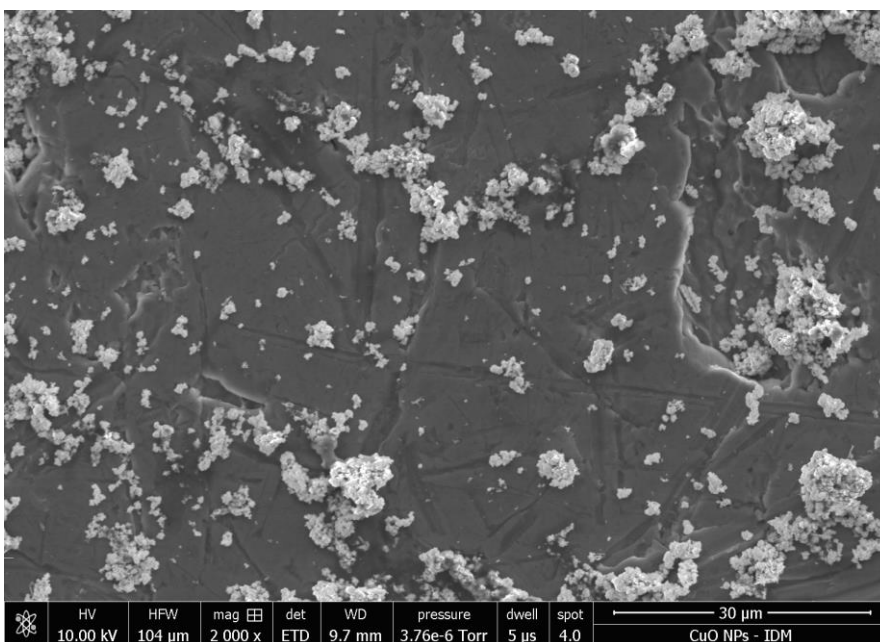
Figure A-13: SEM image of aggregated NPs exposed to IDM SPW. Note large aggregates and few smaller aggregates.

Figure A-14: SEM image of aggregated NPs exposed to GM SPW. Note single, large aggregate.

Figure A-15: SEM image of aggregated NPs exposed to WS SPW. Bacterial cells dominate this image due to contamination after NP collection.
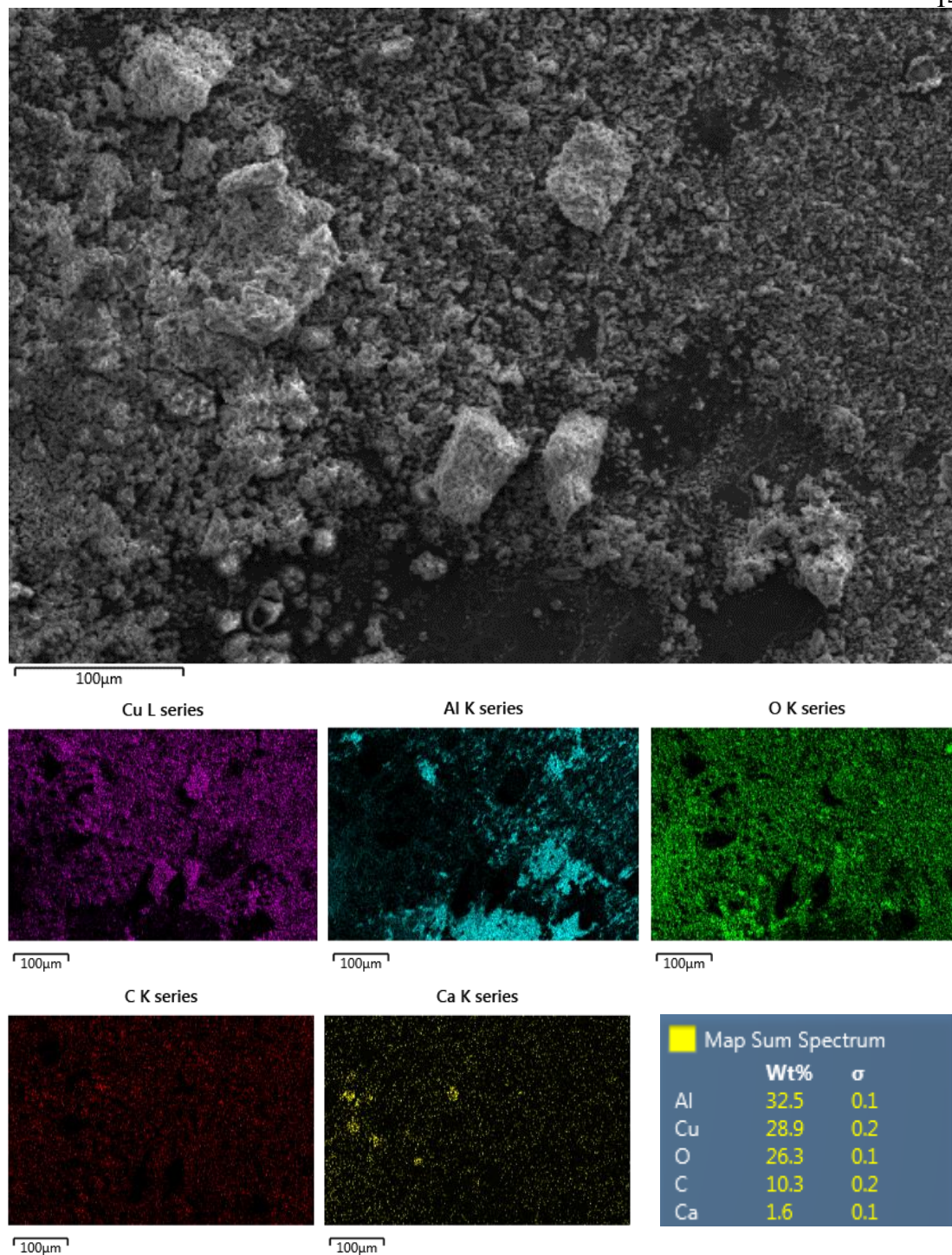
Figure A-16: SEM (top) and colorized EDS images of distribution of individual elements of NPs incubated in 3.34 mM Ca(NO$_3$)$_2$ with FA after 240 hours. Background is aluminum stub. Note the large CuO NP aggregates.
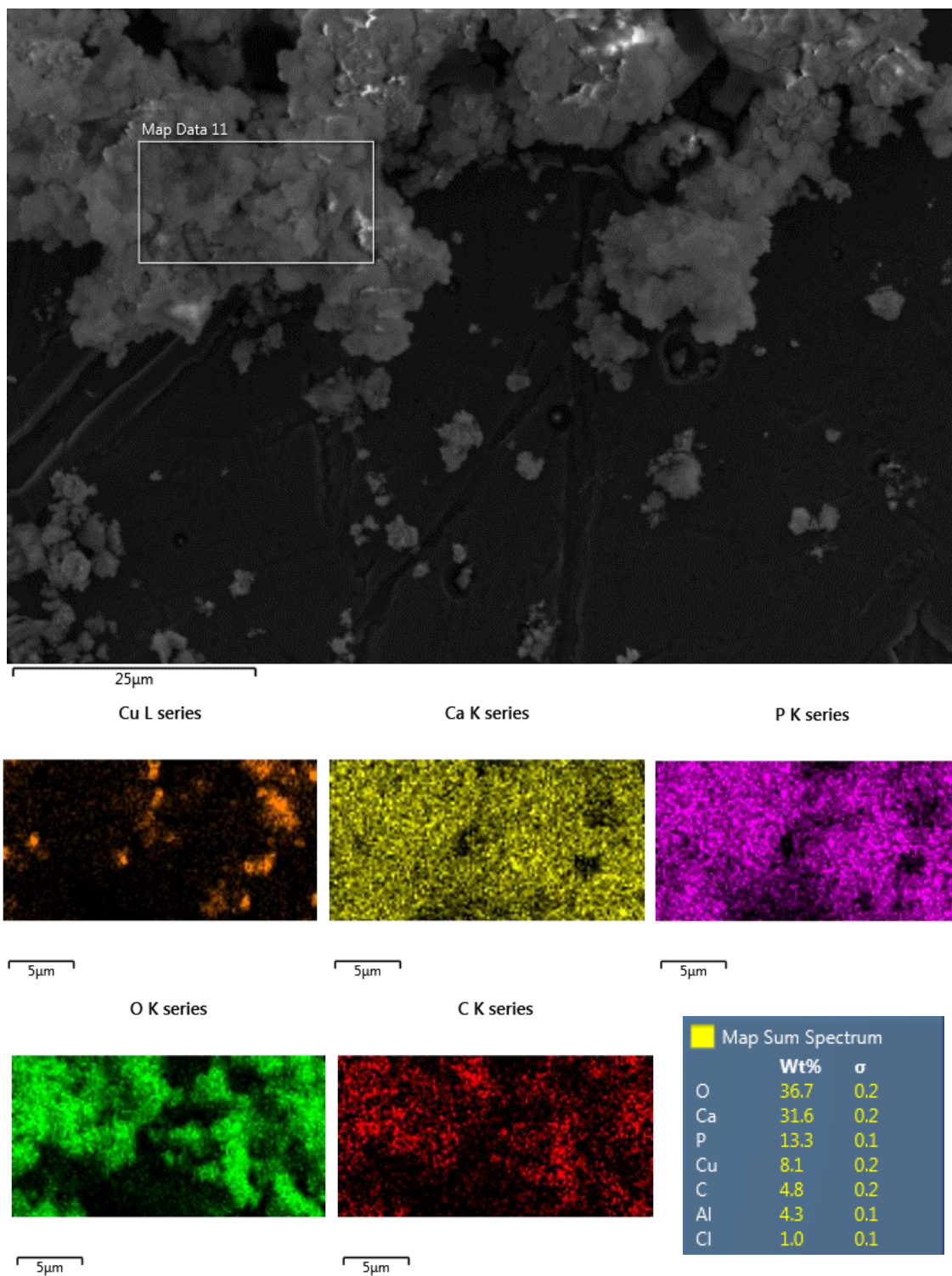
Figure A-17: SEM (top) and colorized EDS images of distribution of individual elements of NPs incubated in phosphate treatment for 240 hours. Background is aluminum stub. EDS is zoomed to avoid excessive Al signature. Note the dispersal of Ca and P indicative of the calcium phosphate solid, and the heteroaggregated CuO NPs.
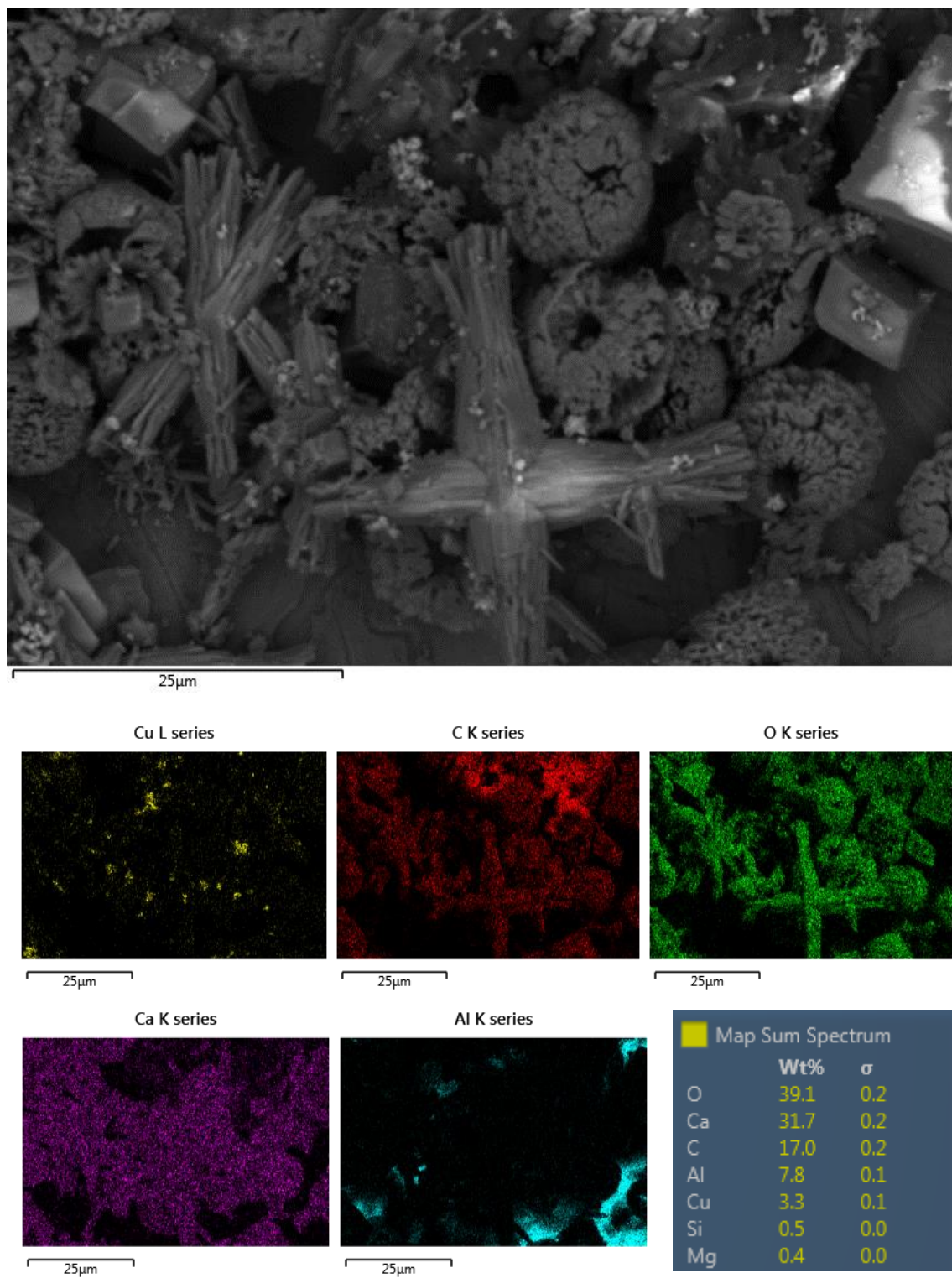
Figure A-18: SEM (top) and colorized EDS images of distribution of individual elements of NPs incubated in alkalinity treatment. Background is aluminum stub. Note the even structure of the crystals (C and O) and heteroaggregated CuO NPs.
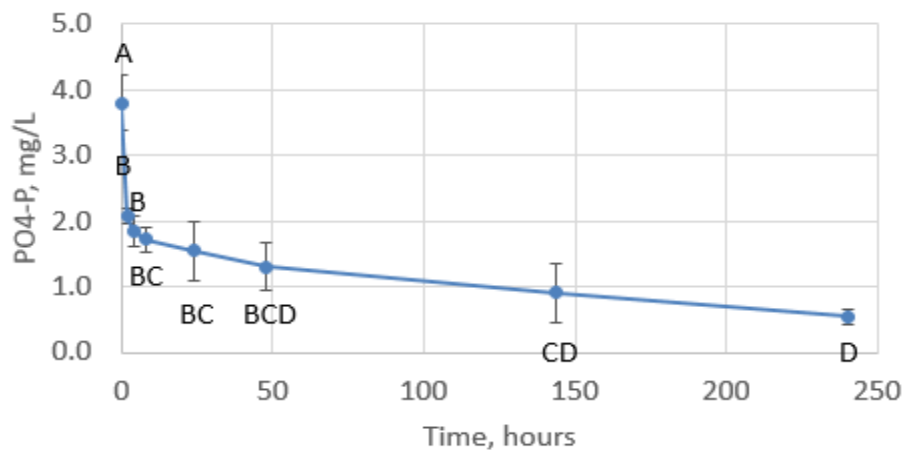
Figure A-19: Phosphate concentration in phosphate treatment. Each point represents the average of three measurements and the error bars represent the standard deviation. Differing letters indicate a significant difference by one-way ANOVA.

Figure A-20: Crystalline, translucent structures containing opaque particles seen under light microscopy in controls (circled in red). The translucent, crystalline structures are predicted to be calcite, and the opaque particles are predicted to be CuO NPs. Clockwise from top left: alkalinity control, alkalinity control, control, control.

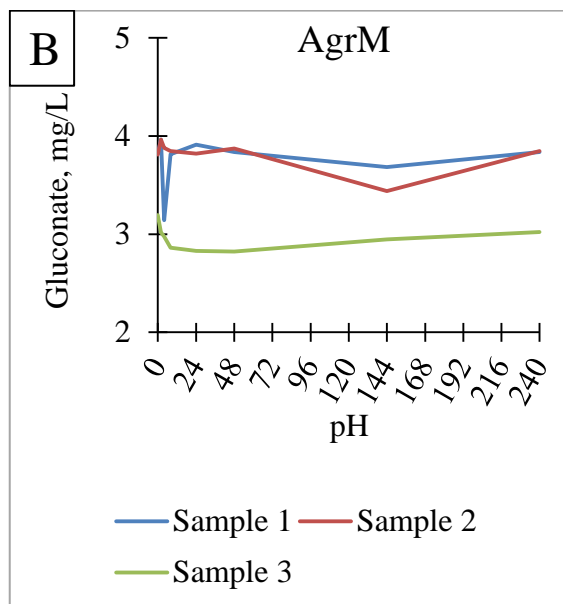|	DOC (mg C/L)
AgrM before incubation	73.4
AgrM sample 3 after incubation	66.2

Figure A-21: Changes in DOC (A) and gluconate (B) seen with time in sterile versus contaminated AgrM samples. All components or samples not shown remained steady.

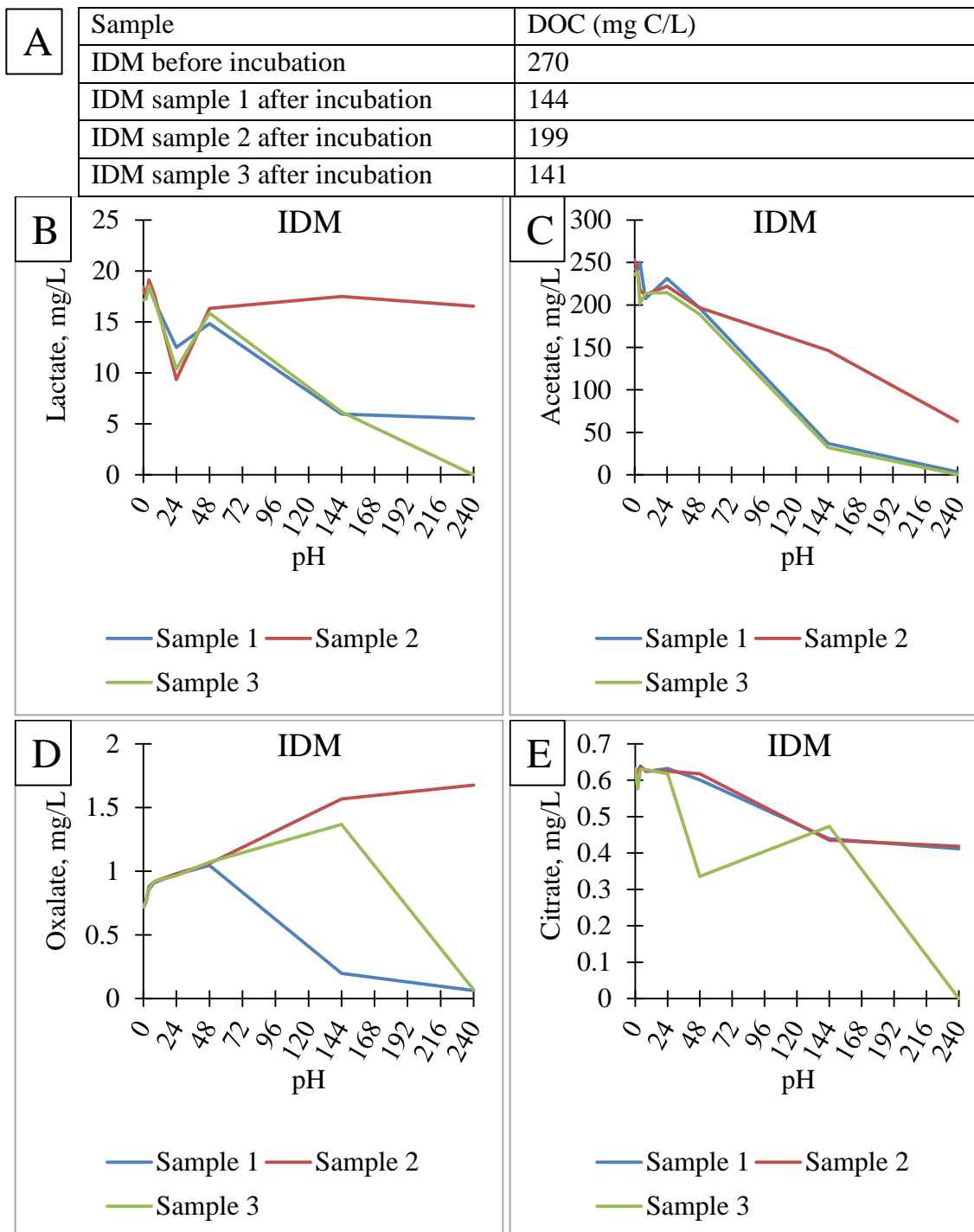| Sample	DOC (mg C/L)
IDM before incubation	270
IDM sample 1 after incubation	144
IDM sample 2 after incubation	199
IDM sample 3 after incubation	141

A

Figure A-22: Changes in DOC (A), lactate (B), acetate (C), oxalate (D), and citrate (E) seen with time in contaminated IDM samples. All components not shown remained steady.
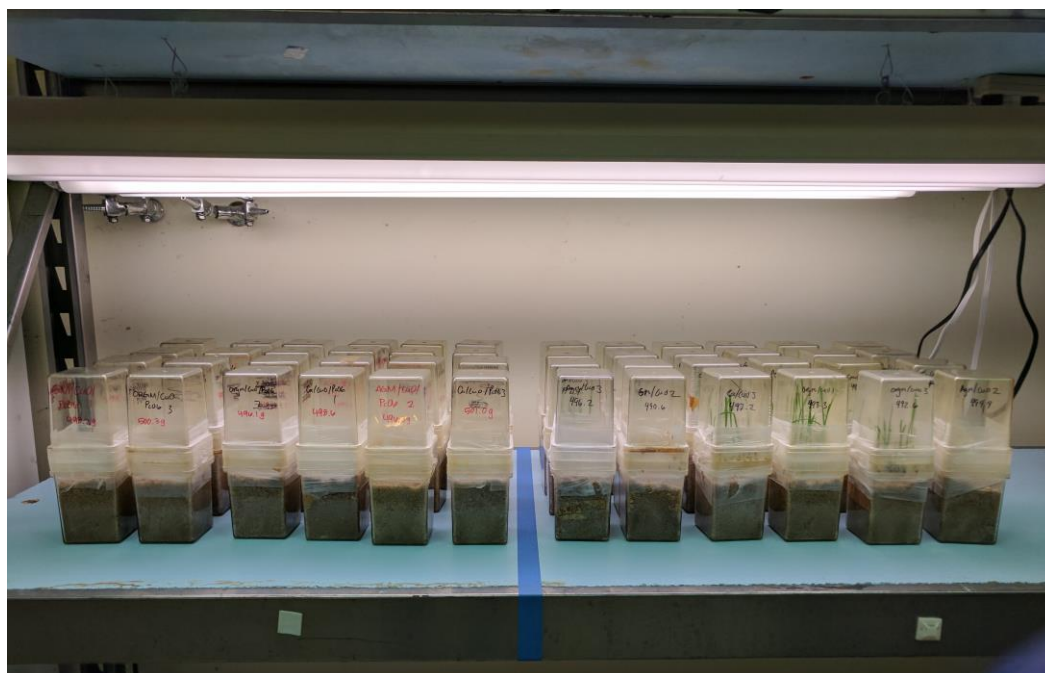
APPENDIX B

CHAPTER 5 SUPPORTING INFORMATION

Figure B-1: Setup of 48 magenta boxes under grow lights, with/without wheat.

Table B-1: Experimental setup for non-PcO6 experiment.

Non-PcO6 experiment setup								
Group	Treatment	Wheat	CuO	*PcO6*	3.4 mM Ca(NO$_3$)$_2$	AgrM SPW	OrgM SPW	GM SPW
Wheat controls (week 2)	1	+	-	-	+	-	-	-
	2	+	-	-	-	+	-	-
	3	+	-	-	-	-	+	-
	4	+	-	-	-	-	-	+
CuO fate controls (week 1)	5	-	+	-	+	-	-	-
	6	-	+	-	-	+	-	-
	7	-	+	-	-	-	+	-
	8	-	+	-	-	-	-	+
SPW controls (week 1)	9	-	-	-	+	-	-	-
	10	-	-	-	-	+	-	-
	11	-	-	-	-	-	+	-
	12	-	-	-	-	-	-	+
CuO treatments (week 2)	13	+	+	-	+	-	-	-
	14	+	+	-	-	+	-	-
	15	+	+	-	-	-	+	-
	16	+	+	-	-	-	-	+

Table B-2: Experimental setup for PcO6 experiment.

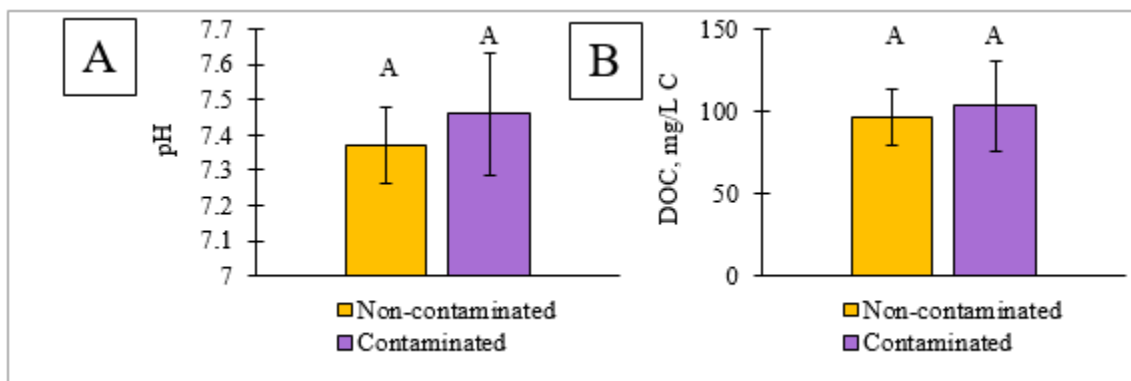| PcO6 experiment setup								
Group	Treatment	Wheat	CuO	$PcO6$	3.4 mM Ca(NO$_3$)$_2$	AgrM SPW	OrgM SPW	GM SPW
Wheat controls (week 4)	1	+	-	+	+	-	-	-
	2	+	-	+	-	+	-	-
	3	+	-	+	-	-	+	-
	4	+	-	+	-	-	-	+
CuO fate controls (week 3)	5	-	+	+	+	-	-	-
	6	-	+	+	-	+	-	-
	7	-	+	+	-	-	+	-
	8	-	+	+	-	-	-	+
SPW controls (week 3)	9	-	-	+	+	-	-	-
	10	-	-	+	-	+	-	-
	11	-	-	+	-	-	+	-
	12	-	-	+	-	-	-	+
CuO treatments (week 4)	13	+	+	+	+	-	-	-
	14	+	+	+	-	+	-	-
	15	+	+	+	-	-	+	-
	16	+	+	+	-	-	-	+

Figure B-2: pH (A) and DOC (B) in contaminated versus non-contaminated samples without wheat, PcO6, or CuO NPs. Bars represent the mean of measurements and error bars represent Tukey HSD statistical significance. No significant changes occurred between sterile and contaminated samples.
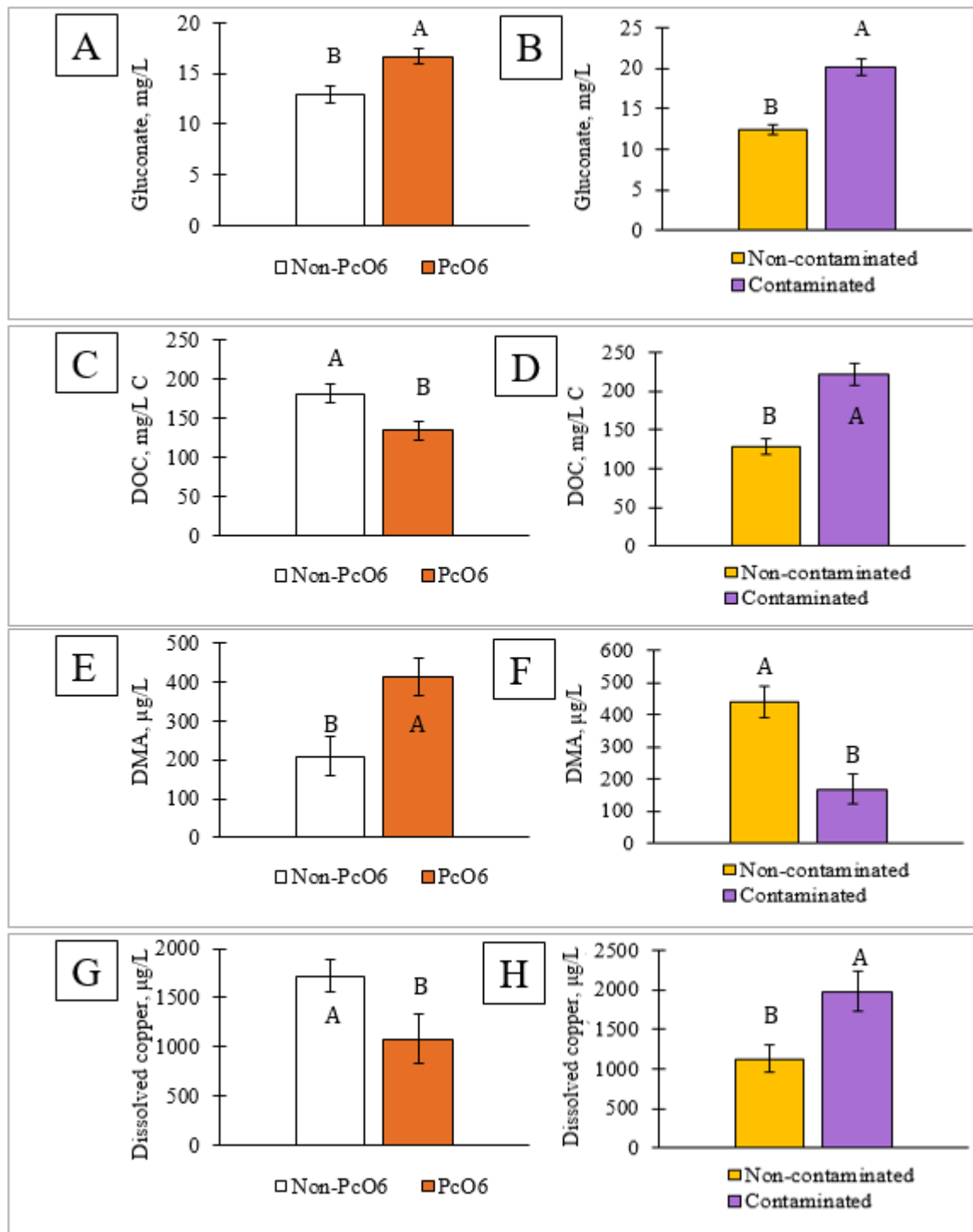
Figure B-3: Gluconate (A), DOC (C), DMA (E), and dissolved copper (G) in contaminated versus non-contaminated samples and gluconate (B), DOC (D), DMA (F), and dissolved copper (H) in *Pc*O6 versus non-*Pc*O6 samples. Bars represent the mean of measurements and error bars represent Tukey HSD statistical significance.
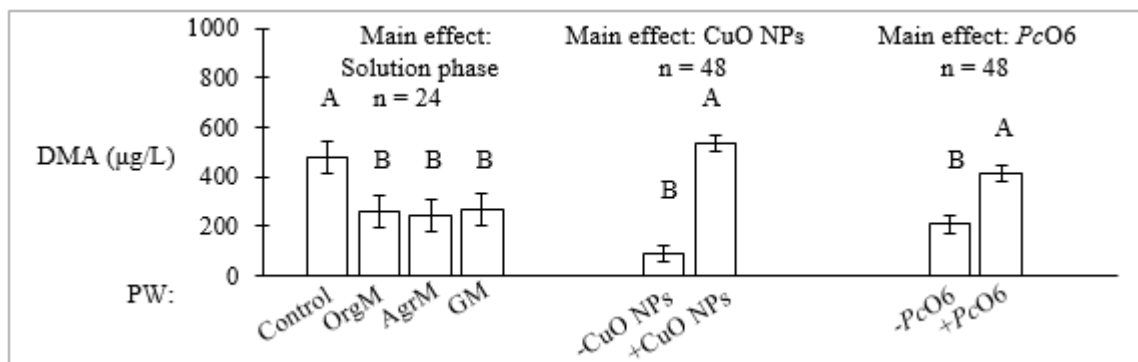
Figure B-4: DMA concentration by main effects PW, CuO NPs, and PcO6.